ABSTRACT

VICKERY, JOHN D. Fundamental Properties and Bond Characteristics of Chlorinated Polyvinyl Chloride and SS340 Adhesive for Evaluation of Steel Tank Linings. (Under the Direction of Dr. Sami Rizkalla.)

Tank linings are used to extend the service life of tanks and to avoid replacement of damaged tanks. Adhesive materials play a major role in the effectiveness of the liner. The main objective of this research is to understand the behavior of the different materials proposed for lining typical bleach tanks used in the pulp and paper industry. This research will focus on the behavior of the selected Structural Adhesive Series 340 (SS340) for a proposed lining system and its interaction with Chlorinated Polyvinyl Chloride material (CPVC) as well as the steel material at various temperatures and sustained stress levels. The experimental program was designed to subject the specimens to a combination of corrosive environments and sustained stresses in order to study their behavior and to determine the effect of those conditions on the behavior and service life. Research findings provide better understanding of the adhesive when subjected to severe environmental conditions and sustained loads. The overall composite behavior of the proposed lining for steel tanks based on testing of small-scale models subjected to high temperature is investigated.

The experimental program focuses on the fundamental material properties and bond characteristics of SS340 when subjected to severe conditions. Test variables include temperature and applied sustained loads, as well as time and soaking solution. Sixty-six SS340 specimens and sixty-six CPVC specimens were examined under severe

environmental exposure to determine the effects of these conditions on the tensile strength. The bond characteristics were investigated using fifty double lap shear specimens to examine the bond behavior of CPVC-to-steel surfaces. The investigation focused on the influence of the environmental exposure on the shear strength of the adhesive bond. Results obtained from tension and lap shear tests were used to identify the performance associated with each variable. Such influences are critical to the future field applications of these materials in extreme environments. Conclusions are focused on ultimate tensile strength and shear strength under various environmental conditions. Test results also provided limitations of the temperature and sustained load level, which can be used safely under service loading conditions.

The final phase of the experimental program consists of small-scale specimens to simulate the lining proposed for a typical steel bleach tank. The specimens were subjected to extreme temperature changes to examine the thermal gradient distribution and the composite interaction of the CPVC liner to the steel wall under the effect of temperature. Strains and temperatures were recorded at each interface. Finite element analysis was conducted to validate test results. The analytical model was used to study the effect of key parameters believed to affect the behavior including boundary conditions and specimen dimensions.

FUNDAMENTAL PROPERTIES AND BOND CHARACTERISTICS OF CHLORINATED POLYVINYL CHLORIDE AND SS340 ADHESIVE FOR EVALUATION OF STEEL TANK LININGS

by
JOHN DAVID VICKERY

A thesis submitted to the Graduate Faculty of
North Carolina State University in partial fulfillment of
the requirements of the Degree of Master of Science

CIVIL ENGINEERING

Raleigh, North Carolina

2006

APPROVED BY:

_____
Chair of Advisory Committee
Dr. Sami Rizkalla

_____ _____
Dr. Emmett Sumner Dr. James Nau

ACKNOWLEDGMENTS

I would like to acknowledge the support of the National Science Foundation Industry/University Collaborative Research Center on the use of FRP for the Repair of Bridges and Buildings with Composites (RB^2C). I also thank the industry partner whom I have had the opportunity to work with during this project, and who provided the materials as well as many tools and ideas to complete the project. Without these support groups this project would not have been possible.

I thank Dr. Sami Rizkalla for giving me the opportunity to work alongside him. His patience and understanding of many of the challenges I faced during this research project was greatly appreciated. His personal sacrifices and contributions to help me complete this research program were more than I could have ever asked for and will not be forgotten. I wish him the best as he continues to make his mark in structural engineering. I also thank Dr. Jim Nau and Dr. Emmett Sumner, whom I have also enjoyed working alongside with. I would like to thank for Dr. Nau for the experience of being his reinforced concrete TA for two semesters. I certainly learned the material better the second and third time around. For all three professors, I enjoyed the many valuable lessons and insight provided, academically and on a personal level. As dedicated as they are to the progression of this university, I have a great deal of admiration for each of them in their respective contributions. Each has made a positive impact in my life as I transitioned into a career as a structural engineer.

Additional thanks and acknowledgement is due to Glen Smith. His willingness to transition over to me his previous adhesive work was much appreciated, both before and after his departure from NC State. This “passing of the torch” could not have been more fluid. Without his design and implementation of the lab’s environmental exposure test setup, my research would have been much more difficult. Through his early guidance and knowledge, I was able to take ownership of this research effort.

To Dr. Tarek Hassan, I cannot thank enough for his exceptional contributions in the final phase of testing. His finite element modeling proved to be one of the primary keys to successful analysis of the bonded plate specimens. In addition, his keen approach to research and problem solving proved invaluable during the study. I greatly appreciate his review of the final phase of this paper. He met and exceeded every expectation I had. I cannot imagine the research coming together in the end without his assistance and dedication.

To the lab technicians, I thank both Jerry Atkinson and Bill Dunleavy for their contributions to the project. Jerry is a great lab technician and uses his wealth of experience to tackle any project needs, several of which I needed help with. Bill provided “the way” for me many times. His expertise with the data acquisition as well as his words of encouragement in the faith was a true blessing. In addition, I also thank the staff members, Amy and Renee, who have been such an integral part in my survival as graduate student.

My family has provided unceasing encouragement and prayers, which I could not begin to place a value on. My wife, Jo Neel, has unfailingly contributed love, personal sacrifice, and understanding as my time was increasingly spent on this project. I thank you for shouldering the load in so many ways, so that I could maximize my research efforts at the lab. My love for you has only grown during this time, as I have realized how truly blessed I am to be to walk through life together with you. I look forward to spending so much more free time together as well as the excitement of discovering a new place to call home.

Finally, I give thanks and praise to the Lord for His faithfulness and Providence during this two year journey. Though at times graduate school was very humbling and challenging, I could see His hand at work as I continue to discover my place in glorifying Him in this world.

TABLE OF CONTENTS

List of Tables vii

List of Figures ix

1.0 Introduction 1

1.1 Background 1
1.2 Objective 2
1.3 Scope 3

2.0 Literature Review 5

2.1 Introduction 5
2.2 Structural Adhesives 8
2.3 CPVC 10
2.4 Chlorine Dioxide 11
2.5 Tank Lining Systems 12
2.6 Effect of Environmental Exposure to Adhesives 14
2.7 Effect of Varying Coefficients of Thermal Expansion of the Liner 14

3.0 Experimental Program 17

3.1 Introduction 17
3.2 Overview 17
3.3 Phase I: Environmental Effect on Tensile Strength of CPVC and SS340 17
3.3.1 Specimen Preparation 18
3.3.1.1 CPVC Specimen Preparation 18
3.3.1.2 SS340 Specimen Preparation 19
3.3.2 Stress and Temperature Effects on Tensile Strength 21
3.3.3 Salt Soaking and Time Effects on Tensile Strength 22
3.3.4 Test Setup 25
3.3.5 Test Method 30
3.4 Phase II: Bond Characteristics of SS340 Adhesive for Steel-to-CPVC Surfaces 31
3.4.1 Double Lap Shear Specimen Preparation 32
3.4.2 Stress and Temperature Effects on Lap Shear Strength 36
3.4.3 Test Setup 38
3.4.4 Test Method 38
3.5 Phase III: Thermal Gradient Test 39
3.5.1 Specimen Preparation 39
3.5.2 Test Setup 42
3.5.3 Test Method 44

4.0 Results, Analysis, and Discussion 47

4.1 Introduction 47
4.2 Phase I: Tensile Strength 47
4.2.1 Tensile Strength of CPVC 47
4.2.1.1 Effect of Combined Sustained Load and Temperature 49
4.2.1.2 Effect of Soak Time with Water and Salt-water 53
4.2.2 Tensile Strength of SS340 58
4.2.2.1 Effect of Combined Sustained Load and Temperature 59
4.2.2.2 Effect of Soak Time with Water and Salt-water 62
4.3 Phase II: Double Lap Shear Strength 67
4.3.1 Double Lap Shear Control Specimens 67
4.3.2 Double Lap Shear Group A Specimens 71
4.3.3 Double Lap Shear Group B Specimens 75
4.4 Phase III: Thermal Strain Gradient 82
4.4.1 Coefficient of Thermal Expansion 82
4.4.1.1 Titanium Silicate Adjustment 83
4.4.1.2 Steel 85
4.4.1.3 CPVC 87
4.4.1.4 Adhesive 90
4.4.2 Bonded Specimens 91
4.4.2.1 Specimen 1 (Adhesive thickness of 80 mils) 92
4.4.2.2 Influence of Boundary Condition 102
4.4.2.3 Development of a Finite Element Model 103
4.4.2.4 Influence of End Restraints and Plate Geometry ... 114
4.4.2.5 Specimen 2 (Adhesive thickness of 50 mils) 116
4.4.2.6 Specimen 3 (Adhesive thickness of 30 mils) 124
4.4.2.7 Effect of Adhesive Thickness 129

5.0 Summary and Conclusions 136

5.1 Summary 136
5.2 Conclusions 137
5.3 Future Research 141

References 142

Appendices 146

Appendix A 147
Appendix B 151
Appendix C 153

List of Tables

Page

3.1 CPVC Environmental Exposure Test Matrix A 21

3.2 SS340 Environmental Exposure Test Matrix A 22

3.3 CPVC Environmental Exposure Test Matrix B 23

3.4 SS340 Environmental Exposure Test Matrix B 24

3.5 Lap Shear Environmental Exposure Test Matrix A 37

3.6 Lap Shear Environmental Exposure Test Matrix B 37

3.7 Lap Shear Environmental Exposure Test Matrix B Salt 38

4.1 Summary of CPVC Control Specimens 48

4.2 Test I-B: Average Strength and Stroke Values for CPVC Specimens 57

4.3 Test I-B: Strength and Stroke Changes from Water to Salt-water Soaking for CPVC Specimens 57

4.4 Summary of SS340 Control Specimens 59

4.5 Test I-B: Average Strength and Stroke Values for SS340 Specimens 66

4.6 Test I-B: Strength and Stroke Changes from Water to Salt-water Soaking for SS340 Specimens 66

4.7 Summary of Control Specimens for Lap Shear Group A: Post-Cured and Non-Post-Cured 68

4.8 Summary of Control Specimens for Lap Shear Group B: Post-Cured and Non-Post-Cured Averages 69

4.9 Summary of Control Specimens for Lap Shear Group B 71

4.10 Material Properties used in the Finite Element Model 105

4.11 Input Surface Temperatures of Finite Element Model 106

4.12 Strain Results of Finite Element Model 111

4.13 Strain Comparisons of 3 Finite Element Models …… 115

4.14 Shear Strain Relationships …….. 135

A.1 Test I-A: CPVC Tabulated Results …….. 147

A.2 Test I-B: CPVC Tabulated Results ……. 148

A.3 Test I-A: SS340 Tabulated Results ……. 149

A.4 Test I-B: SS340 Tabulated Results ……. 150

B.1 Test II-A: Lap Shear Tabulated Results …….. 151

B.2 Test II-A: Lap Shear Tabulated Results …….. 152

List of Figures

Page

2.1 Bleach Tank ……..……... 7

2.2 CPVC Tensile Strength vs. Temperature …… 11

2.3 Titanium Silicate Coefficient of Thermal Expansion ……. 16

3.1 CPVC Unstressed Tension Specimen ……. 18

3.2 CPVC Stressed Tension Specimen ……. 19

3.3 Cutting SS340 Specimens ……... 20

3.4 Measuring SS340 Specimens ……..…... 20

3.5 SS340 Unstressed Tension Specimen ……..……... 20

3.6 SS340 Stressed Tension Specimen ……..... 20

3.7 Galvanizing J-Bolts for Environmental Exposure Setup …….……... 26

3.8 Inserting J-Bolts into Caps …….. 26

3.9 Bolts and Caps Secured …….. 26

3.10 Tubes Sealed onto Caps ……...…….... 27

3.11 Heater and Thermostat ……..... 27

3.12 Damaged Heaters ……..... 27

3.13 Heater, Thermostat and Specimen in Plastic Top ……... 28

3.14 Environmental Exposure Test Setup ……... 29

3.15 Side and Top Views of Detail A of the Loading Systems ……...……... 29

3.16 Initial 1/8” CPVC Double Lap Shear Specimen ……..…... 32

3.17 Cutting CPVC Sheets ……...……... 33

3.18 Drilling Anchorage Holes ……... 33

3.19 Environmental Exposure Lap Shear Specimen A Configuration …… 34

3.20 Environmental Exposure Lap Shear Specimen A ……... 35

3.21 Taped CPVC Tabs ……... 35

3.22 Specimens in Plywood Slots ……... 35

3.23 Environmental Exposure Lap Shear Specimen B Configuration …… 35

3.24 Hand Sanding Steel Tabs ……... 36

3.25 Clamping Specimens ……..…... 36

3.26 Cross Section of Thermal Gradient Specimen …… 41

3.27 Attached Stain Gages …….. 41

3.28 Finished Strain Gages …….. 41

3.29 Test Bath Cross Section …….. 42

3.30 Top View of Open Test Bath …….. 42

3.31 Test Bath with Cover …….. 43

3.32 CPVC Plate on Bath ……..….. 43

3.33 Precision Oven with CPVC, Titanium Silicate, and Steel Specimens ...… 44

3.34 Test Setup for Adhesive Specimens …….…….. 44

3.35 Steel and Ti Silicate ……..….. 45

3.36 Titanium Silicate ……..…….. 45

4.1 Results of CPVC Control Specimens …….. 48

4.2 Test I-A: Measured Strength of CPVC Specimens ……..…….. 50

4.3 Test I-A: Measured Stroke at Failure of CPVC Specimens …….…….. 50

4.4 CPVC 2nd Specimen at 140°F and Varied Induced Stress …….. 51

4.5 CPVC 1st Specimen at 73°F and Varied Induced Stress ……...…….. 52

4.6 CPVC 2nd Specimen at 180°F and Varied Induced Stress …….. 52

4.7 Pre-test CPVC Specimens …….. 53

4.8 Post-test CPVC Specimens ……. 53

4.9 Test I-B: Measured Strength of CPVC Specimens Soaked in Water …….. 54

4.10 Test I-B: Measured Strength of CPVC Specimens Soaked in Salt-water …….. 54

4.11 Test I-B: Measured Stroke at Failure of CPVC Specimens Soaked in Water …….. 55

4.12 Test I-B: Measured Stroke at Failure of CPVC Specimens Soaked in Salt-water ……... 56

4.13 Results of SS340 Control Specimens ……. 58

4.14 Test I-A: Measured Strength of SS340 Specimens ……. 60

4.15 Test I-A: Measured Stroke at Failure of SS340 Specimens …..……. 60

4.16 SS340 1st Specimen at 0% Induced Stress and Varied Temperature …….. 62

4.17 Pre-test SS340 Specimens ……... 62

4.18 Post-test SS340 Specimens ……...…….. 62

4.19 Test I-B: Measured Strength of SS340 Specimens Soaked in Water …….. 63

4.20 Test I-B: Measured Strength of SS340 Specimens Soaked in Salt-water …….. 63

4.21 Test 1B: Measured Stroke at Failure of SS340 Specimens Soaked in Water …….. 64

4.22 Test I-B: Measured Stroke at Failure of SS340 Specimens Soaked in Salt-water …….. 65

4.23 Control Specimens for Lap Shear Group A: Post-Cured and Non-Post-Cured ……..……. 68

4.24 Control Specimens for Lap Shear Group B: Post-Cured and Non-Post-Cured ……..……. 69

4.25 Control Specimens for Lap Shear Group B ……...…. 70

4.26 Test II-A: Lap Shear Days Survived …….……. 72

4.27 Instron Lap A …….……. 72

4.28 Typical Lap A Cohesive Bond Failure ……... 72

4.29 Typical Lap A Adhesive Bond Failure ……... 73

4.30 Test II-A: Lap Shear Strength ……..... 73

4.31 Test II-A: Lap Shear Stroke Displacement at Failure …….…... 74

4.32 Test II-B: Lap Shear Days Survived ……... 75

4.33 Instron Lap B ……..……..... 76

4.34 Typical Lap B Cohesive Bond Failure ……... 76

4.35 Typical Lap B Adhesive Bond Failure in Environmental Test …….. 77

4.36 Typical Lap B Adhesive/Cohesive Bond Failure …….…... 77

4.37 Test II-B: Lap Shear Strength ……..…... 78

4.38 Test II-B: Lap Shear Max Stroke Displacement at Failure ……..... 78

4.39 Corroded Salt Specimens Prior to Failure ……... 80

4.40 Typical Lap B Salt Cohesive Failure …….. 81

4.41 Test II-B Salt: Strength ……..……. 81

4.42 Test II-B Salt: Displacement ……..... 81

4.43 Titanium Silicate Oven and Bath Data ……... 84

4.44 Titanium Silicate Combined Data ……... 84

4.45 Coefficient of Thermal Expansion of Steel …….……... 86

4.46 Typical Steel Plate Thermal Expansions …….……... 87

4.47 Coefficient of Thermal Expansion of CPVC in the X-Direction …… 88

4.48 Coefficient of Thermal Expansion of CPVC in the Y-Direction …… 89

4.49 Typical CPVC Plate Thermal Expansions ……..… 90

4.50 Coefficient of Thermal Expansion of SS340 Adhesive ……..… 91

4.51 Typical Temperature Gradient …..……..... 92

4.52 Measured Steel Strain of Specimen 1 …..……..……..... 93

4.53 Measured CPVC Strain of Specimen 1 …..……..... 94

4.54 Strain Behavior of Specimen 1 in X-Direction …..……..... 96

4.55 Strain Behavior of Specimen 1 in Y-Direction …..……..... 96

4.56 Strain Profile for Specimen 1 at 40 min in the X-Direction …….... 98

4.57 Strain Profile for Specimen 1 at 40 min in the Y-Direction …….... 98

4.58 Strain Profile for Specimen 1 at 80 min in the X-Direction …….... 99

4.59 Strain Profile for Specimen 1 at 80 min in the Y-Direction …….... 99

4.60 Strain Profile for Specimen 1 at 100 min in the X-Direction …….. 100

4.61 Strain Profile for Specimen 1 at 100 min in the Y-Direction …..……... 100

4.62 Strain Profile for Specimen 1 at 120 min in the X-Direction …..……... 101

4.63 Strain Profile for Specimen 1 at 120 min in the Y-Direction …..……... 101

4.65 Strain Behavior of Specimen 1 in the X-Direction
using the Roller Supports ……..…….. 102

4.66 Strain Behavior of Specimen 1 in the Y-Direction
using the Roller Supports ……..…….. 103

4.67 Finite Element 3-D Model ……..……..…….. 105

4.68 Deformed Shape of FE Model ……..…….. 106

4.69 FEM Strain Distribution for Steel Top in Long Direction ……..... 107

4.70 FEM Strain Distribution for Steel Top in Short Direction ……..…….. 108

4.71 FEM Strain Distribution for Steel Bottom in Long Direction ……..…... 108

4.72 FEM Strain Distribution for Steel Bottom in Short Direction ……..... 109

4.73 FEM Strain Distribution for CPVC Top in Long Direction …….... 109

4.74 FEM Strain Distribution for CPVC Top in Short Direction …….... 110

4.75 FEM Strain Distribution for CPVC Bottom in Long Direction ……..…... 110

4.76 FEM Strain Distribution for CPVC Bottom in Short Direction ……...…... 111

4.77 Steel Strain Behavior of Specimen 1 in X-Direction …...……... 112

4.78 Steel Strain Behavior of Specimen 1 in Y-Direction …...……... 112

4.79 CPVC Strain Behavior of Specimen 1 in X-Direction …...……..…….. 113

4.80 CPVC Strain Behavior of Specimen 1 in Y-Direction …...……. 113

4.81 Deformed Shape of Finite Element Model 2 …...……... 115

4.82 Deformed Shape of Finite Element Model 3 …...…….…..... 116

4.83 Strain Behavior of Specimen 2 in X-Direction …...……..... 117

4.84 Strain Behavior of Specimen 2 in Y-Direction …...…….…... 117

4.85 Strain Profile for Specimen 2 at 40 min in the X-Direction …….... 119

4.86 Strain Profile for Specimen 2 at 40 min in the Y-Direction …….... 120

4.87 Strain Profile for Specimen 2 at 80 min in the X-Direction …….... 120

4.88 Strain Profile for Specimen 2 at 80 min in the Y-Direction …….... 121

4.89 Strain Profile for Specimen 2 at 100 min in the X-Direction ……..... 122

4.90 Strain Profile for Specimen 2 at 100 min in the Y-Direction ……..…... 122

4.91 Strain Profile for Specimen 2 at 120 min in the X-Direction ……..... 123

4.92 Strain Profile for Specimen 2 at 120 min in the Y-Direction ……..…... 123

4.93 Strain Behavior of Specimen 3 in X-Direction ……... 125

4.94 Strain Behavior of Specimen 3 in Y-Direction ……..... 125

4.95 Strain Profile for Specimen 3 at 40 min in the X-Direction ……... 127

4.96 Strain Profile for Specimen 3 at 80 min in the X-Direction ……... 127

4.97 Strain Profile for Specimen 3 at 100 min in the X-Direction ……...……... 128

4.98 Strain Profile for Specimen 3 at 120 min in the X-Direction ……...…... 129

4.99 Strain Profile for Specimens at 40 min in the X-Direction ……...…... 130

4.100 Strain Profile for Specimens at 40 min in the Y-Direction ……...…... 130

4.101 Strain Profile for All Specimens at 80 min in the X-Direction ……... 131

4.102 Strain Profile for All Specimens at 80 min in the Y-Direction ……... 131

4.103 Strain Profile for Specimens at 100 min in the X-Direction ……... 132

4.104 Strain Profile for Specimens at 100 min in the Y-Direction ……... 133

4.105 Strain Profile for Specimens at 120 min in the X-Direction ……... 133

4.106 Strain Profile for Specimens at 120 min in the X-Direction ……... 134

C.1 Measured Steel Strain of Specimen 2 …...……..…… 153

C.2 Measured CPVC Strain of Specimen 2 …...…… 153

C.3 Measured Steel Strain of Specimen 3 …...……..…… 154

C.4 Measured CPVC Strain of Specimen 3 …...…… 154

C.5 Time vs. Strain of Specimen 1 in Long Direction …...…… 155

C.6 Time vs. Strain of Specimen 1 in Short Direction …...…… 155

C.7 Time vs. Strain of Specimen 2 in Long Direction …...…… 156

C.8 Time vs. Strain of Specimen 2 in Short Direction …...…… 156

C.9 Time vs. Strain of Specimen 3 in Long Direction …...…… 157

C.10 Time vs. Strain of Specimen 3 in Short Direction …...…… 157

1.0 Introduction

1.1 Background

Environmental conditions and corrosive environments can significantly reduce the service life of a tank. Tank linings and coatings have been used for decades to extend the service life of tanks to avoid replacing of the damaged tanks. Adhesively bonded tank linings continue to play an increasingly vital role in tank applications. The use of fiber reinforced polymers (FRP) has garnered much of the attention for tank lining materials. However, thermoplastic sheet linings have also shown much promise as they offer excellent corrosive resistance and low cost installation. The proposed thermoplastic tank lining material used in this study is Chlorinated Polyvinyl Chloride (CPVC). It has excellent chemical resistance and has been shown to endure thermal conditions up to 180°F. As with all designs, the connection method of the lining to the tank wall is critical. The connection method is typically achieved by adhesive bonding. It acts not only as a connection, but as a buffer between the two surfaces or sometimes a series of layered materials. Therefore, the demands required of the adhesive are usually extreme for most service conditions. When subjected to cyclical heating and cooling conditions, the demands become much more complex due to the differences in coefficients of thermal expansion for the various materials. The primary objective of this research is to understand the behavior of the various materials proposed for lining typical bleach tanks used in the pulp and paper industry. Cyclical heating environment, along with corrosiveness of the chlorine dioxide bleaching agent, presents considerable challenges to the proposed tank lining. This thesis research program provides extensive analysis for

some of the complexities facing the adhesive/CVPC tank liner and offers general guidelines to their composite behavior.

The adhesive supplied in this program is currently used by industry for bonding composites, metals, and other plastics. As described by the manufacturer, the adhesive consists of a two-component methacrylate adhesive, ideal for a variety of applications since it requires minimal surface preparation and excellent environmental resistance. In addition, the working time is sufficiently high and ranges between 38 to 55 minutes. This characteristic is particularly beneficial for their applications to large surface areas. A functional cure time of 80 percent typically occurs within 4 hours for thin film applications.

1.2 Objective

The main goal of this research program is to determine the properties of the adhesive material, chlorinated polyvinyl chloride (CPVC) material, the bond characteristics under the effect of severe environmental conditions typical to tank lining systems. The specific objectives can be summarized as follows:

1. Investigate the effect of severe environmental conditions on the performance and the fundamental characteristics of the adhesive and CPVC materials.
2. Evaluate the engineering properties and bond characteristics of steel-to-CPVC adhesive bonds proposed for tank-lining applications
3. Examine the thermal gradient of the proposed tank lining cross-section.

1.3 Scope

As outlined by the three objectives, the research program consists of three phases. Phase I observes the environmental effect on tensile strength of CPVC and SS340 adhesive. The two materials were evaluated under various environmental conditions including temperature and sustained stress, as well as time and soaking solution. Phase II examines the bond characteristics of SS340 adhesive for steel-to-CPVC surfaces. Specimens were exposed to environmental conditions including temperature and sustained stress. Phase III investigates a cross-section of the proposed steel tank with an adhesively bonded CPVC lining. A small-scale model was constructed to determine the thermal gradient distribution and composite interaction resulting from temperature changes. In addition, finite element modeling was conducted to verify the measured results.

The research findings are presented in five chapters in the following order:

- Chapter 1 provides an introduction to the experimental program.
- Chapter 2 presents an overview of adhesive and CPVC materials in relation to tank lining applications. The chapter summarizes current research findings in relation to the various topics, including the coefficient of thermal expansion. In addition, possible future research requirements are discussed.
- Chapter 3 discusses the experimental program undertaken in this study. The procedural methodology is presented, including specimen design, test setups, and test matrices.

- Chapter 4 summarizes test results of the experimental program. For each phase, detailed analysis with emphasis on the overall significance of the results is discussed.
- Summary and conclusions of the test results are given in Chapter 5.
- Appendices A, B, and C are used to summarize additional tables and figures not included in Chapter 4.

2.0 Literature Review

2.1 Introduction

Adhesives are increasingly being used in a variety of engineering applications today. As research efforts from scientists and engineers continue, the potential seems boundless for adhesive utilization. Many researchers who have been studying adhesives for some time can see the progress made from its beginnings. The advent of glue production occurred in the late 1600's and consisted of animal and vegetable components. Modern adhesive production did not occur until the early 1900's when synthetic polymers became the forefront, which included the "landmark" discovery of epoxy resins (Fay 2005). In terms of future trends, researchers agree in predicting that the market for adhesives will continue to grow in all types of manufacturing (Comyn 2005a). Companies specializing in adhesive research have the ability to tailor adhesive products to maximize specific performance requirements for each application (Air Products). Kanderakis states that adhesive uses "offer remarkable advantages such as mechanical efficiency, repair time, cost reduction, high structural integrity, repair inspectability, damage tolerance..." (2003). In addition, adhesives are lightweight and able to resist corrosion, both of which make it an attractive solution for building materials (Ewerszumrode 1998).

Adhesives are broadly defined as a material that joins surfaces together to resist separation (Comyn 2005a). As with most adhesive applications, the critical factor, especially in with structural adhesives, is to "resist separation." No only are an adhesive's resistive properties important, but must be employed in conjunction with satisfactory, bondable materials. Composites and plastics appear to be at the forefront of

adhesive applications due to the versatility and increased demand of these various materials. Additionally, popular alternative materials, such as fiberglass-reinforced plastic (FRP), must utilize adhesive bonds for connections since traditional connections would compromise the material fibers and performance. A proven and still growing field for composite and plastic applications is found in tank and vessel linings.

The standard application for adhesively-bonded sheet linings is in conjunction with steel tanks (Zarnitz 2002). Almost always, the lining is used to protect the steel from a corrosive environment or solution in the tank, but in some cases, a lining can be used to protect the solution from being corrupted by the steel surface (Skabo 1987). Often, the demands of a tank and lining system can be extremely challenging from an engineering standpoint. Some common demands are as follows:

- Endure various combinations and concentrations of chemicals.
- Tolerate extreme temperature changes for the exposed interior surface as well as the wall cross-section. This includes thermal shock.
- Withstand seasonal temperature changes and weather effects for the exterior surface since most tanks must be positioned outdoors.
- Resist internal or external physical abuse.
- Increase operation, add value, and provide low maintenance.

(Zarnitz 2002). Although this list outlines a wide-range of challenges for the tank and tank lining, ultimately, the tank linings are employed to extend the life of the tank. The designed life for a tank can vary from 20 to 30 years, but some may only last five years

(Sumbry 1990). These premature failures can have a profoundly negative effect on a company's production and costs.

Well documented history of tank linings are found in petroleum storage and production. In particular, the storage tank bottoms have proven to be the most susceptible to corrosion. FRP linings have proven to be extremely effective to resist corrosion and extend service life of the petroleum storage tank bottom (Bogner et al. 1993).

Another key area of tank linings occurs in the pulp and paper industry. Two tank types utilized by the pulp and paper industry are bleach towers and chlorine dioxide (ClO_2) solution storage tanks. A photograph displaying lined bleach towers under construction is shown in Figure 2.1 (Stebbins n.d.). As generally discussed earlier, the demands placed on tank linings can be very severe. Pulp and paper tank linings are considered to be one of the most demanding applications in industry due to the following conditions:



Figure 2.1 – Bleach Tank

- Corrosive chemicals
- Elevated temperatures
- High flow rates and continuous agitation
- Thermal shock and shut-down cycling, which can be especially detrimental to the system in winter months

Conventional tank linings are constructed of glazed tiles. Although resistant to the corrosive environment, the performance of glazed tiles have been less than adequate due to effects of thermal shock, impact forces, and problematic tile adherence (Ford et al. 1995). Additional details and developments of chlorine dioxide tank linings will be discussed shortly.

2.2 Structural Adhesives

In addition to properties mentioned earlier, another valuable aspect of using adhesive bonds is its ability to transfer loads over a large area (Kim et al. 1999). This can play a major factor in design considerations when comparing adhesive versus mechanical joints. Additional key factors must be considered before moving forward with an adhesive design. Such factors include surface preparation of the adherents, environmental effects, and application specific forces.

Selecting the right surface preparation, or pretreatment, is essential to achieving adequate performance during service conditions. In addition, proper application of the adhesive is directly related to the performance (Watts 2005). A rough and uncontaminated surface is critical to maximize the adhesive bond. Pretreatment is divided into two groups, physical and chemical methods, which are frequently used tandem to create ideal performance. For moderate bond requirements, physical methods may be adequate. These consist of degreasing, abrasion, and sand blasting of metal substrates. For more severe conditions, such as water exposure or high stresses, chemical treatments may be crucial. In the case of mild steel, sand blasting in combination with saline is a suggested combination of pretreatments. As a general rule, polymers have lower bond strength than metals due to

their “surface energies” being lower. Three major factors influence the ability of a substrate for bonding: surface mechanical strength, topography, and surface chemistry. Chemical preparation methods can influence all three factors, while mechanical methods only influence two, surface strength and topography. It is interesting to note that adhesives can be created to absorb weak surface layers which would increase mechanical strength. Most joint strengths are high at the outset, but as service time progresses, a careful selection of pretreatments becomes all the more important (Brewis 2005). New research has been directed to discover less complex and time-consuming surface treatments for easier adhesive application in the field. This also includes surface treatments built into the adhesive itself (Comyn 2005b).

Preparation methods are essentially selected and highly dependent on the nature of the environmental conditions. Environmental factors that may have an adverse effect on the adhesive joints include, but are not limited to humidity, water, salt water or spray, temperature, stress, oxygen, and UV. Water can be a significant hindrance in limiting the use of adhesives for two reasons. First, it is absorbed by the adhesive and can alter its properties. Secondly, the more extreme effect is water attacking the adhesive interface. The decrease in bond strength is directly related to water diffusion, which conforms to the Arrhenius equation:

$$k = Ae^{\frac{-E_A}{RT}} \tag{2.1}$$

where k is the rate constant, A is the frequency factor, e is 2.71828, E_A is the activation energy, R is the gas constant, and T is the absolute temperature in degrees Kelvin. This equation shows that the diffusion of water increases rapidly due to a temperature rise,

which does not bode well for adhesives subjected to high temperatures (Comyn 2005b). Thermal expansion mismatches between the adhesive and substrates must also be considered because thermal cycling will cause fatigue in the bond (Comyn 2005a). Comyn found conclusive data in salt water testing showed that by subjecting adhesive joints to a 5% salt spray for a period of three months was "more damaging than exposure to semi-tropical conditions for three years." Research has also proven that joint strength decreases over time due to stressed conditions (2005b). Clearly, environmental effects coupled with surface preparations present a challenging field of research in adhesives.

2.3 CPVC

Chlorinated polyvinyl chloride (CPVC), like PVC, is most commonly used for piping applications. However, CPVC is much more versatile and can be used in a wide range of applications because of its attractive properties and for economical reasons. For an anisotropic, thermoplastic material, it provides a unique combination of corrosion and chemical resistance and high mechanical strength. In addition, CPVC is a cost effective material with easy installation, low maintenance, and excellent workability. It can resist a wide variety of chemicals, which includes most mineral acids, bases, salts, and aliphatic hydrocarbons (Ambler 1996). The material data sheet for CPVC ensures operability at temperatures near 180°F as shown in Figure 2.2 (Corzan n.d.-b). The initial tension strength at room temperature drops by nearly 75% when heated to 180°F. Of the thermoplastic material family, CPVC boasts the lowest coefficient of thermal expansion (Ambler 1996). However, the thermal expansion coefficient of the CPVC material is six times that of mild steel. As an additional limitation, CPVC's mechanical strength is not sufficient for large structures or vessels, but must be used in conjunction with stronger

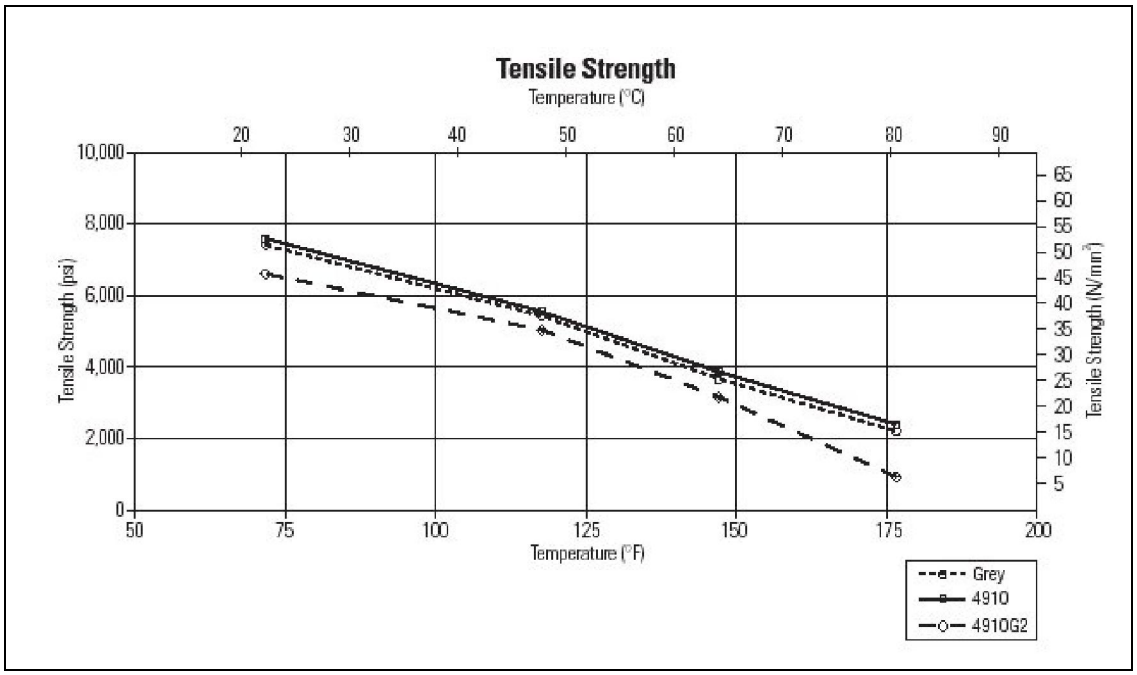

Figure 2.2 – CPVC Tensile Strength vs. Temperature

materials (Habib 1998). For a steel tank lining application, this will not be an issue. Primary concerns are CPVC's performance and interaction with the adhesive and steel at elevated temperatures. In addition, its chemical resistance to chlorine dioxide is essential.

2.4 Chlorine Dioxide

Chlorine dioxide (ClO_2) is an effective disinfectant and oxidizer. It is also used in water treatment applications where it purifies surface waters having odor or taste problems. In more recent years it has become the principal bleaching agent in the pulp and paper industry. Chlorine dioxide minimizes environmental effects as opposed to other bleaching agents, such as chlorine, which can affect the local aquatic life. Though environmentally friendly, ClO_2 can be quite dangerous. It is so highly reactive that transporting the chemical is unlawful; it must be produced on site with a chlorine dioxide generator (Lenntech). At concentrations above 10%, ClO_2 gas will undergo spontaneous

decomposition. In liquid and solid forms, ClO_2 is extremely unpredictable such that explosive decompositions can occur. Optimum control and monitoring of the substance must be achieved in order to safely use chlorine dioxide as a bleaching agent in the pulp and paper industry (Currier 2002).

2.5 Tank Lining Systems

Selecting the right tank lining is fundamentally important for any application. Proper selection severely affects the ability to provide the required protection needed at service conditions. The typical resources that exist to help the designers select the system are published data, including the manufacturers' recommendations, experience based on measured performance, and test studies. The key in utilizing published recommendations is that the previous test data must match the anticipated service conditions. Even though these references are usually reliable, careful consideration must be made before applying these results to a proposed application (Skabo 1987). For a successful tank lining to be effective against corrosion, selecting the right adhesive and reinforcement materials is critical. In addition, surface preparation and suitable application techniques will contribute to the primary goal, which is extending the service life (Bogner et al. 1993).

Tank lining can fall into one of five categories: elastomers, cementitious, organic resins, metallic, and inorganic masonry. Organic resins are nearly unlimited, especially when used in conjunction with inorganic reinforcement materials, such as silica sand or glass fibers. Resins offer the widest selection when faced with resisting chemical environments. Types include but are not limited to epoxy, coal-tar, urethane, polyester, and vinyls. CPVC linings fall under the vinyl category of these organic resins. Skabo

suggests that with a sheet-applied thermal plastic, such as CPVC, a woven cloth is typically used to increase the adhesive bond to the steel substrate. Seams at the sheet junctures are then thermally welded (1987). In the case of CPVC joint welding is accomplished by using a primer and solvent cement. Most liner failures occur due to chemical or moisture seepage through the joints or pipe seal junctures. In addition, roof failures have been known to occur (Sumbry 1990).

Though incidents are rare, releases of ClO_2 have been reported in the pulp and paper industry due to mechanical damage of the storage tanks or due to explosions tanking place. Many of the new ClO_2 tanks are made of fiber-reinforced plastic and have innovative designs, such as a floating roof, to limit damage produced by a possible explosion (Hitztorth et al. 2000). For metal tanks, costly alloys or stainless steels must be used to resist the corrosive environment (Bergquist et al 1996). However, because mild steel is much cheaper, adding a corrosive resistant liner to protect the steel can be an effective and economical solution (Skabo 1987).

According to research findings by Habib, CPVC has excellent resistance up to 80^oC (182^oF) when exposed to chlorine dioxide. For corrosive environments, the use of a "dual laminate composite" composed of a thermoplastic lining, such as CPVC, and FRP structure has proven to be successful. In this application, the FRP replaces the steel tank, instead of retrofitting an existing steel tank with a thermoplastic lining. Proper care and design must be administered to accommodate the anisotropic nature of the composite

tank. Thicknesses the FRP is primarily designed to a factor of safety of 10, which will guarantee low stresses and strains of the structure (1998).

2.6 Effect of Environmental Exposure to Adhesives

Environmental exposure effects of materials, and in particular adhesives, present a challenging and highly complex matter to engineers and researchers. These effects are divided into three categories: they may alter the adhesive, alter the adhered, or affect the bond interface. For adhesive effects, increased plasticization occurs when temperature is increased or moisture is absorbed. The result is a decline in both the modulus and ultimate failure load. Strain and fracture toughness tend to rise simultaneously. Therefore, the likelihood of a brittle failure will decrease, while the likelihood of a creep-fatigue failure will increase. Studies show that high temperature exposure in dry conditions does not affect the failure load. Conversely, the same temperature exposure in wet conditions produces a considerable reduction in strength. For high temperature conditions reaching 180°F or more, the failure is considered "creep enhanced" for a continuously loaded lap-shear specimen (Ashcroft 2005). Mentioned previously, the Arrhenius equation can be invoked for further understanding of temperature and water effects.

2.7 Effect of Varying Coefficients of Thermal Expansion of the Liner

Researchers are working actively to gain a better understanding in the area of bonded specimens of varying materials. Because the materials and the adhesive employed in most bonding situations vary, the coefficients of thermal expansion (CTE) will vary. Therefore, the comparative effects of the movements must be found. Ewerszumrode and Hahn admit it is difficult to apply predictions to an adhesive's CTE effects since material

properties and joint geometry will almost always lack conformity. However, the authors conclude with a few definite result of their study that can be applied broadly. Tests indicated that in all cases relative movement of the adherents during bonding decreases the bond strength. It is also critical to not allow any slippage while curing. Another commonsensical conclusion states that the adhesive bond strength and slip capability will deteriorate the larger the disparity in the adherent and adhesive CTEs (1998). In most cases CTE effects must be studied on a case by case basis. Results can be modeled effectively by using finite element analysis with known material properties (Kanderakis et al. 2003).

CTE measurements using strain gages must be made using the same set of gages on the desired material and a material with a known expansion coefficient. This is necessary because strain gages are designed to temperature compensate for the material being tested, which means a thermal change would ideally produce zero strain in a steel specimen, for example. Titanium silicate glass has such a small CTE that it is an ideal baseline material. Figure 2.3 shows the CTE relationship of titanium silicate for a temperature range of 0 to 150°C. As temperature increases during testing, strain gage results from the titanium silicate produces a negative output, which in turn is subtracted from the steel's strain gage output at corresponding temperatures. Therefore, subtracting the negative values from the titanium silicate to the steel will in fact add to or increase the strain values of the steel specimen. Data for other materials can be correlated in the same manner. For more accurate CTE results, temperature and strain recordings should only be recorded after a dwell time of at least 45 minutes for each temperature stage. This

ensures equilibrium of the strain and temperature has been met. Measurement recordings during a steady increase or decrease in temperature will produce marginally unreliable results (Vishay TN-513).

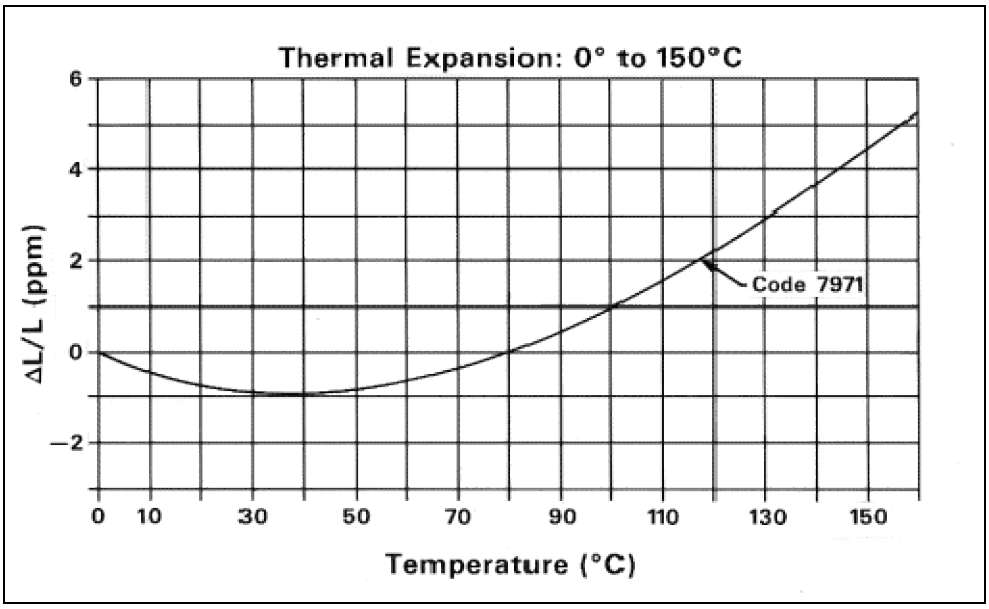

Figure 2.3 – Titanium Silicate Coefficient of Thermal Expansion

3.0 Experimental Program

3.1 Introduction

The program investigates the behaviour and material characteristics of IPS Weld-On® Structural Adhesive 340 (SS340) and Chlorinated Polyvinyl Chloride (CPVC) subjected to environmental conditions. Research findings will be used to develop a CPVC-lining for steel tanks typically used in the pulp bleaching phase of paper-making factories. The findings are not limited to this application alone and will be used for better understanding of SS340 in future industrial applications. The experimental program was conducted at the Constructed Facilities Laboratory at North Carolina State University in collaboration with the research facilities at IPS Corporation in Durham, North Carolina.

3.2 Overview

The experimental program consisted of three phases, which included: 1) Environmental Effect on Tension Strength of CPVC and SS340, 2) Bond Characteristics of SS340 Adhesive for Steel-to-CPVC Surfaces and 3) Thermal Gradient of the tank lining.

3.3 Phase I: Environmental Effect on Tensile Strength of CPVC and SS340

The first phase of the experimental program focused on evaluation of the tensile strength of the two materials under various environmental conditions. The main objective is to determine the effect of environmental conditions such as temperature, induced stress, soaking solution, and time. In order to accomplish this objective, the testing incorporated two sub-phases, A and B. Phase A varied the stress levels and temperatures, while the Phase B included additional variables of exposure time steps and salt water soaking.

3.3.1 Specimen Preparation

Specimens were prepared and tested in accordance to ASTM D 638 – 03, *Standard Test Method for Tensile Properties of Plastics.* CPVC tension specimens were fabricated according to Type I dimensions, and SS340 specimens were fabricated according to Type IV dimensions. Both CPVC and SS340 stressed specimens required adjustments in order to be conformed into the existing environmental exposure test setup.

3.3.1.1 CPVC Specimen Preparation

A 1/8" thick CPVC sheet was machined into ASTM 638 Type I specimens, as shown in Figure 3.1. These specimens were used for the unstressed portion of the environmental testing. 5/8" thick anchorage holes were drilled at each end. Figure 3.2 illustrates the dimensioned, stressed specimens, which have two 3.75" x 1" and 1/16" thick aluminum tabs at each end to strengthen holes for the tension-loaded specimens in the environmental exposure test. These tabs were bonded using SS340 adhesive. In the 2.25" testing section, specimen thicknesses and widths were measured in three places with calipers. The numbers were recorded and averaged to produce the specimen cross-sectional area. The areas were used throughout the testing process to determine the stress on each individual specimen.

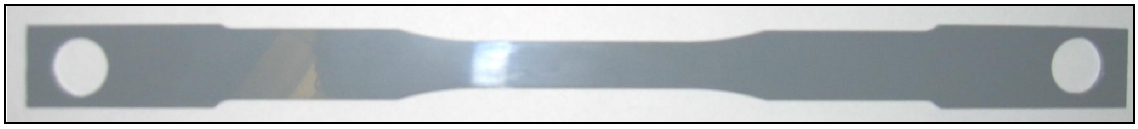

Figure 3.1 CPVC Unstressed Tension Specimen

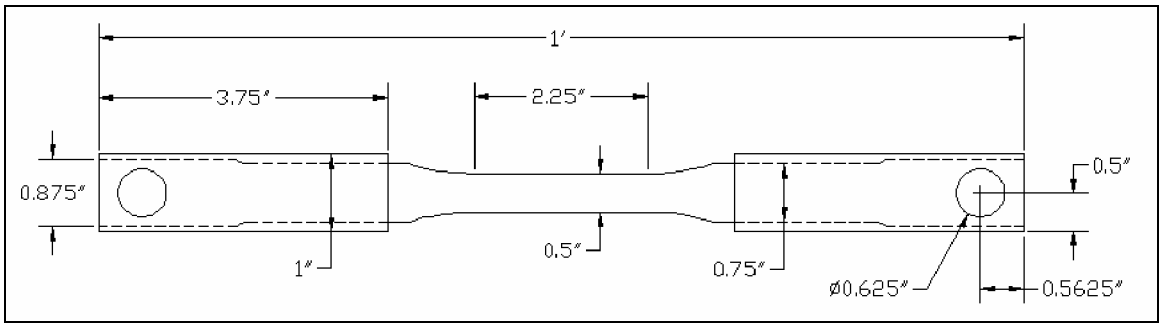

Figure 3.2 CPVC Stressed Tension Specimen

3.3.1.2 SS340 Specimen Preparation

In collaboration with IPS, 1/8" thick SS340 plates were produced to fabricate the test specimens. The two-component methacrylate adhesive has a Part A adhesive and a Part B (SS605B) activator requiring a 10:1 mix ratio. The two part adhesive was dispensed out of a 10:1 ratio canister using a pneumatic gun attached with a mixing nozzle. The adhesive was sandwiched by two 18" x 18" glass plates that were protected by vellum sheets. The glass had 1/8" spacers at each corner and weighted by a 20 lb bucket to produce even spreading and thickness. After a minimum 24-hour curing period, the adhesive plates were cut into several specimens using an ASTM 638 Type IV specified dye. The Carver hydraulic hand jack, shown in Figure 3.3, provided the necessary pressure for cutting. Visible bubbles in the adhesive plates were avoided during cutting. Cut specimens found having bubbles in the narrow section were removed from testing consideration. Dog bone specimens were then placed in an oven at 180°F and post-cured for one hour. Specimen thicknesses and widths were then measured in three places along the length with digital calipers, seen in Figure 3.4. The numbers were recorded and averaged to produce the specimen cross-sectional area. Figure 3.5 shows the unstressed specimen after cutting and labeling. Figure 3.6 displays 1/16" thick stainless steel tabs

with 5/8” diameter anchorage holes at each end to lengthen the specimen in order to be integrated into the environmental exposure test for loading. The dimensions of the specimen are also shown here. Tabs were bonded using SS340.



Figure 3.3 Cutting SS340 Specimens

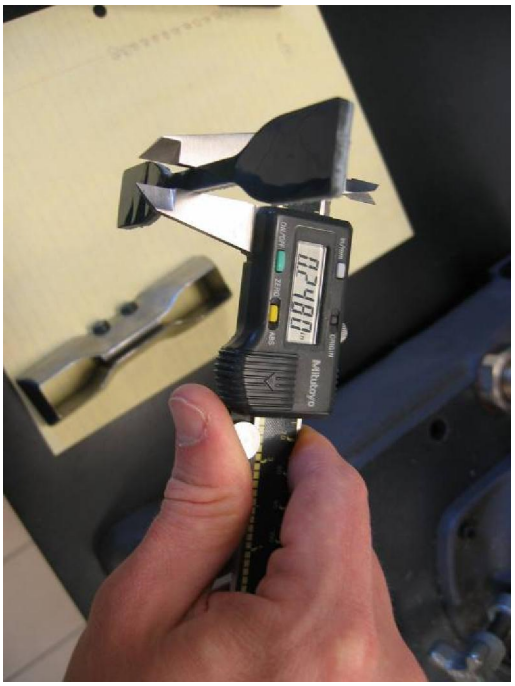

Figure 3.4 Measuring SS340 Specimens



Figure 3.5 SS340 Unstressed Tension Specimen

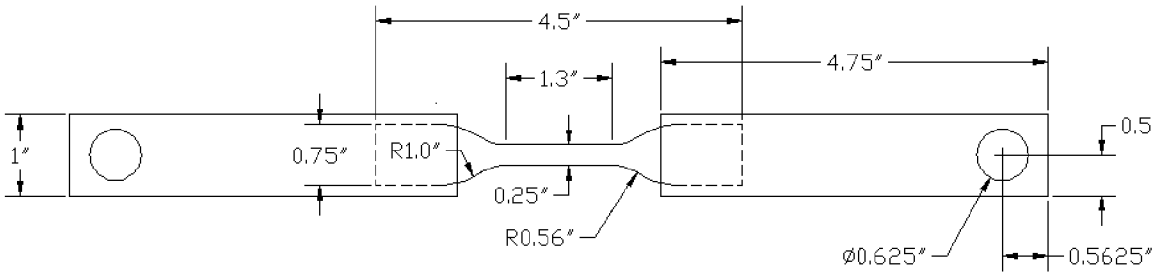

Figure 3.6 SS340 Stressed Tension Specimen

3.3.2 Stress and Temperature Effects on Tensile Strength

The test matrices for environmental exposure tests of SS340 and CPVC specimens were developed and are shown in Tables 3.1 and 3.2. Table 3.1 consists of CPVC specimens, and Table 3.2 consists of SS340 specimens. Five control specimens were used to determine the average ultimate strength of the respective materials. Specimens were placed in the test setup, where the effects of temperature and stress were observed. Two specimens were used at each condition for a total of 18 CPVC and 18 SS340 specimens. The variables tested include:

- Temperatures of 73^0, 140^0, and 180^0F
- Induced sustained stress equivalent to selected percentage of 0, 15, and 30 percent based on ultimate strength of 8000 psi for CPVC and 2100 psi for SS340

For specimens survived 30-day exposure, they were tested to failure using an Instron 8801 Servo-hydraulic Dynamic Testing Machine in order to examine the environmental effect on the material behavior.

Table 3.1 CPVC Environmental Exposure Test Matrix A

Temperature	Selected Percentage	Induced Stress (psi)
T_1 - 73 ^{o}F	0%	0
	15%	1200
	30%	2400
T_2 - 140 ^{o}F	0%	0
	15%	1200
	30%	2400
T_3 - 180 ^{o}F	0%	0
	15%	1200
	30%	2400

Table 3.2 SS340 Environmental Exposure Test Matrix A

Temperature	Selected Percentage	Induced Stress (psi)
T_1 - 73 ^oF	0%	0
	15%	315
	30%	630
T_2 - 140 ^oF	0%	0
	15%	315
	30%	630
T_3 - 180 ^oF	0%	0
	15%	315
	30%	630

3.3.3 Salt Soaking and Time Effects on Tensile Strength

In addition to temperature and the induced stress, Tables 3.3 and 3.4 incorporate soaking solution and time variables into the test matrix. Table 3.3 consists of CPVC specimens, and Table 3.4 consists of SS340 specimens. Five control specimens were used to determine the average ultimate strength of the respective materials. Specimens were placed in the test setup, where the effects of temperature, stress, soaking solution, and time were observed. One specimen was used at each condition for a total of 48 CPVC and 48 SS340 specimens. The variables tested include:

- Temperatures of 73^0, 140^0, and 180^0F (presented in Tables 3.1 and 3.2)
- Induced sustained stress equivalent to selected percentage of 0 and 10 percent based on ultimate strength of 8000 psi for CPVC and 2100 psi for SS340
- Water and 5% NaCl water solution
- Exposure times of 1, 7, 14, and 28 days

Again, for the specimens survived the respective exposure times, the specimens were tested in tension to failure using an Instron 8801 Servo-hydraulic Dynamic Testing Machine in order to examine the environmental effect on the material behavior.

Table 3.3 CPVC Environmental Exposure Test Matrix B

Temperature	Solution	Selected Percentage	Induced Stress (psi)	Soak Time (days)
T_1 - 73 ^oF	Water	0%	0	1
				7
				14
				28
		10%	800	1
				7
				14
				28
	5% NaCl	0%	0	1
				7
				14
				28
		10%	800	1
				7
				14
				28
T_2 - 140 ^oF	Water	0%	0	1
				7
				14
				28
		10%	800	1
				7
				14
				28
	5% NaCl	0%	0	1
				7
				14
				28
		10%	800	1
				7
				14
				28
T_3 - 180 ^oF	Water	0%	0	1
				7
				14
				28
		10%	800	1
				7
				14
				28
	5% NaCl	0%	0	1
				7
				14
				28
		10%	800	1
				7
				14
				28

Table 3.4 SS340 Environmental Exposure Test Matrix B

Temperature	Solution	Selected Percentage	Induced Stress (psi)	Soak Time (days)
T_1 - 73 ^{o}F	Water	0%	0	1
				7
				14
				28
		10%	210	1
				7
				14
				28
	5% NaCl	0%	0	1
				7
				14
				28
		10%	210	1
				7
				14
				28
T_2 - 140 ^{o}F	Water	0%	0	1
				7
				14
				28
		10%	210	1
				7
				14
				28
	5% NaCl	0%	0	1
				7
				14
				28
		10%	210	1
				7
				14
				28
T_3 - 180 ^{o}F	Water	0%	0	1
				7
				14
				28
		10%	210	1
				7
				14
				28
	5% NaCl	0%	0	1
				7
				14
				28
		10%	210	1
				7
				14
				28

3.3.4 Test Setup

In order to execute the environmental exposure test matrices, the load was applied to the test specimens using a specially designed test setup. To study the environmental conditions, the setup allowed for placing each specimen in a CPVC cylindrical container with water, a heater, and a thermostat. These containers were fabricated by securing and sealing J-bolts through a CPVP cap. Because these bolts would be submersed in water they were painted with a zinc-rich primer. Photographs of the spray-painting process and of inserting the J-bolts are shown in Figures 3.7 and 3.8, respectively. The bolts and caps were then secured to wooden 6" x 6" beams located on the basement floor of the lab, as shown in Figure 3.9. CPVC tubes were sealed to the anchored caps, as shown in Figure 3.10, by use of an IPS Corporation CPVC solvent cement. Immersion heaters wired into thermostats were used to control the temperature of the water. Acrylic tops with holes cut out were used to hold the heaters and thermostats in place as well as to minimize evaporation of the water. The heaters and thermostats are shown in Figure 3.11. Over the course of the project, heaters and thermostats were replaced as the highly corrosive environment began damaging the equipment and causing heater failures. The thermostats would fail in the "open" position, causing the heater to ramp up to its maximum temperature. If not detected in time, this would cause the water to boil out and permanently damage the specimen because of the extreme temperature. Thus, several specimens had to be replaced and restarted from the beginning. Figure 3.11 exhibits two damaged heaters, where the outer protective sleeve ruptured due to corrosion. The newer, flanged-top heater is shown resting on the acrylic disc in Figure 3.12. A total of 18 environmental test setups were constructed (Smith 2005).



Figure 3.7 – Galvanizing J-Bolts for Environmental Exposure Setup



Figure 3.8 – Inserting J-Bolts into Caps



Figure 3.9 – Bolts and Caps Secured



Figure 3.10 – Tubes Sealed onto Caps

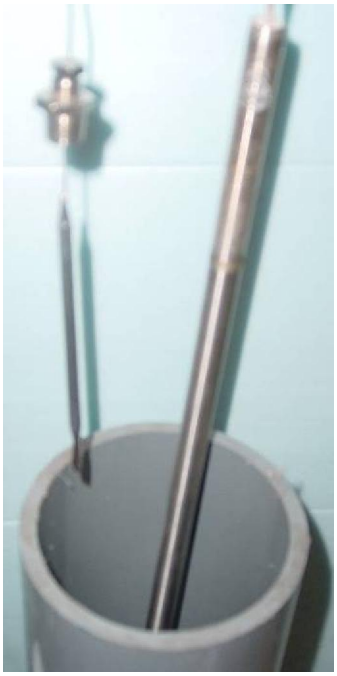

Figure 3.11 – Heater and Thermostat

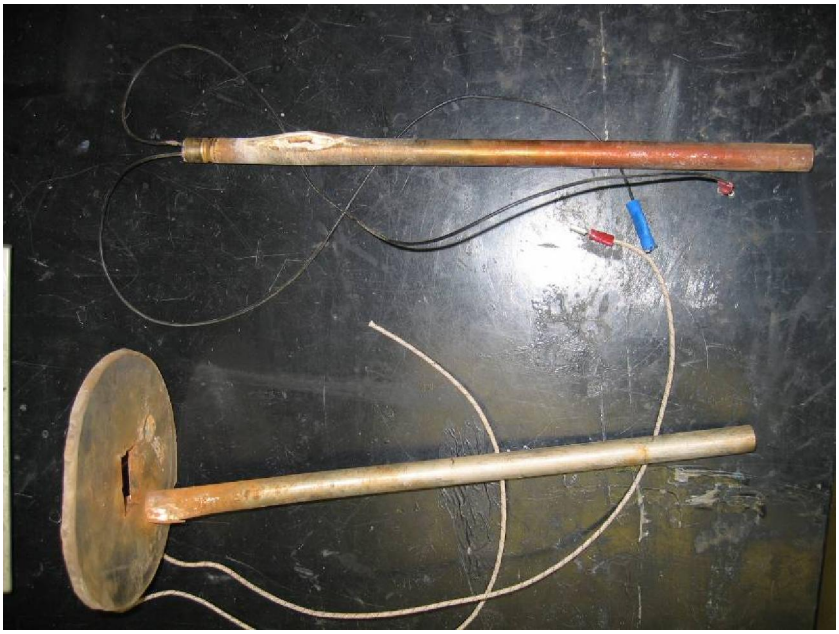

Figure 3.12 – Damaged Heaters



Figure 3.13 – Heater, Thermostat and Specimen in Plastic Top

The loading mechanism utilizes a lever system to apply various levels of sustained tensile load to the tension specimens. Posts were placed between the ceiling and the wooden boards, to hold the horizontal wood member in place. One end of each specimen was hooked onto the J-bolt in one of the CPVC tubes. The other end of the specimen was hooked onto another J-bolt that was secured to a 63 inch long, 52 pound HSS member. The HSS member pivots about a roller, which was welded to a plate and secured onto a movable wooden support frame. This support frame and corresponding roller position could be moved lengthwise along the lever arm to adjust for the desired force. As basic statics proves, the closer the roller to the midpoint of the lever arm, the less force is produced. Since SS340 specimens have a smaller cross-section and ultimate tensile strength than CPVC specimens, the SS340 specimens required much less force. Therefore, the roller was positioned 9” from the midpoint while the roller was 17.5” from the midpoint for CPVC specimens. At the other end of the HSS member, another J-bolt was secured, and 22 pound steel plates could be hung from that bolt to add weight to the system. Using the weight of the HSS members and the steel plates, the roller position

varied according to the dimensions above to achieve the tension force necessary for the induced sustained stress, which are found in Tables 3.1 through 3.4. Another wooden support was also built up at the weighted end to catch the HSS and steel plates after failure. The complete environmental exposure test setup is shown in Figure 3.14, along with details of a tube and specimen shown in Figure 3.15 (Smith 2005).



Figure 3.14 – Environmental Exposure Test Setup



Figure 3.15 – Side and Top Views of Detail A of the Loading Systems

3.3.5 Test Method

Each environmental exposure test began by emptying the water from the CPVC cylinder from the previous test. The cylinder was then refilled with water, the heater, thermostat, and plastic top were put in place, and the thermostat was set to the appropriate temperature. Two to three hours later the temperature of the water was checked with a digital thermometer and any necessary adjustments to the thermostat were made. After the temperature was settled at the desired level, the tension specimen was placed into the cylinder. For unstressed specimens, fishing line was tied to one end. Then the specimen was dropped into the cylinder and secured by the fishing line to a screw outside the cylinder so it would not touch the bottom. If the specimen were to rest on the bottom, it would settle at an angle, which would cause undesired warping. The heater and the thermostat were then replaced to cover the top of the cylinder. No cover was needed for room temperature specimens at 73°F. For stressed specimens, one end was secured on the hook in the water; the other end secured on the J-bolt and run through the end of the HSS member, which was supported at the free end by a 2 x 4 support block. While holding the J-bolt in place, the nut was tightened on top of the HSS member, thus securing the specimen from movement. At this point, the specimen was only slightly loaded since HSS member was supported horizontally at the free end. The specimen was allowed to become acclimated to the water for a minimum of five minutes before loading. The load was applied by removing the support block from the free end, and if necessary, adding steel plates for increased loading. As soon as the specimen was loaded, the starting time was recorded. All specimens were observed for at least the first 10 minutes of testing, in order to get a more accurate failure time in case that time was unusually

short. For those specimens that lasted prolonged amounts of time, the temperature and lever arm position were monitored daily. When failure occurred, the specimen was removed, and the cylinder and loading mechanism was prepared for another test. A maximum testing time of 30 days was set for environmental exposure specimens in matrix A specimens. Testing times of 1, 7, 14, and 28 days were set for environmental exposure specimens in matrix B specimens. Those specimens that did not fail after the required time were tested in tension in order to determine the effect of severe environmental conditions on the material behavior.

3.4 Phase II: Bond Characteristics of SS340 Adhesive for Steel-to-CPVC Surfaces

The purpose of this phase of the project was to examine the bond characteristics of SS340 using steel-to-CPVC double-lap specimens. Primary considerations were focused on determining the effect of environmental conditions such as temperature and stress. Additional observations of salt soaking effects were conducted at ambient conditions only. To accomplish these objectives, the testing incorporated two groups, A and B. Both groups A and B used varied stress levels and temperatures, as in Phase I-A. However, due to the poor performance of group A specimens, the stress level and temperature were changed. Furthermore, additional preparation methods were made to enhance the performance, which included bond area, steel surface preparation, and weighted curing. These observations and enhancements will be discussed in greater detail in the next section. Salt soaking for lap shear specimens occurred only for a small portion of group B specimens.

3.4.1 Double Lap Shear Specimen Preparation

A double lap shear specimen was used in order to eliminate eccentricity typically induced by using a single lap specimen. Type A lap shear specimens were prepared according to ASTM D 3528, *Standard Test Method for Strength Properties of Double Lap Shear Adhesive Joints by Tension Loading*. However, unique design considerations were necessary for the CPVC tabs because of its inferior strength to steel. In addition, the total specimen length was required to be 12" in order to fit in the environmental test setup. Two lengths of steel tabs were employed, both having thicknesses of 1/16". Three-inch long tabs were bonded in between the CPVC tabs to strengthen the hole, while 6.5" tabs were used for the bond overlap. The latter steel tab bond was the investigated bond. Throughout the double lap shear test several adjustments were necessary. Initially, specimens were created with 1/8" CPVC tabs and 1/2" bond overlap. Out of the five double-lap shear control specimens, all had one side fail adhesively while the other failed in the CPVC substrate. A visual display of this failure is found in Figure 3.16. It was unclear which failure occurred first, the bond or the substrate, so the obvious solution was to increase the CPVC thickness. This new method was tested using two approaches. The first approach was by bonding reinforcement tabs along the outside edges of the existing CPVC tabs, essentially increasing the thickness from 1/8" to 1/4". Results were improved, but the effort and time required to bond the specimens in two rounds was



Figure 3.16 – Initial 1/8" CPVC Double Lap Shear Specimen

undesirable. The second approach, yielding group A specimens, required only a single round of bonding, but required more effort to create the CPVC tabs. The new tabs were cut one inch wide out of 3/8" CPVC sheets by a band saw as shown in Figure 3.17. 5/8" holes were drilled out of each tab so that they could be secured to hooks for loading purposes in the environmental exposure test. Figure 3.18 displays tabs being drilled. In order for the Instron grips to be used in lap shear failure testing, the CPVC thickness at the end had to be reduced. Therefore, the tab thicknesses at the hole-end of the CPVC were cut by the band saw, nearly halving their thickness for a grip length of two inches. Shown at the bottom right of Figure 3.19, the resulting thickness for the bonded 3" steel tab and two CPVC tabs was 1/2", which was sufficient to fit in the Instron grips and the environmental exposure test. The bond overlap between the steel and CPVC was 1/2" because of doubts that CPVC stressed at high temperatures could withstand a one-inch overlap without failing in the substrate. A bonded group A, double-lap shear specimen is shown in Figure 3.20. For steel tab preparation, the 3" and 6.5" tabs were grinded, sandblasted, and wiped with acetone before bonding. For CPVC tab preparation, the bonding surface was visually inspected and wiped with a dry paper towel to remove



Figure 3.17 – Cutting CPVC Sheets



Figure 3.18 – Drilling Anchorage Holes

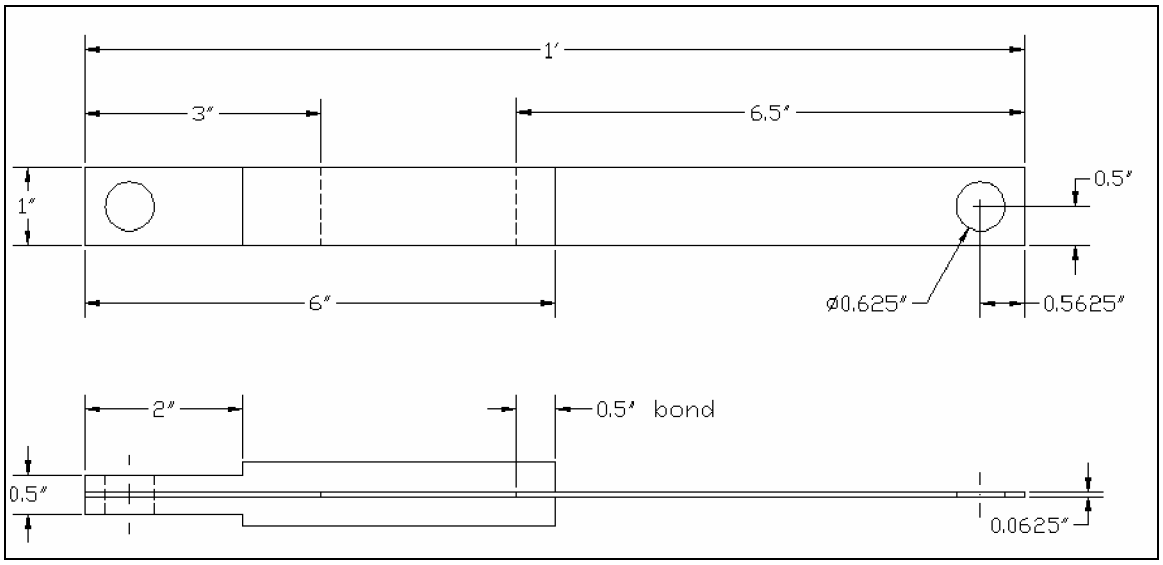

Figure 3.19 – Environmental Exposure Lap Shear Specimen A Configuration

debris. Clear tape was applied to the inside surface of the CPVC above the 1/2" bond overlap as displayed in Figure 3.21. This prevented excess SS340 trapped in between the tabs from bonding to the CPVC, which would have increased the load resistance. The adhesive was hand-mixed using an 8.75:1 weight ratio as specified by the material data sheet. During bonding, 30 mils (or 0.03") glass beads were placed in the adhesive layer to ensure consistent bond thickness. A steel plate weighted specimens during the 24-hour curing process in a piece of plywood cut with one-inch slots. A picture of the plywood with half bonded and half unbonded specimens is seen in Figure 3.22. With assistance provided by IPS lab technicians, group B specimens were designed to increase the bond overlap from 1/2" to 1" in order to improve the adhesive resistance to the environmental conditions. CPVC tabs were lengthened from 6" to 6.5" to adjust for the additional half-inch overlap. Figure 3.23 illustrates the group B specimen configuration. As mentioned earlier other enhancements were made to Type B specimens to improve performance. Because sandblasting proved to be inadequate, hand sanding the steel with 180 grit

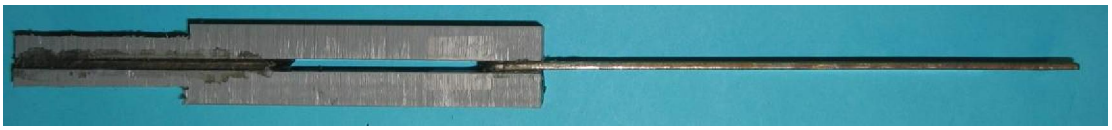

Figure 3.20 – Environmental Exposure Lap Shear Specimen A



Figure 3.21 –Taped CPVC Tabs



Figure 3.22 – Specimens in Plywood Slots

sandpaper removed scale from the steel tabs and allowed for better molecular penetration of the adhesive into the steel. Instead of hand mixing the adhesive, the 10:1 canister of SS340 with mixing nozzle and gun was used for bonding to ensure the correct mix ratio. To help in the curing process, spring clamps were used to apply a more evenly distributed force at the bond areas. Illustrations of these methods are displayed in Figures 3.24 and 3.25. Finally, a 180°F, one hour heat curing process was implemented.

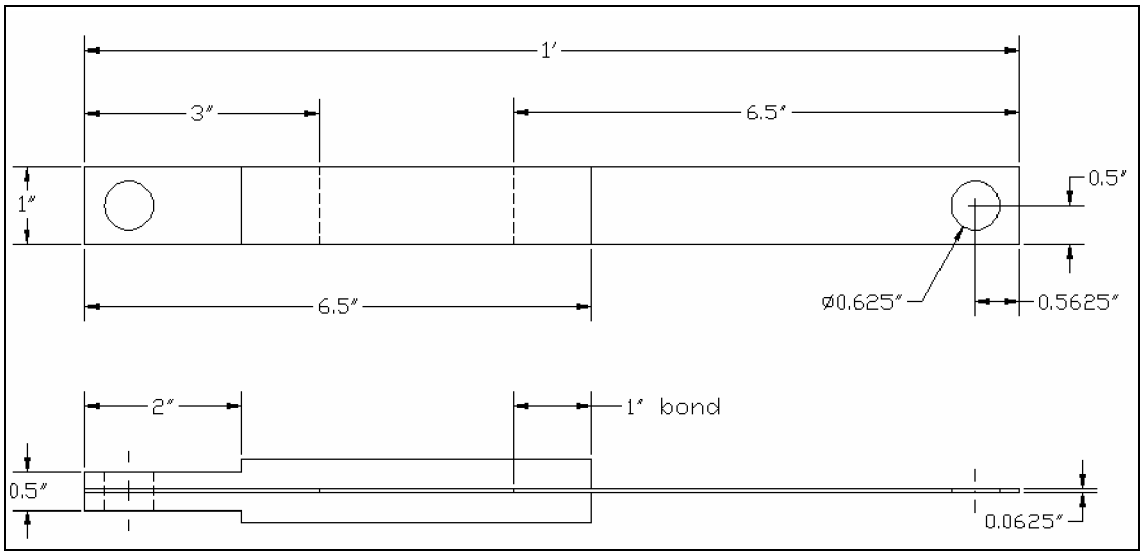

Figure 3.23 – Environmental Exposure Lap Shear Specimen B Configuration

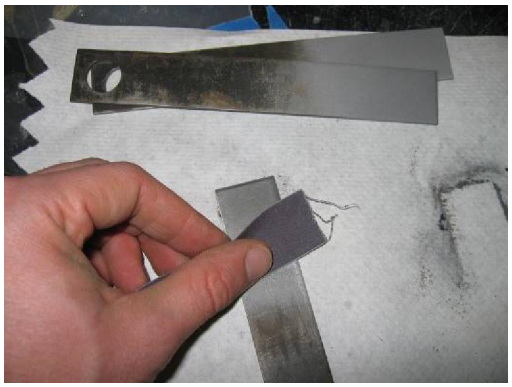

Figure 3.24 – Hand Sanding Steel Tabs



Figure 3.25 – Clamping Specimens

3.4.2 Stress and Temperature Effects on Lap Shear Strength

The test matrices for environmental exposure tests of double lap shear specimens were developed and are given in Tables 3.5 through 3.7. Table 3.5 consists of group A specimens, Table 3.6 consists of group B specimens, and Table 3.7 consists of group B salt soaked specimens. Five control specimens were used to determine the average ultimate shear strength of the adhesive, which was found to be 1400 psi. Specimens were placed in the test setup, where the effects of temperature and stress were observed. Group A specimens used two specimens at each condition for a total of 18 lap shear specimens. For group A specimens, the variables tested include:

- Temperatures of 73^0, 140^0, and 180^0F
- Induced sustained stress equivalent to selected percentage of 0, 15, and 30%

Similarly, group B specimens used two specimens at each condition. However, two additional specimens were used at stressed conditions heated to 120^0 and 140^0F for a total of 26 lap shear specimens. For group B specimens, the variables tested include:

- Temperatures of 73^0, 120^0, and 140^0F
- Induced sustained stress equivalent to selected percentage of 0, 8, and 15%

Salt-soaked group B specimens used two specimens at each condition for a total of 6 lap-shear specimens. For group B salt specimens, the variables tested include:

- Temperature of 73^0
- Induced sustained stress equivalent to selected percentage of 0, 8, and 15% based

For the specimens survived 30-day exposure, they were tested to shear failure using an Instron 8801 Servo-hydraulic Dynamic Testing Machine in order to examine the environmental effect on the material behavior.

Table 3.5 – Lap Shear Environmental Exposure Test Matrix A

Temperature	Selected Percentage	Induced Load (lb)	Induced Stress (psi)
T_1 - 73 ^oF	0%	0	0
	15%	220	220
	30%	420	420
T_2 - 140 ^oF	0%	0	0
	15%	220	220
	30%	420	420
T_3 - 180 ^oF	0%	0	0
	15%	220	220
	30%	420	420

Table 3.6 – Lap Shear Environmental Exposure Test Matrix B

Temperature	Selected Percentage	Induced Load (lb)	Induced Stress (psi)
T_1 - 73 ^oF	0%	0	0
	8%	220	110
	15%	420	210
T_2 - 120 ^oF	0%	0	0
	8%	220	110
	15%	420	210
T_3 - 140 ^oF	0%	0	0
	8%	220	110
	15%	420	210

Table 3.7 – Lap Shear Environmental Exposure Test Matrix B Salt

Temperature	Selected Percentage	Induced Load (lb)	Induced Stress (psi)
T_1 - 73 ^{o}F	0%	0	0
	8%	220	110
	15%	420	210

3.4.3 Test Setup

The environmental exposure test setup was used again. Here, the double lap shear test setup was identical to Phase I testing, with one exception. Instead of varying the roller position, as in Phase I, the position of the roller was maintained at 6.2 inches from the J-bolt connecting the specimen or slightly less than 24" from the center of the lever arm. From static calculations, the 6.2 inch distance provided 220 pounds of tension force with just the HSS member. With a steel plate added, an additional 200-pound force was created for a total of 420 pounds at maximum loading.

3.4.4 Test Method

The test method used in the second testing phase was almost identical to the first phase with the exception of the load level which is quite high in comparison to the first phase. Because the lap shear specimens were much more robust than the tension specimens, un-stressed specimens, placed in the cylinders, were not supported by the fishing line. Warping was not of a concern. All specimens were exposed to a maximum testing time of 30 days for environmental exposure testing. Specimens that did not fail after the specified time were tested in to failure in order to determine if the severe environmental conditions had any adverse effects on the bond characteristics.

3.5 Phase III: Thermal Gradient Test

The purpose of the final phase of this investigation is to examine the thermal gradient distribution and the composite interaction as affected by temperature changes. The test consists of a small scale model to simulate the proposed tank lining, including the steel, adhesive, and CPVC lining. The model was built to determine the thermal gradient from the liner to the steel wall and to evaluate the induced strains at the interface layers. Finite element analysis was conducted to validate the test results and to provide an additional resource for the behavior of the bonded specimen.

3.5.1 Specimen Preparation

All materials were provided by IPS Corporation. The dimensions of the steel plates were 4" x 8" with a thickness of 1/4". Due to their existing surface corrosion characteristics, the surface was initially cleaned by steel wire. Sanding with an 80-grit grinding wheel was also used for further cleaning. As the last step in the surface preparation of the steel prior to the installation of the strain gages, the surface was hand sanded with 120-grit paper. The thickness of the CPVC sheets was 1/8" thick and was cut using a band saw. The dimensions of the CPVC plate were 4.375" x 8.25", which was slightly larger than the steel plate. This increase was provided to be able to support the steel plate after bonding. For thermal expansion measurements, both the steel and the CPVC plates were instrumented by Vishay Micro-Measurement 350 Ohm electric resistant strain gages attached on both sides of the plates in the x and y-directions. According to Vishay Micro-Measurements, "a 350Ω gage is preferable in order to minimize self-heating by the excitation current. The 350Ω gage is also advantageous in reducing the effects of small imbalances which may occur due to unsymmetric resistance changes in the leadwires

with temperature." The selected strain gages were also designed to temperature compensate for steel, which in theory means that the strain gage and the steel would expand at the same rate. Therefore, when tested individually, strain readings for the steel specimens would produce zero output for any temperature change. However, by using a material with a known infinitesimal coefficient of thermal expansion (CTE), the strain data for steel can be adjusted by the strain data for the known material. Details of this method will be discussed in a following chapter. For temperature measurements, Omega 36-gage wire, calibration type-K thermocouples were attached on each of the outer surfaces of the steel and CPVC plates as well as the adhesive layer for a total of three thermocouples to measure the temperature distribution along the composite specimen. A cross-section sketch of the instrumentation including the strain gage and thermocouple placements is shown in Figure 3.26, while a plan view of actual strain gages used is displayed in Figure 3.27. Due to the excellent durability of the M-Bond AE-10 epoxy at high temperatures, it was used to bond strain gages and thermocouples. Surface preparation of the materials, application of the epoxy, and installation method of the gages were conducted according to the instructions set by Vishay Bulletin B-137, which is given in appendix A. The adhesive was set to cure for 24 hours, after which the gage wires were soldered to the lead wires. Three, five foot gage wires were used for each stain gage, two soldered to one lead and one soldered to the other lead. This third wire was used to zero out any temperature effects that may influence the apparent strain in the wires. The gages were tested by a multi-meter to ensure 350 Ohms of resistance. For steel plates, the leads and soldiered portions of the wire were brushed with M-Coat A polyurethane to prevent the gages from shorting out when touching the steel. Tape

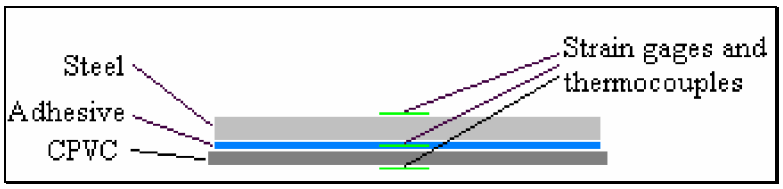

Figure 3.26 – Cross Section of Thermal Gradient Specimen

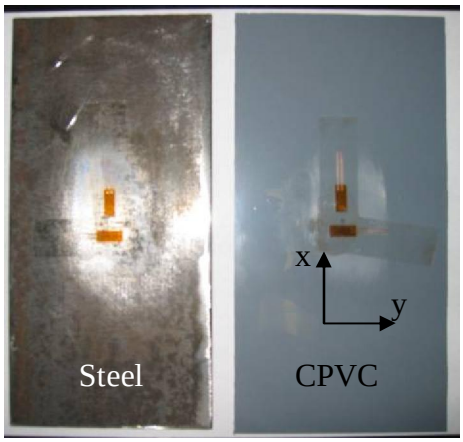

Figure 3.27 – Attached Stain Gages

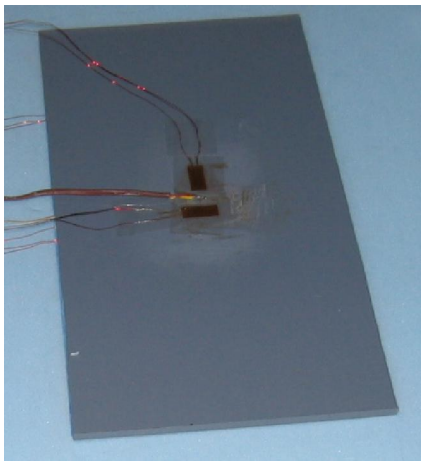

Figure 3.28 – Finished Strain Gages

protecting the exposed side of the stain gages was peeled back and M-Bond was used again to coat the gages, thus adding a permanent protection from environmental effects. An illustration of the CPVC plate after installation of strain gages is shown in Figure 3.28. As the final stage of specimen preparation, the adhesive was applied using a 10:1 volume ratio of SS340 adhesive and activator to bond the steel and CPVC plates. The thermocouple positioned in the adhesive layer was secured with epoxy to prevent possible movement during the squeezing out the excess adhesive. These procedures ensured that the thermocouple was positioned in the center of the specimen. Glass beads were used as spacers to ensure uniform distribution of the adhesive thickness. All the specimens were weighted with a 20 pound steel plate and allowed to cure for 24 hours. Three specimens were constructed with adhesive thicknesses of 30, 50, and 80 mils. This had adhesive layer thickness was the only variation between the bonded specimens.

3.5.2 Test Setup

A square stainless steel box with sides measuring 12," a depth of 10," and an opening at the top was used as the testing container. To maintain a fairly constant temperature, 2" thick Styrofoam Scoreboard insulation was taped around the sides and the bottom of the box. Another piece of insulation was used as the top cover. A rectangular opening, slightly smaller than the plate specimens, was cut out of the cover. During testing, the specimens rested on top of this opening so that they were only supported in the vertical direction at their outer edges. This produced direct heat exposure to the bottom surface while minimizing the escape of heat or moisture to the top of the specimens. Figure 3.29 shows a side view of the container with a specimen resting on top. An insulating cover was used to protect the specimen and to subject the bottom surfaces of the steel and CPVC to the desired temperature. Otherwise, the ambient temperature on the top surface of the steel plate kept the bottom surface from reaching temperatures greater than 140°F. A Lindberg/Blue immersion heater with a dial thermostat fit into container, located just off the bottom surface. The heater can be seen in the top view of the open test bath from Figure 3.30. Figure 3.31 shows the test bath with top cover and Figure 3.32 shows a steel

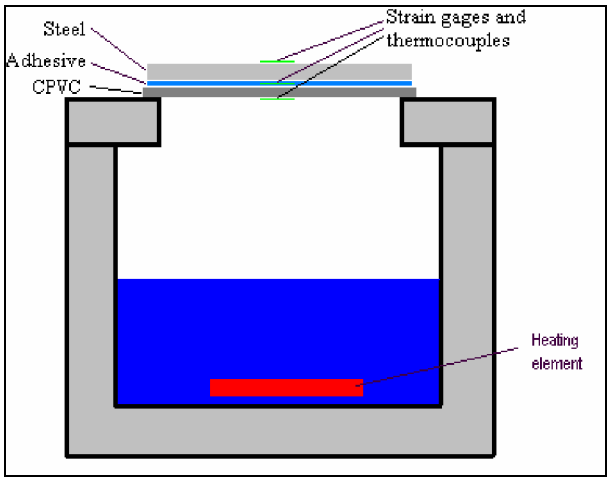



Figure 3.29 – Test Bath Cross Section **Figure 3.30 – Top View of Open Test Bath**



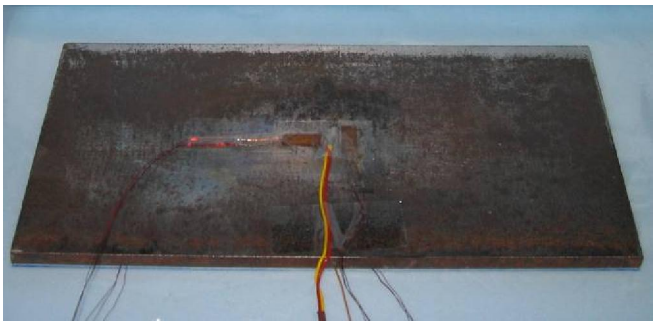

Figure 3.31 – Test Bath with Cover **Figure 3.32 – CPVC Plate on Bath**

plate resting on the test bath, attached with a thermocouple and strain gages. Strain gages and thermocouples were attached to a data acquisition system for measurement and recordings at thirty second intervals. For CTE measurements, the titanium silicate was tested in conjunction with the bath. Similar CTE measurements were also made in an oven. Not only would the additional oven tests provide more accurate data, but it would also indicate the effect moisture from the test bath on the CTE results. For the oven tests, a steel and CPVC plate were tested simultaneously with the titanium silicate. Each material had a single strain gage with a thermocouple attached next to the gage. Because there were only three strain gages, a four-input strain indicator box was used in conjunction with a multi-meter for temperature recordings. Measured values were hand recorded. The steel, CPVC, and titanium silicate were placed in the oven and simply supported by rollers to minimize the expansion resistance. Figure 3.33 displays the test setup in the oven and provides a close-up of the specimens with rollers. Two adhesive samples measuring 1” by 2” were also tested for CTE determination using the oven with the strain indicator box. These samples each had two strain gages, one in the short (y)

and long (x) directions, and a thermocouple for temperature readings. Figure 3.34 shows the test setup for the adhesive test as well as a close-up of the specimens in the oven.



Figure 3.33 – Precision Oven with CPVC, Titanium Silicate, and Steel Specimens

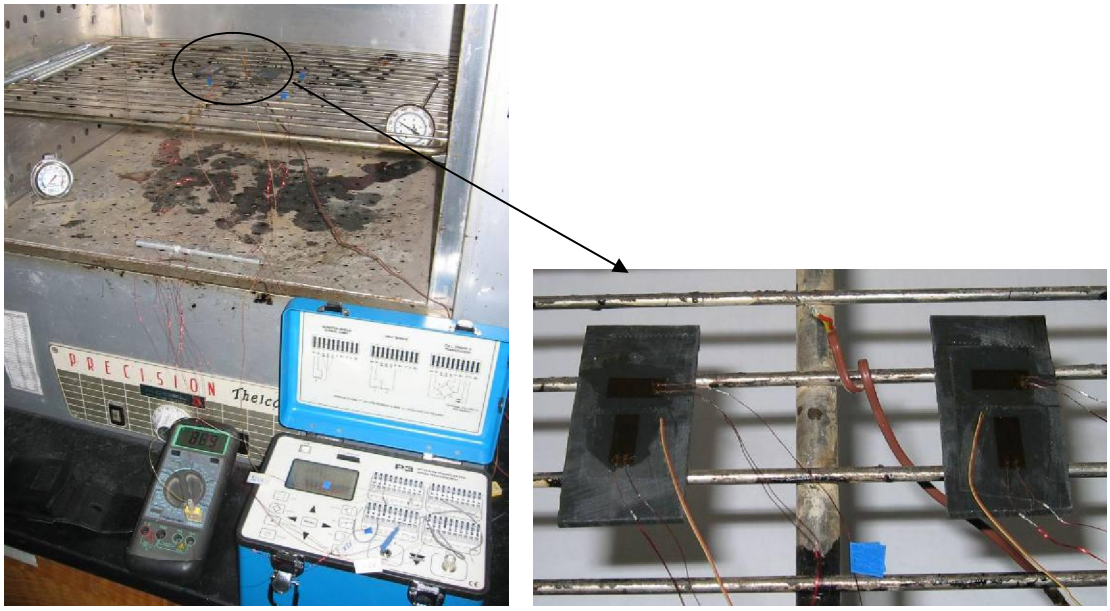

Figure 3.34 – Test Setup for Adhesive Specimens

3.5.3 Test Method

The heated bath with the rectangular opening at the top cover was used to expose the material surfaces to a temperature range of 73 to 180°F. A smaller opening to fit the titanium silicate was cut out from one cover. The titanium silicate opening was positioned next to the plate specimen opening, so that the CTE test could be verified in conjunction with a steel specimen as shown in Figure 3.35. A close up view of the

titanium silicate is illustrated in Figure 3.36. With the oven tests, the materials were exposed to identical temperature ranges and stabilized at various temperatures. Three tests were performed using both the test bath and the oven for the titanium silicate. The test bath was used for the remainder of the steel and CPVC tests to simulate actual field conditions. To gain a better understanding of the interaction caused by the bonded steel and CPVC plates, the materials were initially tested by themselves. Each of the steel and the CPVC specimens were individually subjected to a temperature range of 73°F to 180°F while strains and temperatures were continuously recorded using the data acquisition system. Once the bottom surface of the specimen reached 180°F, the heat was maintained for several minutes. This allowed the data to stabilize, so that temperatures and corresponding strains were accurately represented at the maximum temperature range. After observing the data stabilization, the insulating cover was removed, and the top cover was slid partway to one side. The hot water in the bath was then removed and replaced with cooler water. These steps allowed for faster cooling of the specimen while at the same time not disturbing the integrity of the data collection during the cool-down cycle. The complete heating and cool down cycle lasted from four to five hours. If the

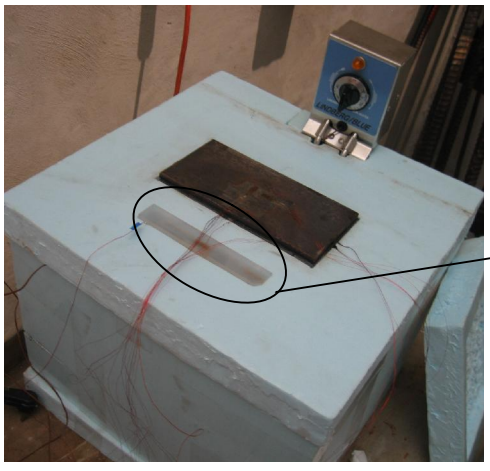

Figure 3.35 – Steel and Ti Silicate



Figure 3.36 – Titanium Silicate

specimen had been allowed to cool without removing the top cover and replacing the water, the process would have taken around 24 hours due to the insulating effect of the bath. This temperature cycle and data collection was repeated on each steel and CPVC plate for three trials in order to ensure test accuracy. A total of 18 tests were performed, 9 for the steel and 9 for the CPVC. After collecting this data, the steel and CPVC were bonded following the previously discussed method using adhesive thicknesses of 30, 50, and 80 mils. The bonded specimens were then tested as a unit until three successful trials of accurate data were compiled. To examine the influence of the boundary conditions, a test on the 80 mils thick specimen was performed with rollers at the four corners. These rollers were placed on the cover to support the corners of the bonded specimen as displayed by Figure 3.37. This test was performed to minimize the friction effects caused by supporting all the sides of the CPVC bottom surface on Styrofoam. The rollers were brushed with oil as an additional measure to decrease resistance and provide a free thermal expansion. For additional understanding of the bonded specimen behavior, a linear elastic finite element model was developed to verify the observed behavior. The 80 mils thick specimen was modeled to compare finite element results with measured test results. Additional models were analyzed to investigate boundary conditions and rectangularity effects on the behavior of the specimen.



Figure 3.37 – Bonded Specimen with Rollers

4.0 - Results, Analysis, and Discussion

4.1 Introduction

This chapter describes the test results and analysis of three experimental phases considered to study the behavior of CPVC and adhesives used for lining steel tanks. The chapter provides critical discussion of the behavior and includes detailed information presented in graphical format, tables and illustrations. The results are presented in the same segments used in Chapter 3.

4.2 Phase I: Tensile Strength

Tension specimens described in Section 3.3 subjected to environmental exposure were tested to failure using an Instron testing machine. Loading was applied using a displacement control rate of 0.2 in/sec according to the ASTM Standard D-638. A load cell, with maximum capacity of 10,000 lbs, was used to measure the applied load. Movement of the piston, known by the stroke, was used to measure the overall displacement. Tension stress and the displacements were recorded every 0.1 seconds and stored in an electronic data acquisition system.

4.2.1 Tensile Strength of CPVC

Control specimens were used to determine the tensile strength of the CPVC without the effect of the various parameters considered in this investigation. A total of five control specimens, not subjected to the environmental exposure test, were tested. The measured average tensile strength was used to determine the applied load to be used as sustained loads to study the effect of the environmental exposure. Results of the control specimens are shown in Figure 4.1 and the values are given in Table 4.1. The standard deviation of the measured maximum tensile stresses, which occurred at stroke values around 0.25

inches, was relatively low. The results indicate significant drop in the ultimate strength of the material, about 25 percent, before reaching a constant level or "yielding" plateau. Based on these results, the ultimate tensile strength of 8000 psi was used for the CPVC material for duration of the project to calculate the percentage of sustained loading. These sustained loads were used during the environmental exposure tests.

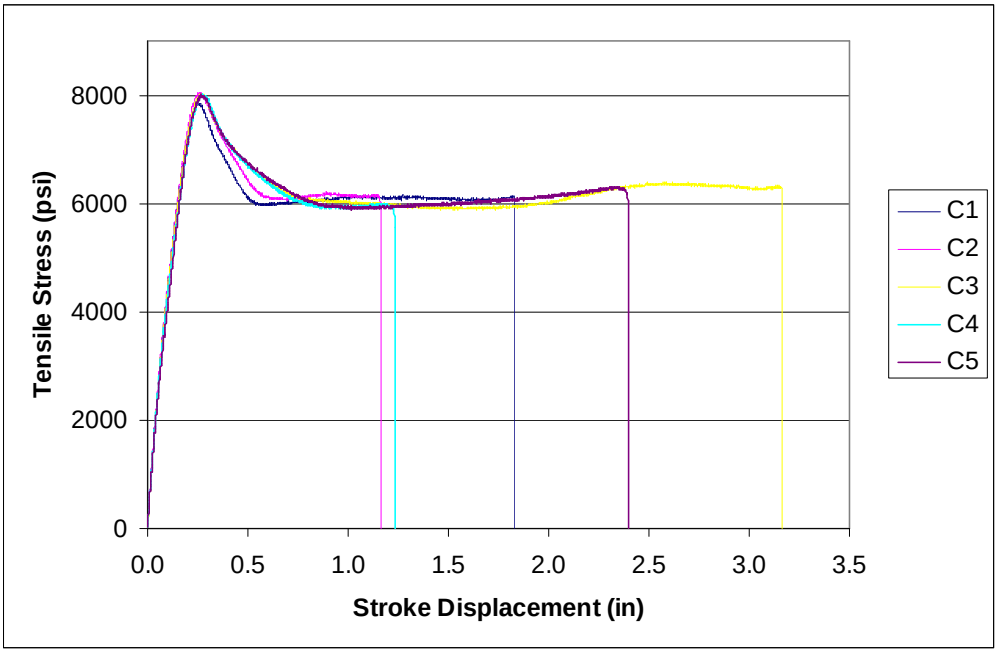

Figure 4.1 – Results of CPVC Control Specimens

Table 4.1 – Summary of CPVC Control Specimens

Specimen	Tensile Stress at Failure (psi)	Stroke Displacement at Failure (%)
C1	7844	1.8
C2	8044	1.2
C3	8015	3.2
C4	8016	1.2
C5	8009	2.4
AVG	**7986**	**2.0**
Std Dev	80.6	0.84

4.2.1.1 Effect of Combined Sustained Load and Temperature

To study the effect of the environments on the behavior of the CPVC material, the experimental program described in Table 3.1 for CPVC Test I-A was undertaken. The behavior under the environmental conditions was evaluated using different levels of both sustained loads and temperatures. In each case, two specimens were tested at each condition and were subjected to the specified environmental conditions for 30 days. Figures 4.2 and 4.3 show the measured maximum stress and stroke at failure in each case. Test results indicate that the CPVC material could maintain at least 75 percent of the tensile strength of 8000 psi quite well throughout all the conditions with the exception of specimens subjected to a high temperature of 180°F and high sustained load of 30 percent. Failure of the specimens subjected to sustained stresses of 15 and 30 percent was typically due to rupturing in a brittle manner as shown in Figure 4.3 by the low stroke measurement. For example, the first specimen subjected to 30 percent sustained stress and tested at 73°F ruptured slightly above 6000 psi and achieved a 0.1 inch stroke compared to a 3.0 inch stroke measured at zero sustained load. Failure of the specimens subjected to sustained stresses and tested at high temperatures was brittle and did not achieve the same stroke measured at ultimate for the unstressed specimens tested at the same temperature. Control specimens shown in Figure 4.1 also produced high stroke prior to failure. Since these specimens reached a high stress greater than 75 percent of the 8000 psi strength, this indicated that exposing CPVC to water does not cause a significant degrading effect to the material in comparison to the sustained load which alters the nature of failure of the material. The measured strength of the unstressed specimens tested at 140°F and 180°F were even higher than the strength measured for the

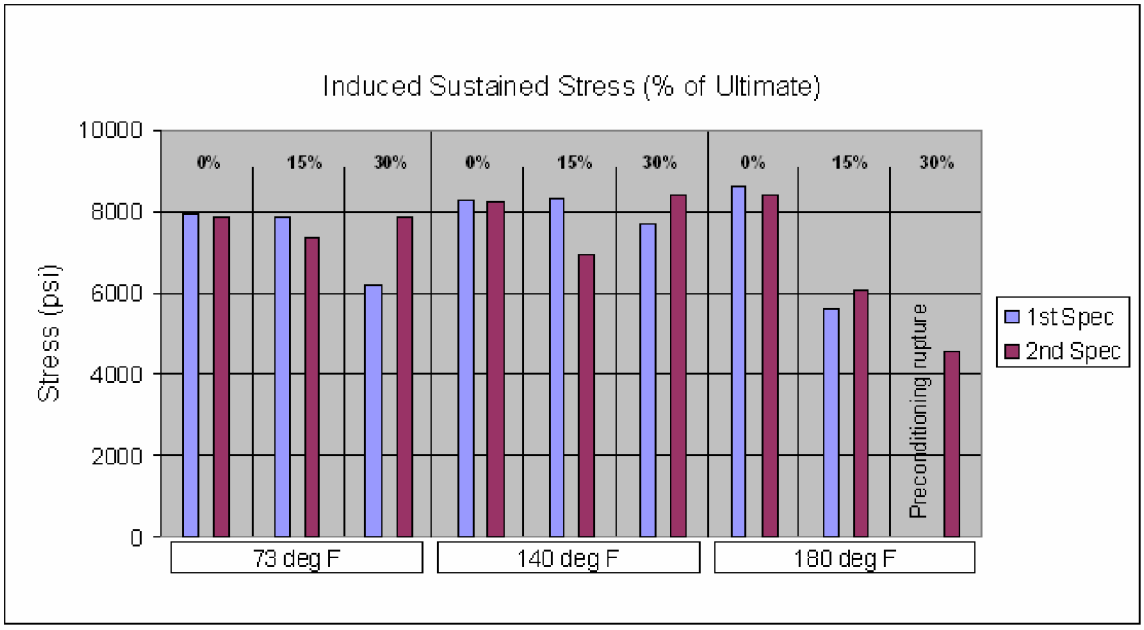

Figure 4.2 – Test I-A: Measured Strength of CPVC Specimens

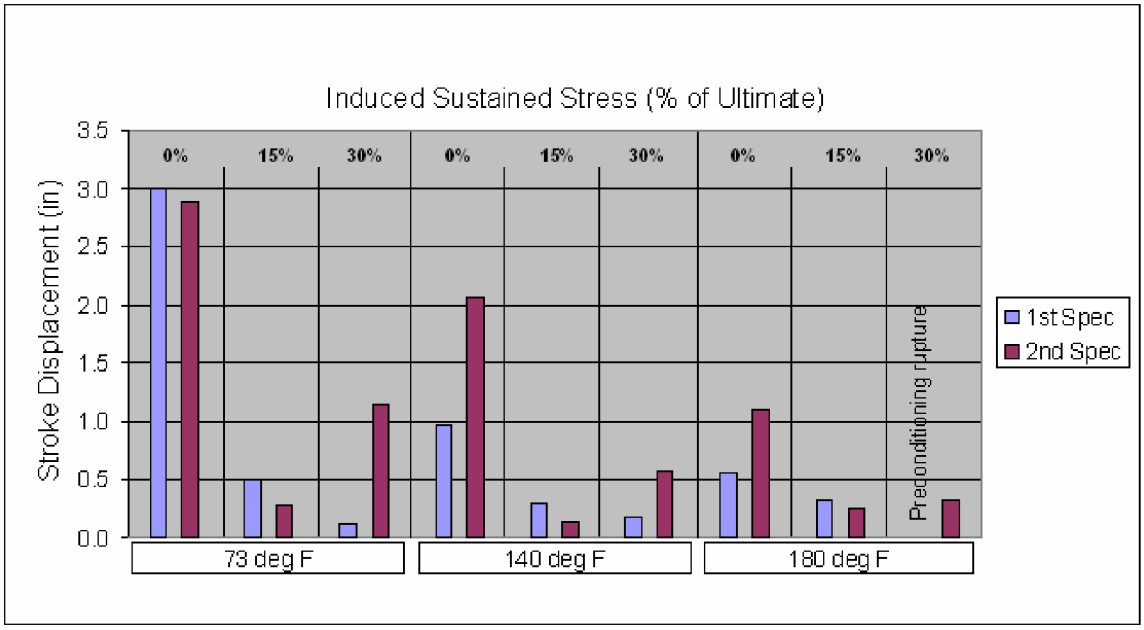

Figure 4.3 – Test I-A: Measured Stroke at Failure of CPVC Specimens

specimens tested at 73°F. The results also eliminate the effect of the temperature in altering the behavior of CPVC and suggest that the permanent load level combined with high level of sustained stress is more effective in influencing the behavior. This conclusion is evidence by the results of the specimens tested at 180°F and high sustained

load of 30 percent where the specimen had significant reduction of the strength. This suggests that a combination of high sustained load with high temperature cause significant reduction of the strength as well as brittle failure of the CPVC. These results also suggest limiting the sustained load to be less than 30 percent and possibly the temperature load level to be less than 180°F. Several of the discussed properties can be clearly seen in the stress vs. stroke graph shown by Figure 4.4 for the specimens subjected to 140°F under different sustained load levels. The unstressed specimen achieved significantly greater stroke at failure in comparison to the specimens subjected to 15 and 30 percent sustained stress. The specimen subjected to 15 percent loading failed at a much lower stroke displacement and only reached a strength of 7000 psi. The specimen subjected to a sustained load of 30 percent also achieved lower stroke at failure, but reached a similar strength value as the unstressed specimen. Figures 4.5 and 4.6 exhibit comparable behavior to the effect of sustained load for specimens tested at140°F.

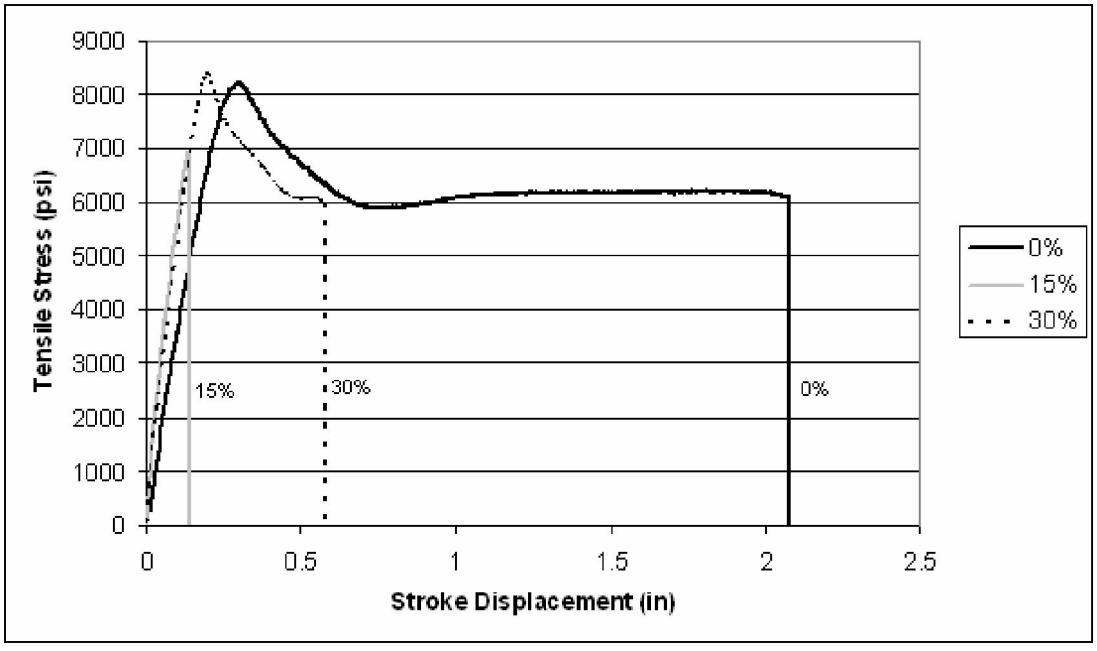

Figure 4.4 – CPVC 2nd Specimen at 140°F and Varied Induced Stress

In all three figures, the unstressed specimen measured the highest strength and displacement at failure. Figure 4.5 shows the brittle nature of failure for the specimen subjected to a sustained load of 30 percent. In this instance, the strength dropped to the 6000 psi level. Figure 4.6 indicates clearly the effect of stressed environments and high

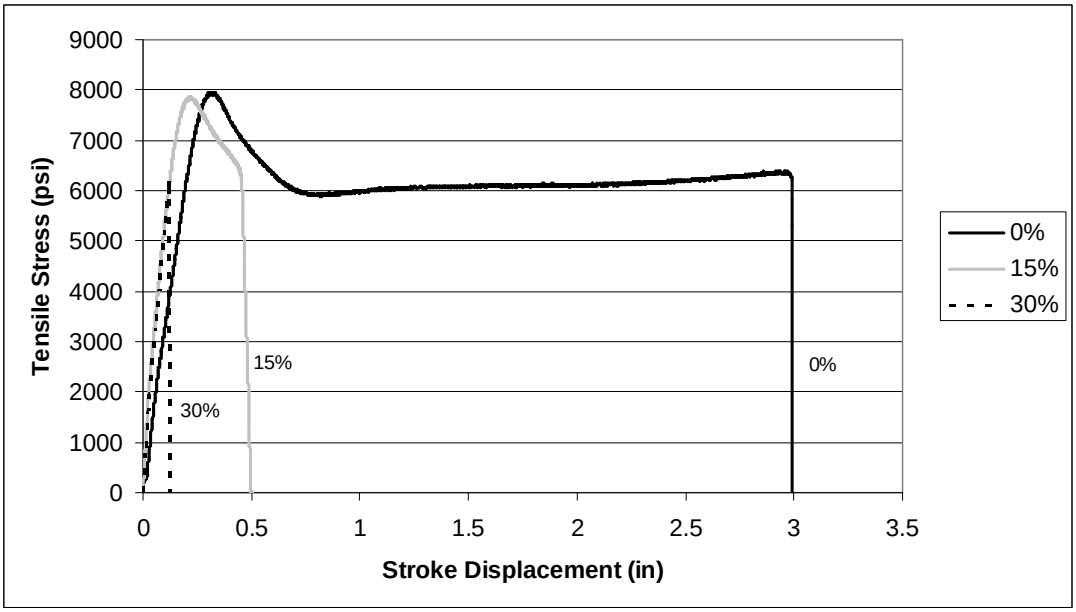

Figure 4.5 – CPVC 1st Specimen at 73°F and Varied Induced Stress

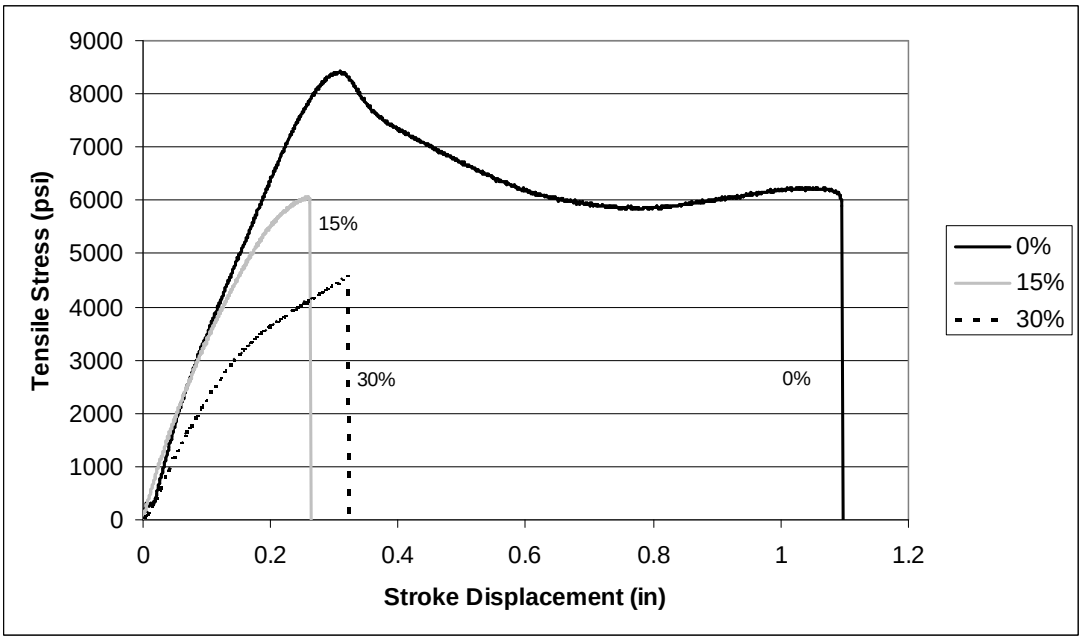

Figure 4.6 – CPVC 2nd Specimen at 180°F and Varied Induced Stress

temperatures of 180°F. The adhesive loses a significant portion of its strength and deformation at failure. Figure 4.7 shows the specimens before being subjected to sustained loads. Figure 4.8 shows unstressed specimens after testing where the large and permanent deformations which occurred before failure can be clearly observed. The results indicate that high levels of sustained loading alter the characteristics of the CPVC. A combination of the high sustained load beyond 30 percent of the ultimate load and temperature higher than 140°F could significantly reduce the strength and deformation at ultimate. Presence of the sustained load reduced the stroke at ultimate but not the strength with temperature levels less than 140°F.



Figure 4.7 – Pre-test CPVC Specimens

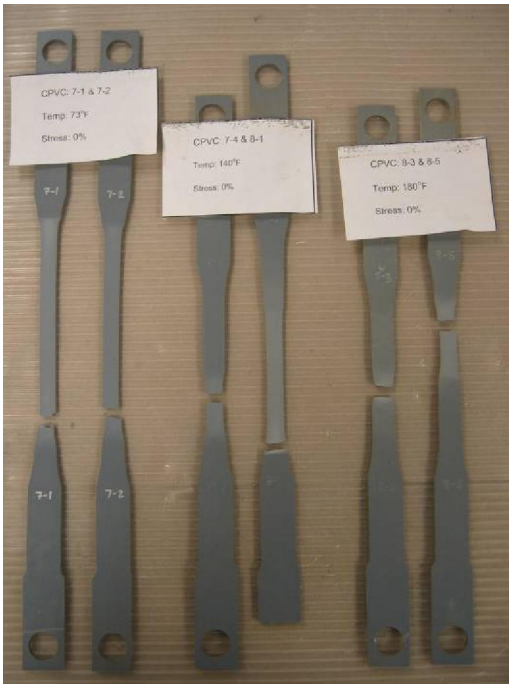

Figure 4.8 – Post-test CPVC Specimens

4.2.1.2 Effect of Soak Time with Water and Salt-Water

To study the effect of the water versus salt water soaking with time variation, the experimental procedure described in Table 3.3 for CPVC Test I-B was undertaken. One specimen was subjected to each environmental condition for a varying number of days.

Figures 4.9 and 4.10 represent the maximum measured strength for specimens subjected to water soaking and salt-water soaking, respectively, using exposure times of 1, 7, 14, and 28 days. Figures 4.11 and 4.12 represent the measured deformation at failure for water and salt water soaking, respectively. Comparing each individual line on one of

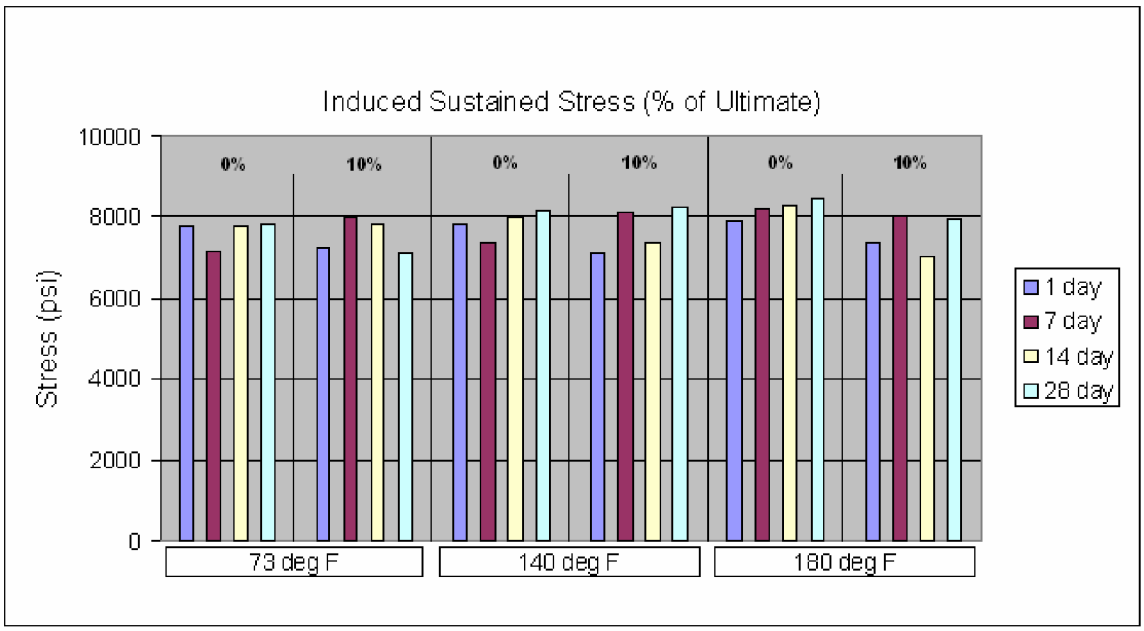

Figure 4.9 – Test I-B: Measured Strength of CPVC Specimens Soaked in Water

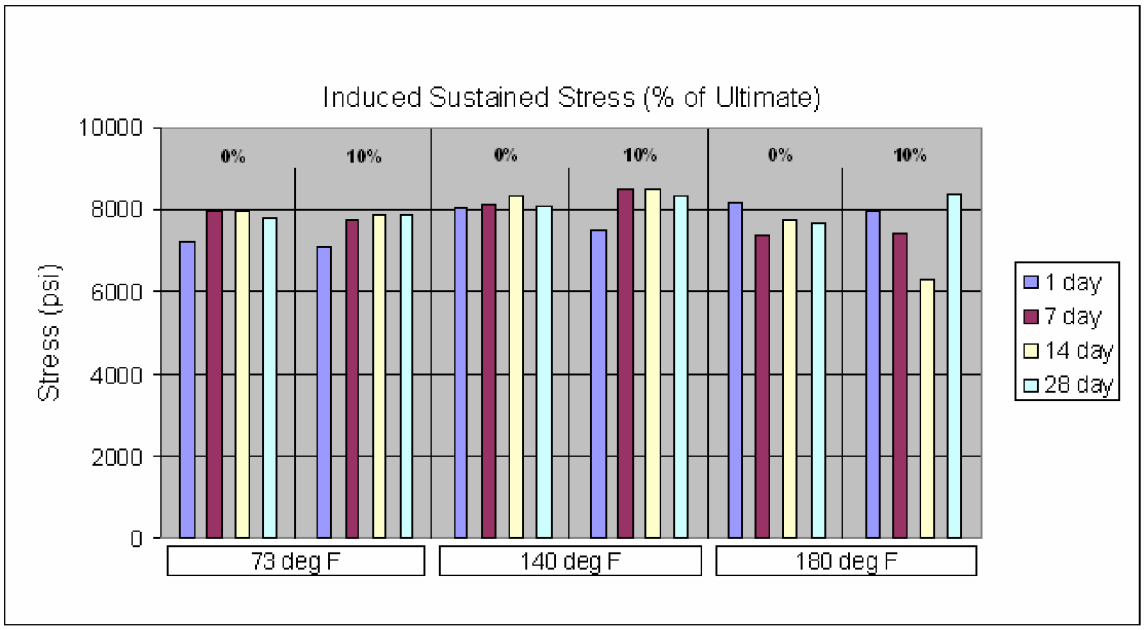

Figure 4.10 - Test I-B: Measured Strength of CPVC Specimens Soaked in Salt-water

these graphs with the identical conditions on the corresponding graph provides the effect of salt soaking versus the effect of water soaking. Unlike Test I-A results, the 180°F water and high sustained stress conditions do not have a significant effect on the strength. However, the measured deformations are reduced at higher temperatures. These results would indicate that for sustained stress less than 10 percent of the ultimate strength use of salt water or water is acceptable up to temperatures of 180°F. From a maximum strength standpoint, it is difficult to determine clear conclusions on the effect of soaking time. Therefore, Table 4.2 provides all test results for both cases. The table groups all the results of unstressed specimens and the specimens subjected to sustained stress of 10% tested at each of the three temperatures using their respective soak times. The average of the results allows evaluation of the effect of soaking time for both water and salt-water soaked specimens. Each strength and stroke value in the table represents the average reading from six specimens. Test results indicate that the soaking time has a slight effect

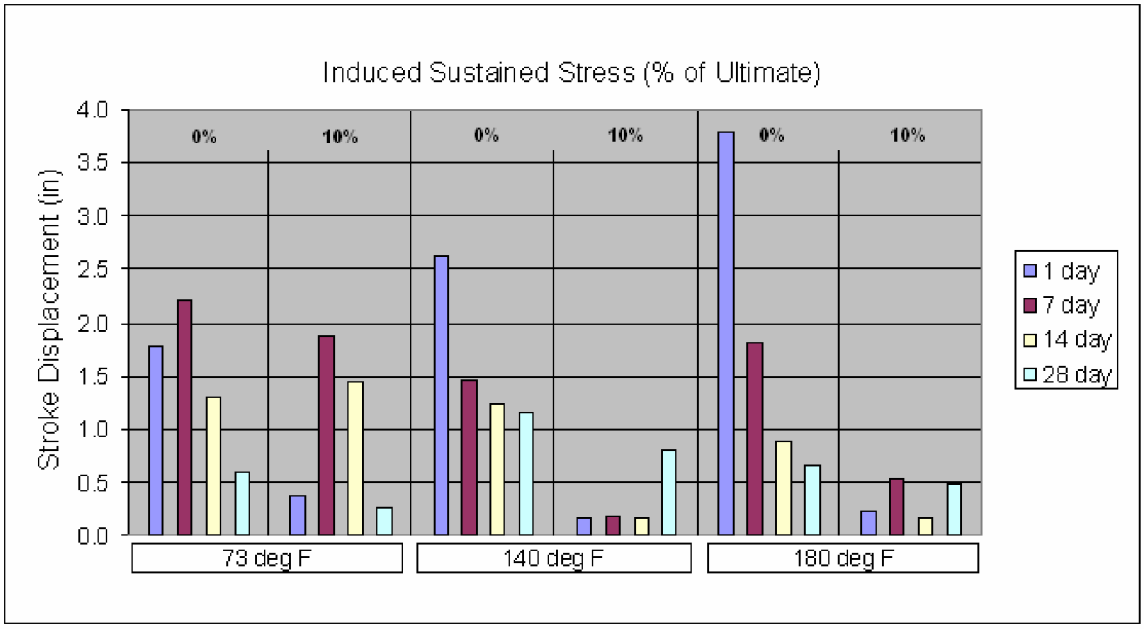

Figure 4.11 – Test I-B: Measured Stroke at Failure of CPVC Specimens Soaked in Water

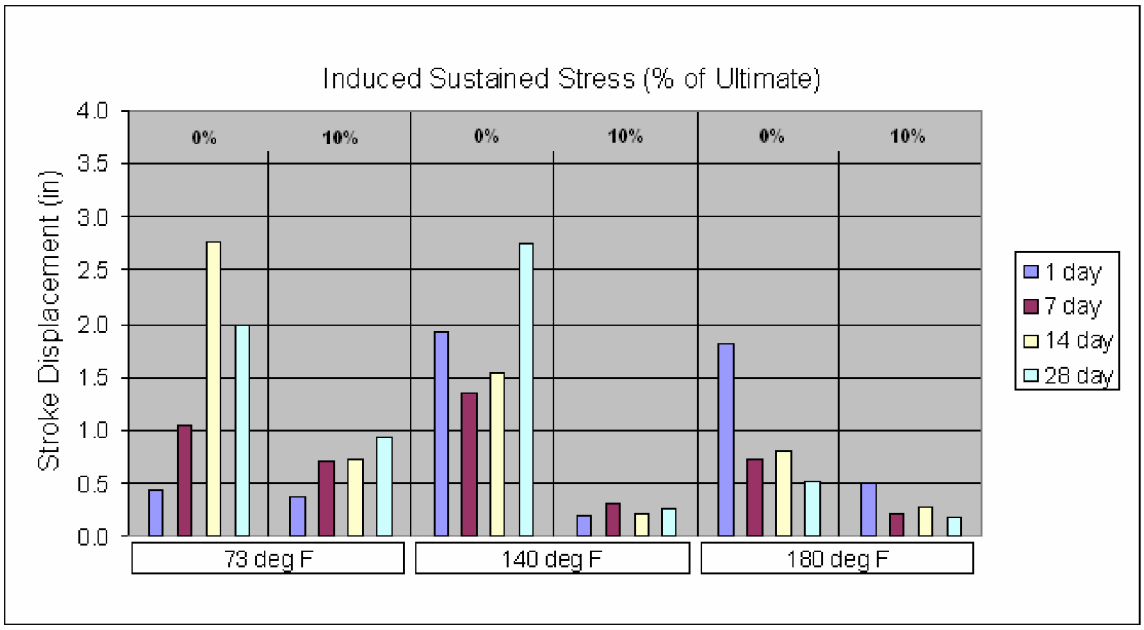

Figure 4.12 – Test I-B: Measured Stroke at Failure of CPVC Specimens Soaked in Salt-water

to the strength. For example, the average strength for 1-day water soaked specimens is 7535 psi, and for 28-day water soaked specimens the average increases to 7961 psi. A similar strength trend is followed for the salt-water soaked specimens. The variation of measured higher strength in some cases cannot be used to conclude a general trend since it is within the accuracy of the instruments used this program. For water soaked specimen, the average measured displacements indicate that soaking time could reduce the stroke at failure and therefore affects the overall deformability of the material. A clear correlation between water soak time and stroke reduction can be seen Figure 4.11. From Table 4.2, the average of the 1-day soaked specimens have an average stroke of 1.5 inches but drops to0.7 inches for the 28-day specimens. For salt-water soaked specimens, the table indicates that the trend could be reversed. However, this observation is not correct by examining the readings shown in Figure 4.12, where the stroke averages are greatly influenced by some measurements at 73°F and 140°F. Accordingly, no

conclusive trend can be made at this stage due to the limited specimens tested to examine this variable. The overall comparison of water versus salt-water specimens can be seen in Table 4.3. The comparison indicates that using a 5 percent solution of salt-water has the same effect on the strength as water soaking. The strength increased from water to salt-water exposure is insignificant and ranges from 1 to 2%. Further testing may be required to study the effect on the overall deformation, however, based on the positive and negative values given in Table 4.3, there is no significant difference between water or salt-water solution on the behavior of the CPVC material.

Table 4.2 – Test I-B: Average Strength and Stroke Values for CPVC Specimens

	Water Soaked		Salt Water Soaked	
Soak Time (days)	**Average Strength (psi)**	**Average Stroke at Failure (%)**	**Average Strength (psi)**	**Average Stroke at Failure (%)**
1	7535	1.50	7673	0.87
7	7798	1.34	7862	0.73
14	7721	0.87	7795	1.05
28	7961	0.67	8025	1.10
Average	**7754**	**1.09**	**7839**	**0.94**

Table 4.3 – Test I-B: Strength and Stroke Changes from Water to Salt-water Soaking for CPVC Specimens

Soak Time (days)	Strength Change from water to salt-water	Stroke Change from water to salt-water
1	1.8%	-41.5%
7	0.8%	-46.0%
14	1.0%	21.1%
28	0.8%	65.7%
Average	**1.1%**	**-14.1%**

4.2.2 Tensile Strength of SS340

A total of five control specimens were used to determine the tensile strength of SS340 adhesive without the effect of the environmental conditions. The resulting average tensile strength was used to determine the sustained load that should be applied as a percentage of the ultimate strength to the loaded specimens subjected to environmental exposure. Results of the SS340 control specimens are given in Figure 4.13 and Table 4.4. The behavior shown in the charts were nearly identical with the exception of ultimate stroke. Thus, the standard deviation is small for the maximum tensile stresses, which was achieved prior to rupture. The initial yield strength occurs at around 1800 psi, followed by a small drop, and then increases by an average of 18 percent accompanied with large deformation. Based on these results, an ultimate tensile strength of 2100 psi was used for the SS340 adhesive for the duration of the project to determine the induced sustained stress levels as a percentage of the ultimate strength. An average value of

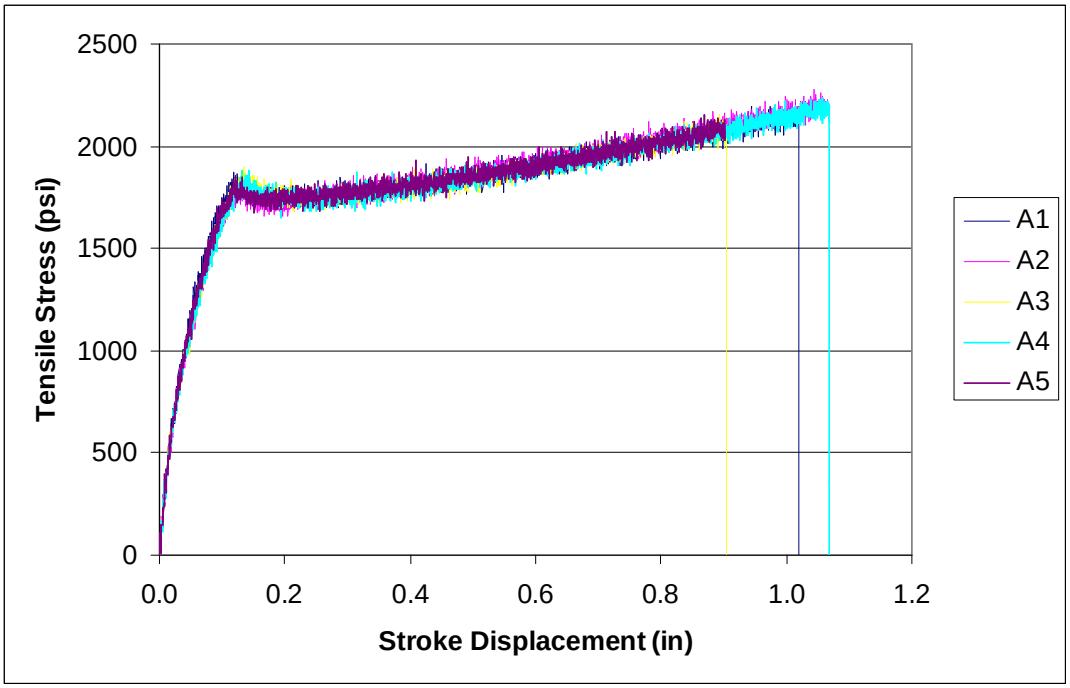

Figure 4.13 – Results of SS340 Control Specimens

Table 4.4 – Summary of SS340 Control Specimens

Specimen	Tensile Stress at Failure (psi)	Stroke Displacement at Failure (%)
A1	2197	1.0
A2	2281	1.1
A3	2154	0.9
A4	2239	1.1
A5	2152	0.9
AVG	**2205**	**1.0**
Std Dev	55.7	0.08

2100 psi was chosen instead of the 2200 psi average measured strength since the material data sheet tensile strength provided by the manufacturer stated a range of 2000-2200 psi.

4.2.2.1 Effect of Combined Sustained Load and Temperature

To study the effect of the environments on the behavior of the SS340 adhesive, the experimental program was performed as described in Table 3.2 for SS340 Test I-A. Two specimens at each condition were subjected to environmental conditions for 30 days. Figures 4.14 and 4.15 show the measured maximum stress and stroke, respectively. Several correlations can be obtained from these figures. SS340 reached or exceeded the 2100 psi level when exposed to 73°F for all levels of applied sustained load up to 30 percent. These results indicate that exposing SS340 to water a sustained load under room temperature has no degrading effect on the tension strength of the adhesive. Results indicate that for unstressed specimens at 140°F and 180°F, the ultimate strength decreased slightly when compared to the specimens at 73°F. This suggests that exposure to hot water without any sustained load could have some small degree of degradation to the material. Measured stroke displacement did not reach the measured values found in the control specimens, which indicates that water soaking does have an adverse effect on the deformability of the adhesive. When specimens ruptured during the environmental

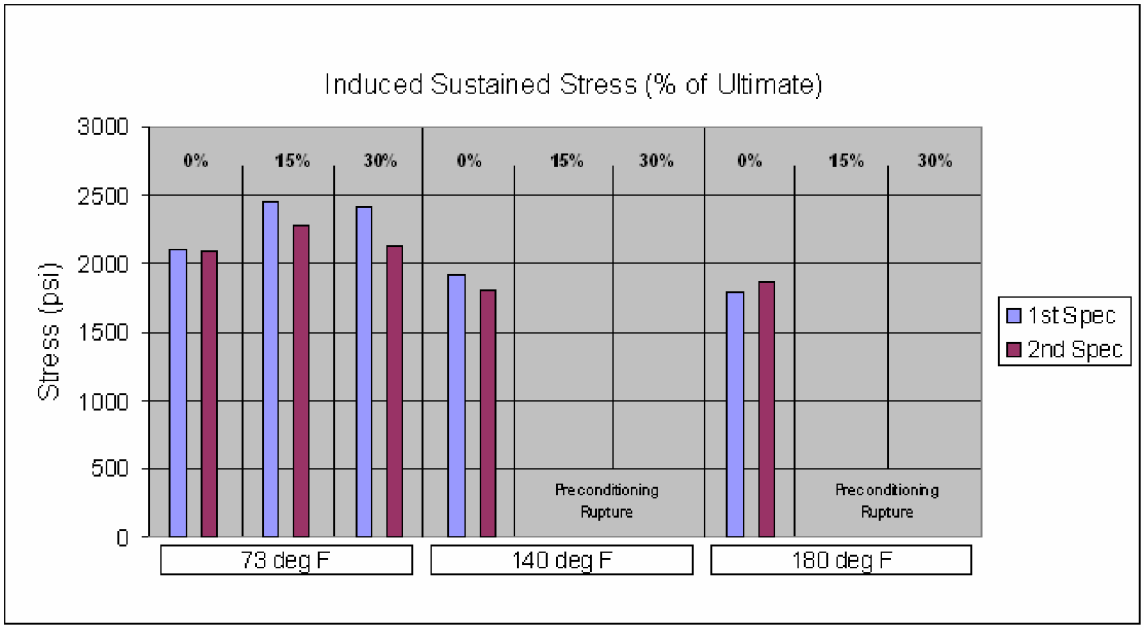

Figure 4.14 – Test I-A: Measured Strength of SS340 Specimens

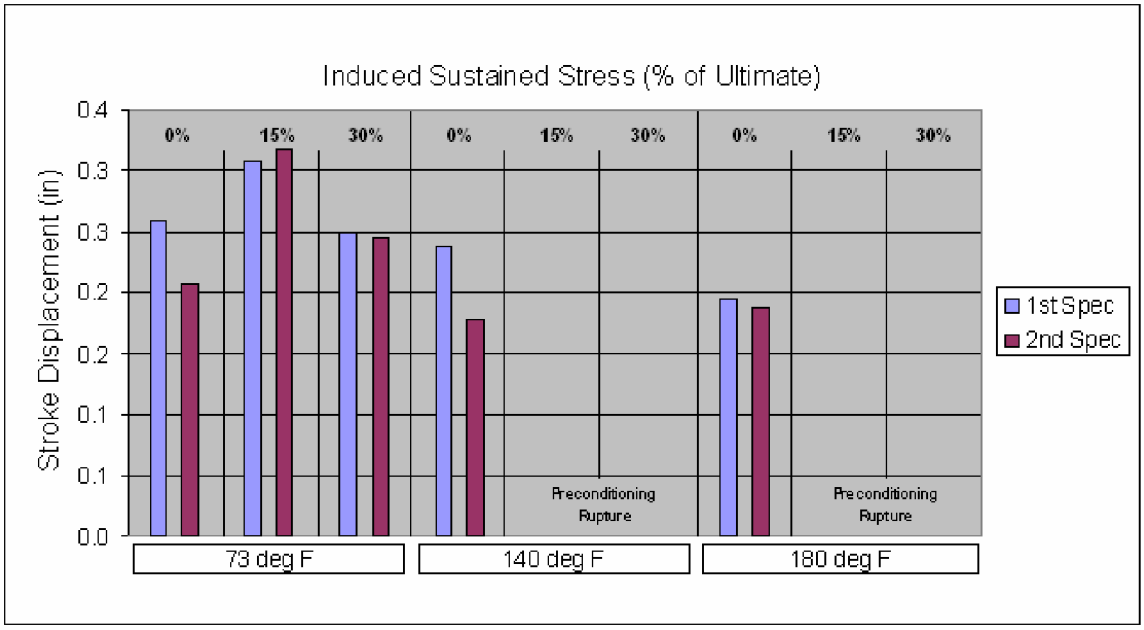

Figure 4.15 – Test I-A: Measured Stroke at Failure of SS340 Specimens

test portion, the rupture date was recorded. Specimens subjected to the most extreme conditions (30 percent sustained stress and 180°F) did not survive more than a few minutes. The specimens subjected to 15 percent sustained loading and 180°F as well as the specimens subjected to 30 percent and 140°F survived less than one day. Specimens

subjected to 15 percent sustained stress and 140°F nearly completed the test, but survived for 20 days only. Test results indicate that SS340 should not be exposed to a combination of high temperatures and high sustained loads of 15 percent of the ultimate. Based on these results, the program was altered to examine a different range of combinations of high temperature and sustained load which be used on the adhesive. The stress-stroke relationship shown in Figure 4.16 is for the unstressed specimens subjected to different temperature levels. The behavior of the three specimens matches well up to a stress level of 1500 psi, at which the behavior started to deviate. This performance indicates that the temperature could slightly influence the behavior for even unstressed specimens. Figure 4.17 shows pre-tension test results of unstressed specimens subjected to different temperatures. Exposed temperatures of the specimens start from left to right in increasing order. The photo indicates that heated water changes the color of the adhesive from black to a yellowish-brown when subjected to 180°F. Although this color change would seemingly indicate a significant change in the material properties, the decrease of the strength and deformation was within 15 to 20 percent as shown in Figure 4.16. Figure 4.18 displays the unstressed specimens subjected to tension failure. Overall results show the presence of sustained loads combined with high temperature could dramatically reduce the strength and causes early failure of the adhesive. Further research is needed to determine the maximum temperature that could be used with minimal reduction of tensile strength. This temperature should be less than the 140°F used in this program.

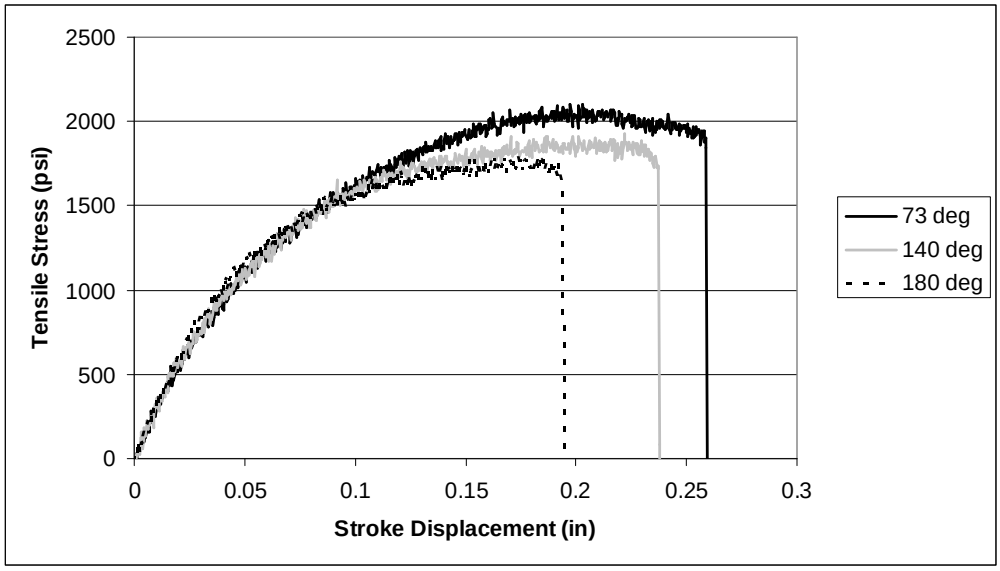

Figure 4.16 – SS340 1st Specimen at 0% Induced Stress and Varied Temperature



Figure 4.17 – Pre-test SS340 Specimens



Figure 4.18 – Post-test SS340 Specimens

4.2.2.2 Effect of Soak Time in Water and Salt-Water

To study the effect of the water versus salt water soaking with time variation, the experimental procedure was performed as described in Table 3.4 for SS340 Test I-B. One specimen was subjected to each pf the selected environmental conditions for a varying number of days. Figures 4.19 and 4.20 represent the maximum measured strength for specimens subjected to water soaking and salt-water soaking, respectively, using exposure times of 1, 7, 14, and 28 days. Figures 4.21 and 4.22 represent the stroke at failure for water and salt water soaking, respectively. Comparing each individual line

on one of these graphs with the identical line on the corresponding graph provides the relationship of salt soaking versus water soaking. It should be noted that the sustained applied load was limited to 10 percent of the ultimate strength based on the results obtained in the previous test to study the effect of the sustained load on the adhesive.

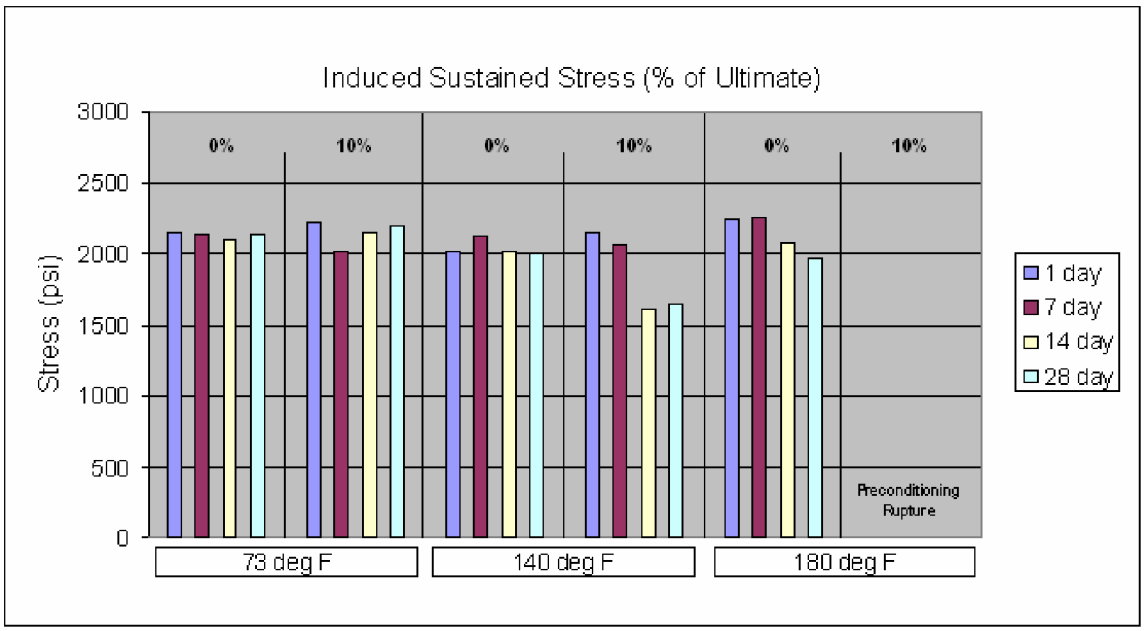

Figure 4.19 – Test I-B: Measured Strength of SS340 Specimens Soaked in Water

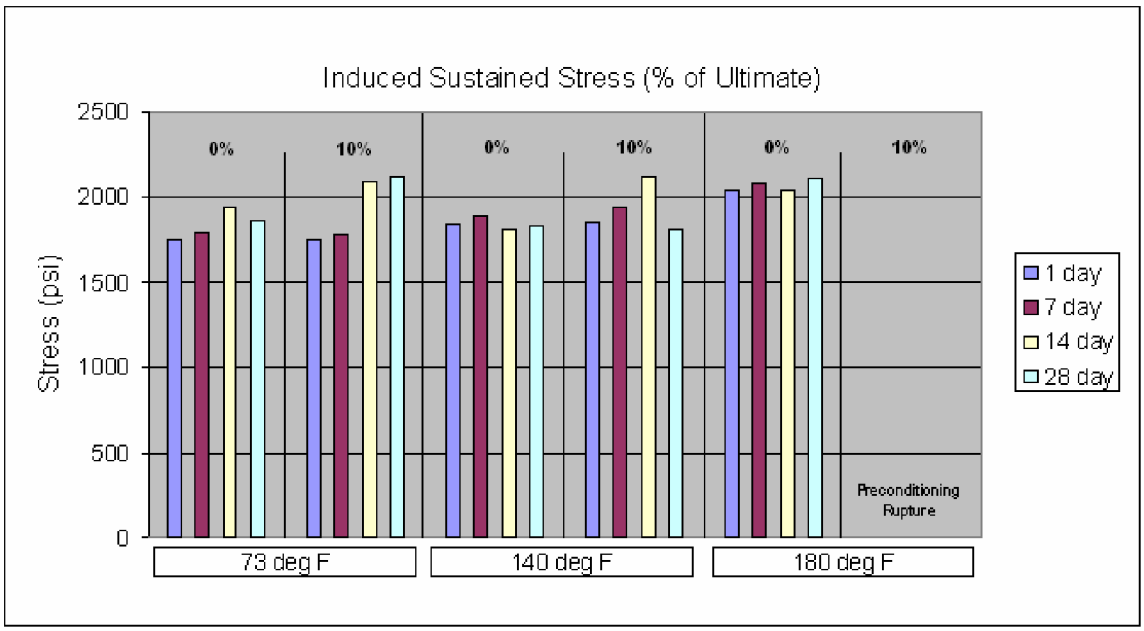

Figure 4.20 – Test I-B: Measured Strength of SS340 Specimens Soaked in Salt-water

As previously discussed in Test I-A, specimens subjected to a temperature of 140°F and sustained loading of 15 percent failed after an average of 20 days. Here in Test I-B, the adhesive's performance is subjected to 140°F conditions at slightly reduced sustained loads of 10 percent. Specimens soaked in 140°F water at 10 percent sustained stress show a 25 percent reduction in strength for the 14 and 28-day specimens when compared to the 1 and 7-day specimens. Test results indicate that the adhesive exposed to sustained stresses up to 10 percent and temperatures of 140°F or higher, could produce strength reduction in the range of 25 percent. The results show also that the adhesive can not be subjected to combined temperature of 180°F for any sustained load. Results suggest that maximum temperature exposure should be around 120°F with sustained load in the range of 10 percent. From Figure 4.21, the measured deformation for specimens soaked in water is shown to decrease deformability in the range of 25 to 45 percent when exposed to temperatures of 140°F and 180°F. This trend was not observed for the case of salt-

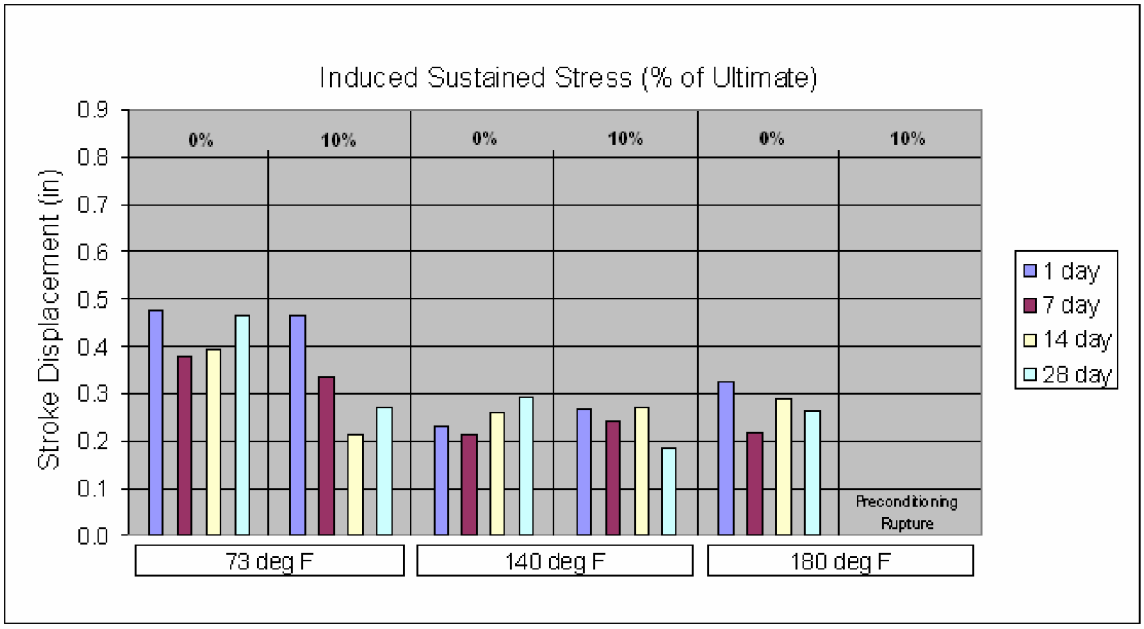

Figure 4.21 – Test 1B: Measured Stroke at Failure for SS340 Specimens Soaked in Water

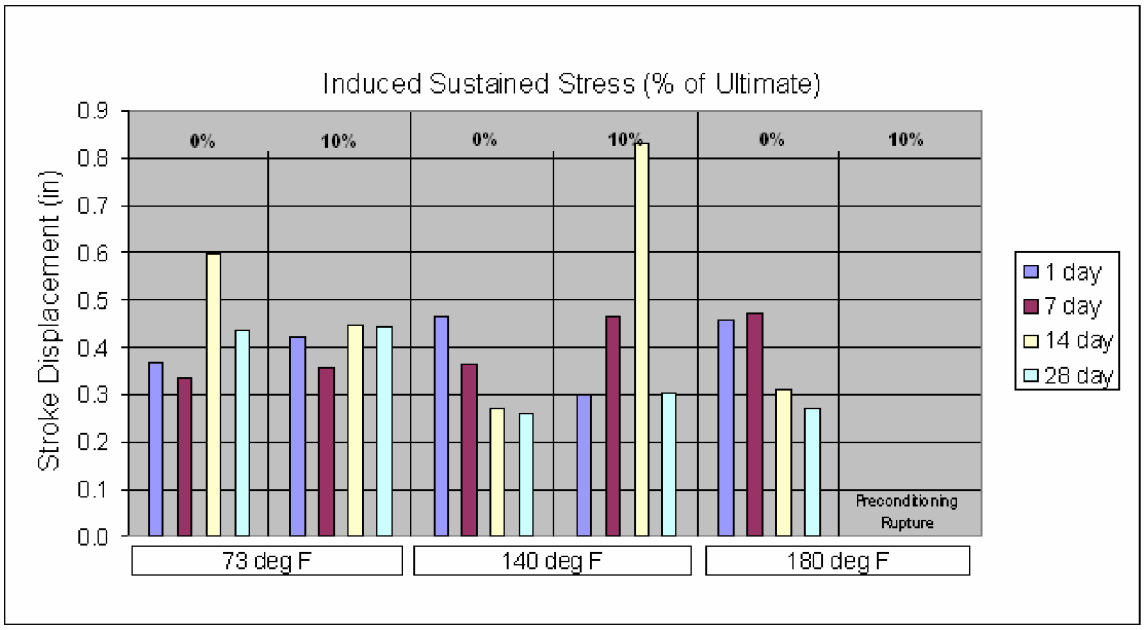

Figure 4.22 – Test I-B: Measured Stroke at Failure of SS340 Specimens Soaked in Salt-water

water soaked specimens as shown in Figure 4.22, where results indicate no overall influence on deformability by increasing the temperature. In terms of exposure time variation, it is difficult to conclude definite correlations for the strength in each case. Therefore, Table 4.5 was used to provide overall numerical values to evaluate the effect of the soaking times. The table groups all the results of unstressed specimens and the specimens subjected to sustained stress of 10% tested at each of the three temperatures using their respective soak times. The average of the results allows evaluation of the effect of soaking time for both water and salt-water soaked specimens. Each strength or stroke average in the table represents six specimens. Based on this approach, several observations can be made. Soaking time has a minimal effect on strength. For water soaked specimens, the strength slightly decreased as soak time increased. On the other hand, for salt-water specimens results show that the strength slightly increased with an increase in soak time. This variation in the average strength measurements in some cases

is insignificant and cannot be used to conclude a general trend since it is within the range of the measurements' accuracy used in this program. Table 4.6 gives the percentage changes for strength and stroke at ultimate of the salt water soaking as compared to water soaking specimens. Here again, results indicate that salt water does not have a significant reduction on the strength. However, results show an increase of the measured stroke for the specimens soaked in salt-water by 35 percent in comparison to water soaking. These results suggest that salt water soaking improves overall deformability when compared to the water soaked condition. However, there is no real justification that can be used to support this observation. Further investigation with multiple specimens at each condition should be performed to improve the accuracy and confirm these unexpected results. At this state it can be concluded that salt water does not have an adverse effect on the strength behavior or the deformability.

Table 4.5 – Test I-B: Average Strength and Stroke Values for SS340 Specimens

	Water Soaked		Salt Water Soaked	
Soak Time (days)	**Average Strength (psi)**	**Average Stroke at Failure (%)**	**Average Strength (psi)**	**Average Stroke at Failure (%)**
1	2157	0.35	1847	0.40
7	2119	0.28	1898	0.40
14	1990	0.28	2001	0.49
28	1989	0.30	1949	0.34
Average	**2064**	**0.30**	**1924**	**0.41**

Table 4.6 – Test I-B: Strength and Stroke Changes from Water to Salt-water Soaking for SS340 Specimens

Soak Time (days)	Strength Change from water to salt-water	Stroke Change from water to salt-water
1	-14.4%	14.4%
7	-10.4%	44.2%
14	0.6%	72.4%
28	-2.0%	16.2%
Average	**-6.8%**	**35.3%**

4.3 Phase II: Double Lap Shear Strength

Double lap shear specimens, survived the environmental exposure test, were tested to failure using an Instron testing machine. The load was applied using a displacement control rate of 0.05 in/sec according to the ASTM Standard D-3528. A load cell, with a maximum capacity of 10,000 lbs, was used to measure the applied force. Displacement of the hydraulic piston (stroke) was used to measure deformation. Stress and stroke displacement were recorded every 0.1 seconds by an electronic data acquisition.

4.3.1 Double Lap Shear Control Specimens

A series of trials using different preparation methods were performed to ensure the success of the undertaken experimental program. The initial double lap specimens were designed using 1/8" CPVC tabs. This configuration was not successful since failure occurred away from the lap splice zone. The second generation of the specimens used 3/8" CPVC tabs to examine bonding of the CPVC-to-steel interface. This configuration required additional cutting at the end in order to fit in the environmental chamber as well as meet the 1/2" maximum width limitation of the Instron testing grips. The first successful specimen, Group A specimens used 1/2" bond overlap, sandblasting of the steel tab, and used weight to induce pressure during the curing process. Group B specimens used a 1" bond overlap, hand sanding of the steel tab, and clamps for curing. Control specimens for each group were used to determine the baseline shear strength of the two lap shear designs. These control specimens were not subjected to the environmental exposure. The measured average shear strength was used to determine the applied sustained load as a percentage of the ultimate strength during the environmental exposure. Results of group A control specimens are shown in Figure 4.23 and Table 4.7,

where two specimens were post-cured and two were non-post-cured, respectively. Post-curing of the adhesive, include subjecting the specimens to high temperature of 180°F for one hour as recommended by the manufacture to increase the bond characteristics of the adhesive. Test results indicate a slight increase of the strength. The average measured strength of the post-cured specimens was 1360 psi. The average measured strength of the

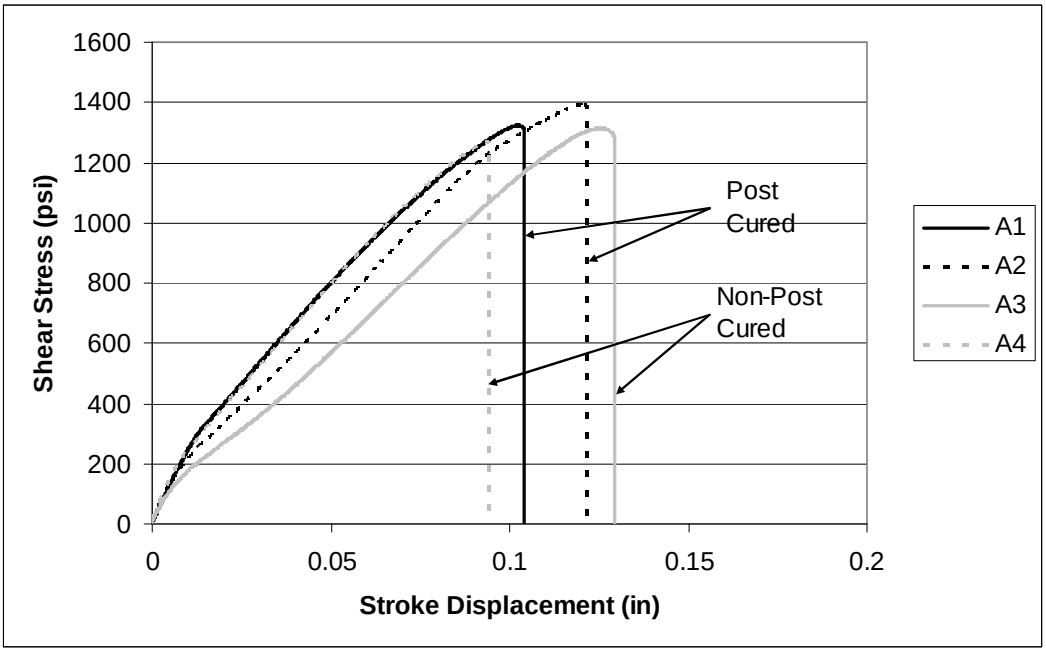

Figure 4.23 – Control Specimens for Lap Shear Group A: Post-Cured and Non-Post-Cured

Table 4.7 – Summary of Control Specimens for Lap Shear Group A: Post-Cured and Non-Post-Cured

Specimen	Post Cured	Shear Stress at Failure (psi)	Stroke Displacement at Failure (in)
A1	Yes	1325	0.10
A2	Yes	1394	0.12
A3	No	1315	0.13
A4	No	1270	0.09
Post Cured AVG		**1360**	**0.11**
Std Dev		31.9	0.025
Non Post Cured AVG		**1293**	**0.11**
Std Dev		31.9	0.025
Total AVG		**1326**	**0.11**
Std Dev		51.4	0.016

non-post-cured specimens was 1293 psi. The difference is within 5 percent. Based on these results, the ultimate shear strength of the control specimens was selected to be 1360 psi and was used to determine the level of the sustained loading to be used for the environmental exposure study. Test results of the control specimens, group B, are shown in Figure 4.24 and Table 4.8. Initially, two specimens were post-cured and two were not

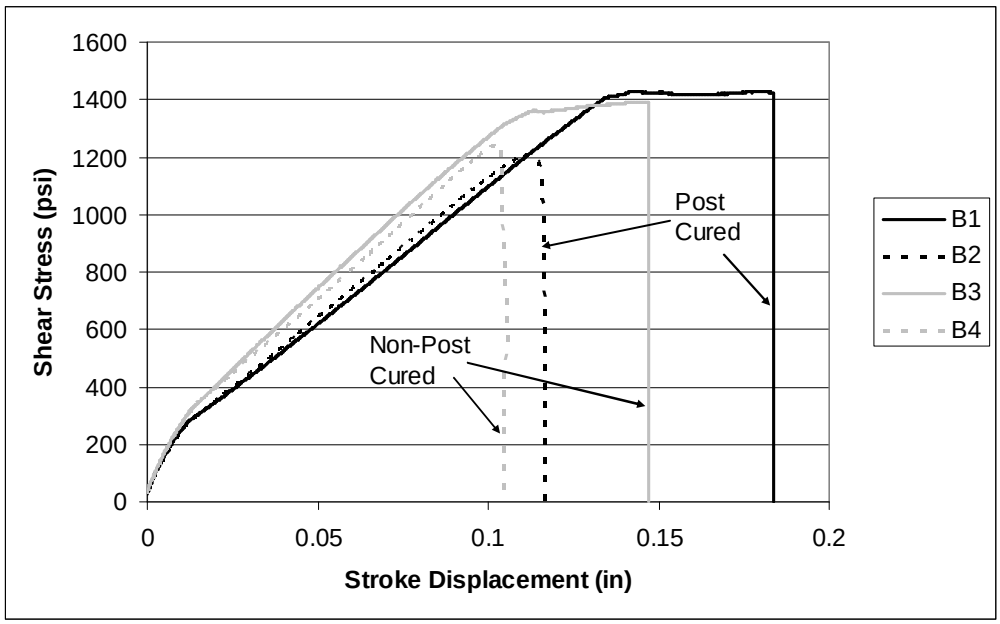

Figure 4.24 – Control Specimens for Lap Shear Group B: Post-Cured and Non-Post-Cured

Table 4.8 – Summary of Control Specimens for Lap Shear Group B: Post-Cured and Non-Post-Cured Averages

Specimen	Post Cured	Shear Stress at Failure (psi)	Stroke Displacement at Failure (in)
B1	Yes	1430	0.18
B2	Yes	1209	0.12
B3	No	1392	0.15
B4	No	1247	0.11
Post Cured AVG		**1319**	**0.15**
Std Dev		102.3	0.029
Non Post Cured AVG		**1319**	**0.13**
Std Dev		102.3	0.029
Total AVG		**1319**	**0.14**
Std Dev		107.6	0.035

post-cured. Test results indicate that there is no need for post-curing since the averages for post cured and non-post cured were at the same magnitude of 1319 psi. Since the maximum value occurred for a post-cured specimen, all test specimens used in this program were post-curing to comply with the manufacture's recommendation. Three additional post-cured specimens were tested to validate the measured value obtained from the first tests. The measured data for group B control specimens, shown in Figure 4.25 and Table 4.9, provide even higher strength from the first test group. Overall, the average post-cured values were 1413 psi. Based on these results, the ultimate shear strength of 1400 psi was selected for the group B lap shear specimens and was used to determine the level of the sustained loading to be used for the environmental exposure study.

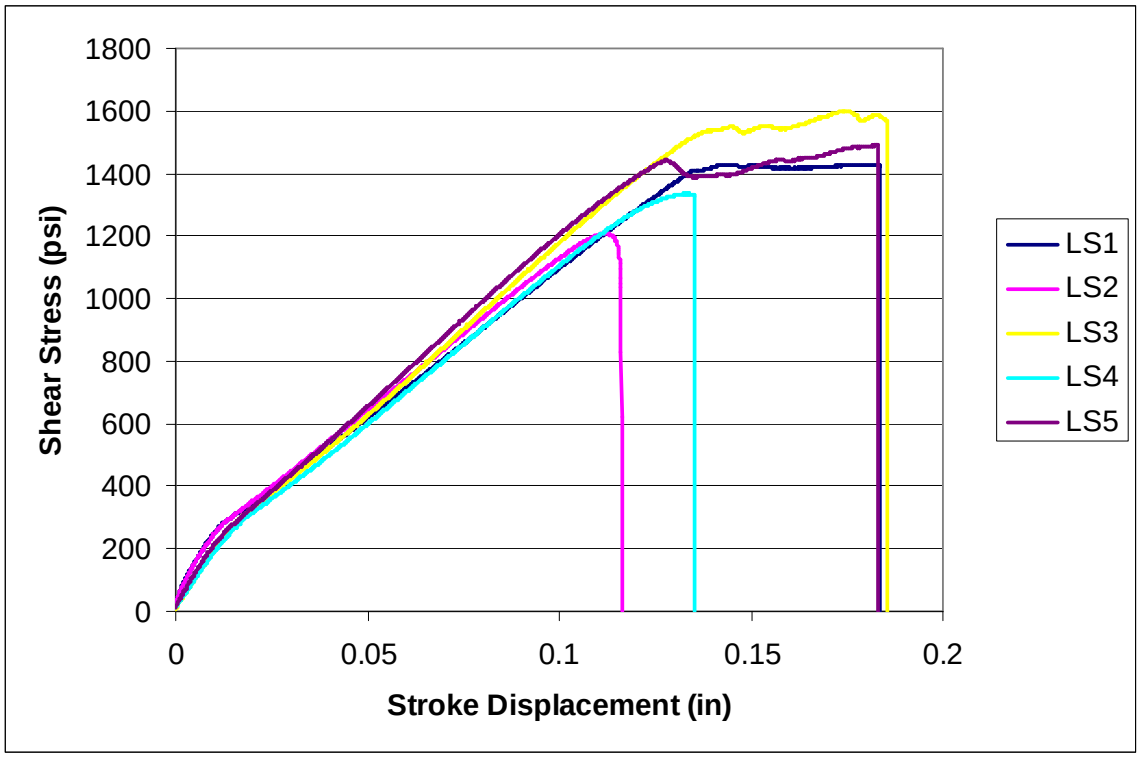

Figure 4.25 – Control Specimens for Lap Shear Group B

Table 4.9 – Summary of Control Specimens for Lap Shear Group B

Specimen	Post Cured	Shear Stress at Failure (psi)	Stroke Displacement at Failure (in)
LS1	Yes	1430	0.18
LS2	Yes	1209	0.12
LS3	Yes	1601	0.18
LS4	Yes	1336	0.14
LS5	Yes	1491	0.18
	AVG	**1413**	**0.16**
	Std Dev	149.3	0.032

4.3.2 Double Lap Shear Group A Specimens

To study the effect of the environments on the behavior of the adhesive for steel-to-CPVC specimens, the length of the overlap for the shear specimens was1/2" according to the experimental program described in Table 3.5. The behavior under the environmental condition was conducted at different sustained load levels and different levels of temperature. In each case, two specimens were tested at each condition and were subjected to environmental conditions for 30 days or until failure. Figure 4.26 shows the days survived by the test specimens. Results indicate that specimens either failed within the first few days or lasted the entire 30-day period. The only specimens survived were the unstressed specimens and those subjected to a sustained stress of 15 percent at a temperature of 73°F. Test results for the failed specimens indicate a substantial loss of adhesive shear strength when exposed to high temperatures in water. Figure 4.27 illustrates a typical failure of a lap shear specimen loaded by the Instron testing machine. Figure 4.28 shows the typical bond failure for specimens exposed to temperatures of 73°F. The failure in this case is a cohesive failure, where the failure occurs in the adhesive layer. A rough adhesive layer remains on both the steel and CPVC surfaces in a cohesive failure. Figure 4.29 displays a typical adhesive bond failure for specimens

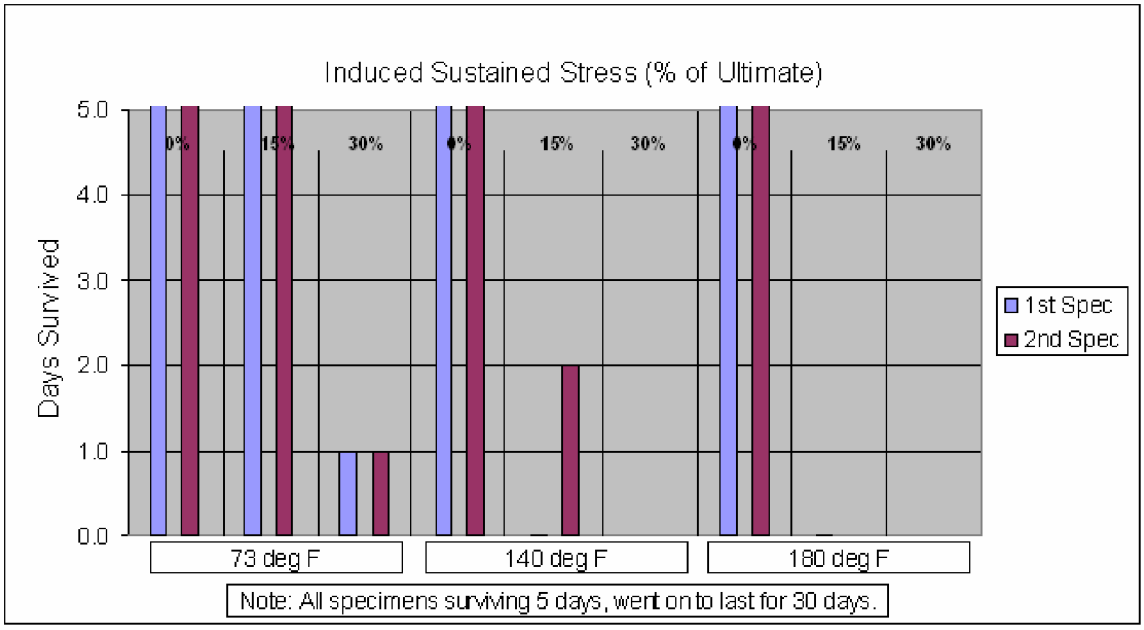

Figure 4.26 – Test II-A: Lap Shear Days Survived



Figure 4.27 – Instron Lap A



Figure 4.28 – Typical Lap A Cohesive Bond Failure

tested at temperatures of 140°F and 180°F. Adhesive failure occurs when the failure takes place between the adhesive and the steel substrate. The failure in this case produces a smooth layer of adhesive still fixed to the CPVC. No adhesive remains on the steel surface, evident by the observed smooth surface. Figures 4.30 and 4.31 show the

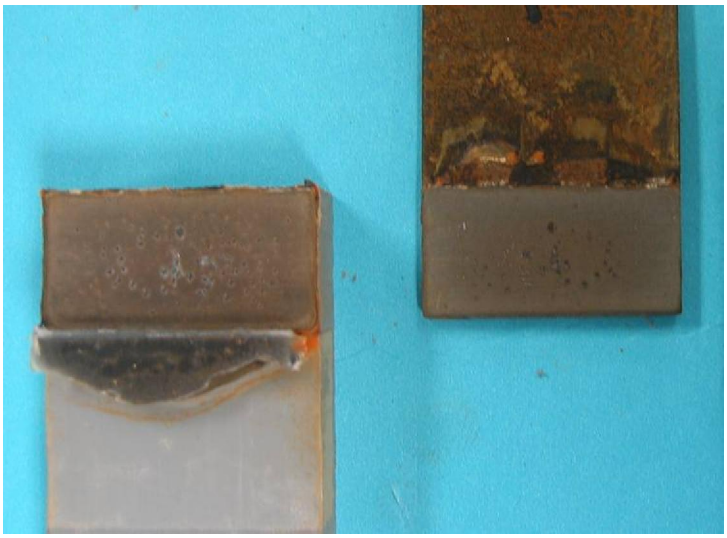

Figure 4.29 – Typical Lap A Adhesive Bond Failure

measured maximum shear stress and stroke at failure for ach case. Results indicate that both strength and overall specimen displacement decrease for unstressed specimens soaked at high temperatures. The measured strength of specimens tested at 140°F dropped by about 25 percent compared to specimens at 73°F. Additionally, the measured strength of specimens tested at 180°F dropped by about 50 percent compared to

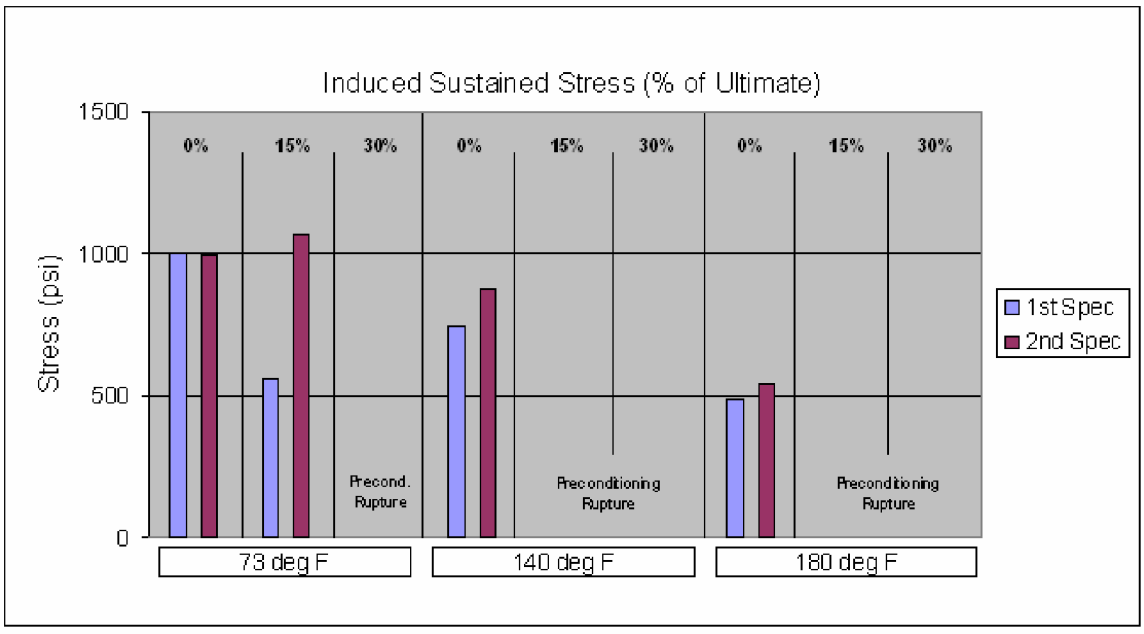

Figure 4.30 – Test II-A: Lap Shear Strength

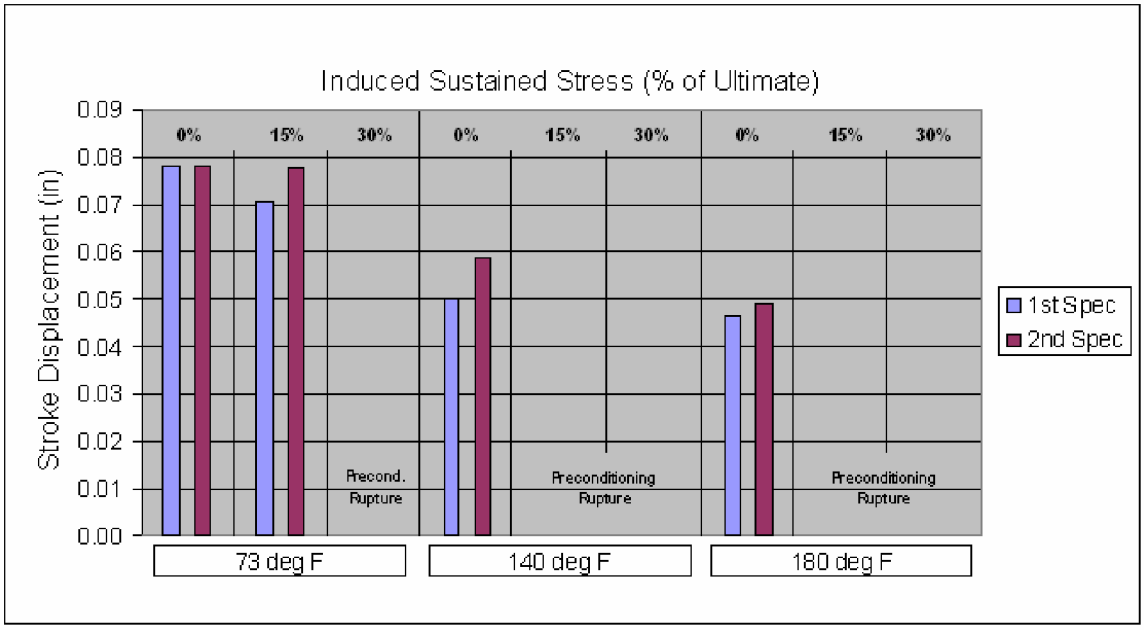

Figure 4.31 – Test II-A: Lap Shear Stroke Displacement at Failure

specimens subjected to 73°F. The displacement at failure has a similar decreasing trend. The strength variation measured for specimens survived the temperature exposure of 73°F and sustained loading of 15 percent could be due to possible variation of the application of the adhesive used in each case. Great care and consistency was followed throughout the bonding phase, still some specimens measured significantly reduced strengths and/or displacement at ultimate. In this instance, the first specimen only achieved half the strength of the second specimen. The strength reduction could likely be attributed to the weighted curing of the specimen. If the weight distribution was uneven or at a slight angle, the bond produced for the lap shear would likewise be undistributed and contribute to a premature failure. For group A specimens alone, the results suggest limiting the sustained load to a maximum level of 15 percent and to a temperature range of 73°F but less than 140°F. Other than the unstressed specimens, group A specimens provided insufficient results to identify the effects of temperature and sustained stresses. Therefore, adjustments were made by altering the design and environmental conditioning

to produce more consistent results by using another set of specimens, identified as group B presented in the following section.

4.3.3 Double Lap Shear Group B Specimens

To study the effect of the environments of the behavior of the adhesive for the steel-to-CPVC 1" bond overlap shear specimens, the experimental program was performed according to the procedue described in Table 3.6. Environmental conditions were less severe for group B than for group A. Instead of 15 and 30 percent induced sustained stresses, a sustained load range between 8 and 15 percent were used. For temperature, 180°F was replaced with 120°F, therefore the 140°F became the maximum exposure temperature. Two specimens were tested for all conditions, and two additional specimens were tested for the more extreme temperature and sustained stress conditions. This produced more conclusive results and averages for the more unpredictable environmental conditions. All specimens were subjected to environmental conditions for 30 days or until failure. Figure 4.32 shows the days survived by each specimen. Results indicate

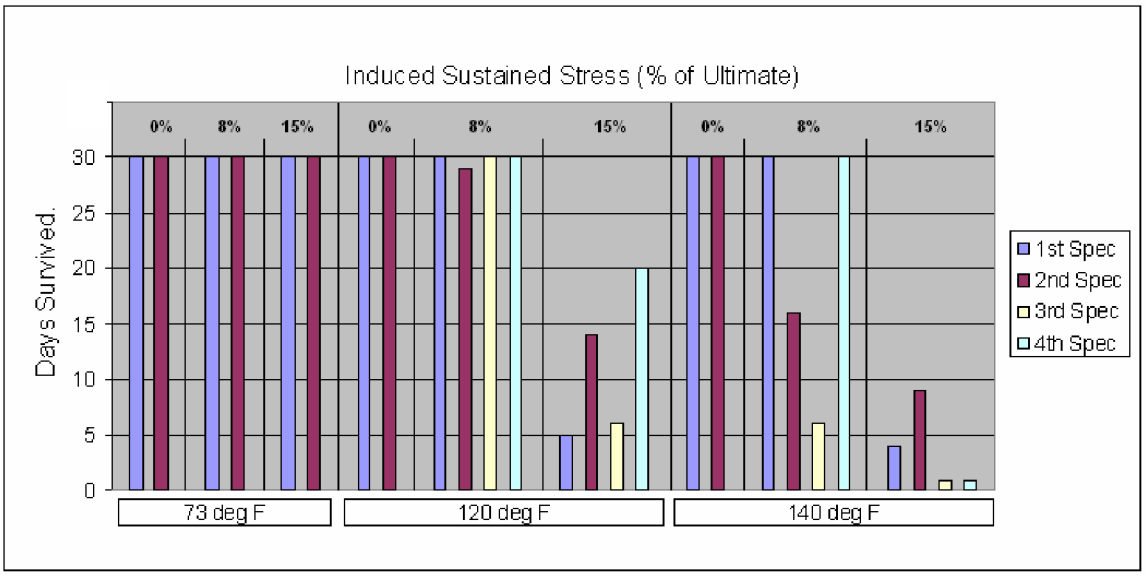

Figure 4.32 – Test II-B: Lap Shear Days Survived

that the lap bond did not survive combined sustained stresses of 15 percent at temperatures of 120°F and 140°F. Specimens loaded at 15 percent stress and heated to 120°F survived an average of 11 days, while specimens heated to 140°F survived an average of 4 days. Results also indicate that the majority of the lap bond subjected to temperatures of 140°F and 8 percent sustained stress can survive these imposed environmental conditions. Although two specimens survived the 30 day period, two failed prematurely for a survival average of 20 days. Figure 4.33 illustrates a typical lap shear failure in the Instron testing machine. Figure 4.34 shows the typical bond failure after being tested in the Instron for specimens exposed to temperatures of 73°F. This cohesive type failure indicates that the adhesive bond remains intact at the steel and CPVC interfaces, since a rough adhesive layer remains on both the steel and CPVC surfaces. Figure 4.35 displays a typical bond failure occurring in the environmental exposure test for specimens subjected to temperatures of 140°F and 180°F. This is a combination type bond failure. Most of the failure is adhesive from the steel substrate,



Figure 4.33 – Instron Lap B

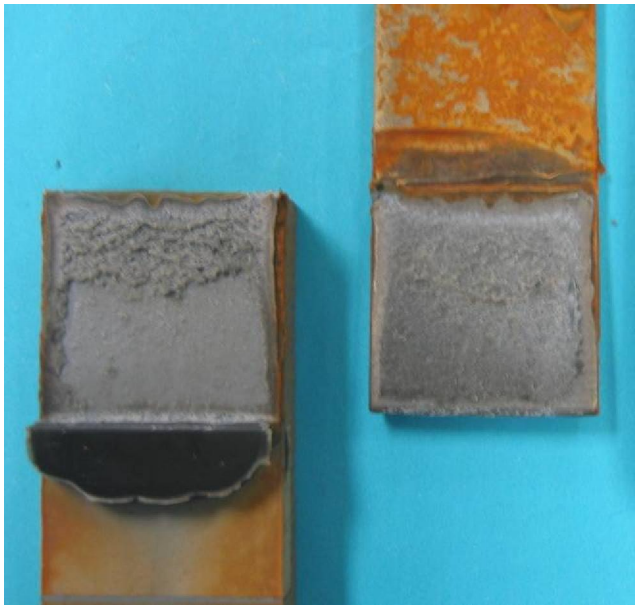

Figure 4.34 – Typical Lap B Cohesive Bond Failure

while a small portion of the adhesive remains intact as a cohesive failure on the steel. Figure 4.36 shows a typical failure of a heated and stressed specimen that survived the environmental test. Some of the specimens exhibited a combination adhesive/cohesive failure. Here, the bond adhesively failed on both the steel and CPVC surfaces. The adhesive failure on the steel was located around the perimeter of the bond, while the adhesive failure on the CPVC was located in the center. Some cohesive failure was also



Figure 4.35 – Typical Lap B Adhesive Bond Failure in Environmental Test



Figure 4.36 – Typical Lap B Adhesive/Cohesive Bond Failure

located in the center of the bond area, as shown in Figure 4.36. These figures clearly display the influence of the water, stress, and temperature to the adhesive's lap shear properties. Analysis of the survived specimens can be made by referencing Figures 4.37 and 4.38. Figure 4.37 shows the measured maximum shear stress and Figure 4.38 shows the overall specimen displacement at failure. Results for specimens tested at 73°F exhibit

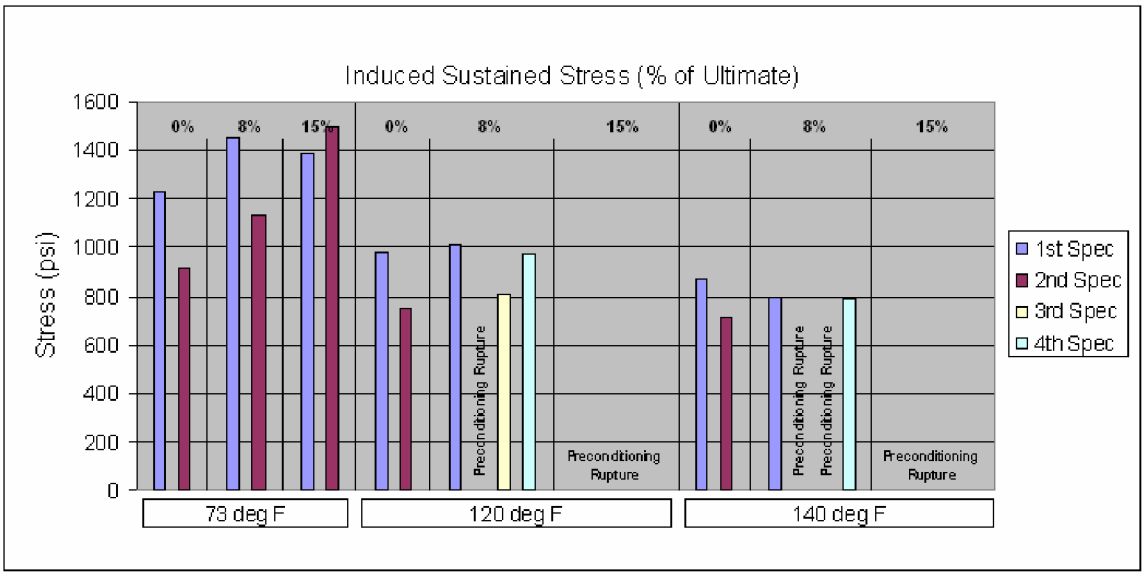

Figure 4.37 – Test II-B: Lap Shear Strength

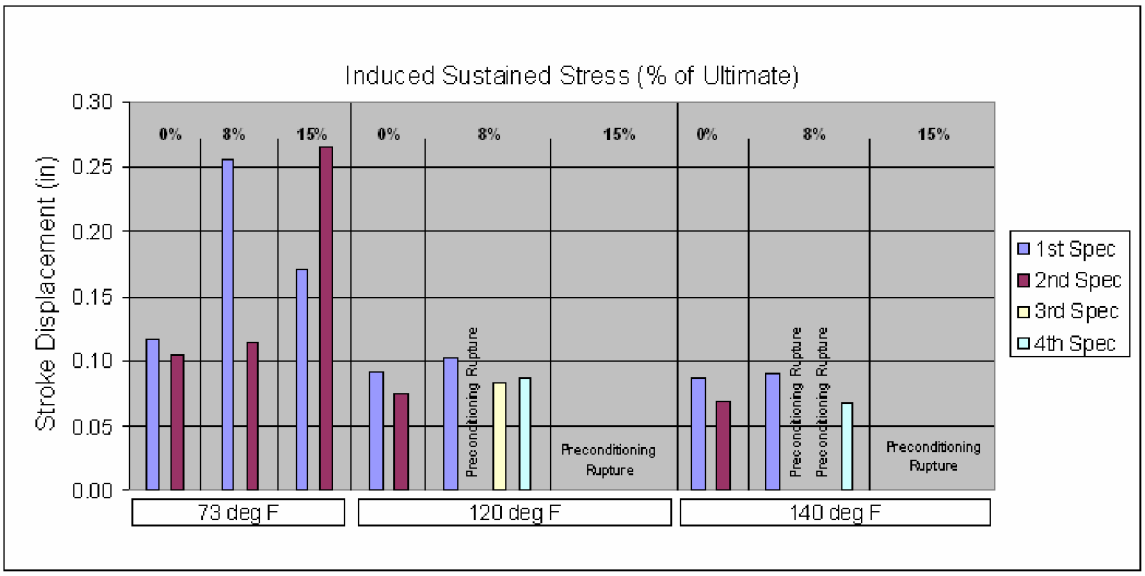

Figure 4.38 – Test II-B: Lap Shear Max Stroke Displacement at Failure

some irregularity, however, clear correlations can still be observed. Test results indicate that the adhesive can carry sustained load up to 15 percent at room temperature without any sign of degradation. Two of the specimens achieved 0.25"stroke displacement at failure of the CPVC substrate while being tested in tension. This behavior indicates that the adhesive bond was stronger than the CPVC tensile strength. For the specimens subjected to 120°F and 140°F, the strength was reduced by one third. The displacement at failure as also significantly reduced. For specimens tested at 8 percent sustained load and 120°F, three specimens survived and one failed at day 29. These results indicate that such loading and temperature conditions would likely be acceptable with extremely rigid bonding specifications. However, specimens with 8 percent sustained load and 140°F soaking would likely be unacceptable despite two of the four specimens surviving. One of those failures occurred after six days in the environmental exposure test, while the other failure occurred at 15 days only. Visual inspection of these two failures indicated no presence of bonding irregularities. Therefore, field use of the adhesive subjected to the same conditions could potentially be hazardous. Further investigation of specimens soaked at 140°F and lower induced sustained stresses would likely yield acceptable results. Results clearly indicate that to bond CPVC-to-steel subjected to sustained loads of 8 percent of adhesive ultimate strength, the maximum temperature that can be used without significant reduction of strength and deformability is 120°F.

Double lap shear salt-soaked specimens were tested according to the experimental program described in Table 3.7. The six specimens were subjected to ambient conditions of 73°F. All specimens survived the 30 day testing period. The corroded specimens, stacked two-high, are shown in Figure 4.39 prior to failure testing. Bond failures were similar to the 73°F water soaked specimens. Figure 4.40 shows a typical cohesive failure for the lap specimens. Figures 4.41 and 4.42 show the measured maximum shear stress and stroke displacement at failure for each case. Results show that the induced sustained stresses of 15 and 30 percent do not have an effect on the strength or overall specimen displacement for the lap bond. Average specimen lap strength is only marginally lower than the 1400 psi control specimens, which indicates no effect of salt soaking. Comparing the salt-soaked specimens with water-soaked specimens at 73°F (found in Figures 4.37 and 4.38) may indicate that salt-soaking results in no difference from water soaking.



Figure 4.39 – Corroded Salt Specimens Prior to Failure



Figure 4.40 – Typical Lap B Salt Cohesive Failure

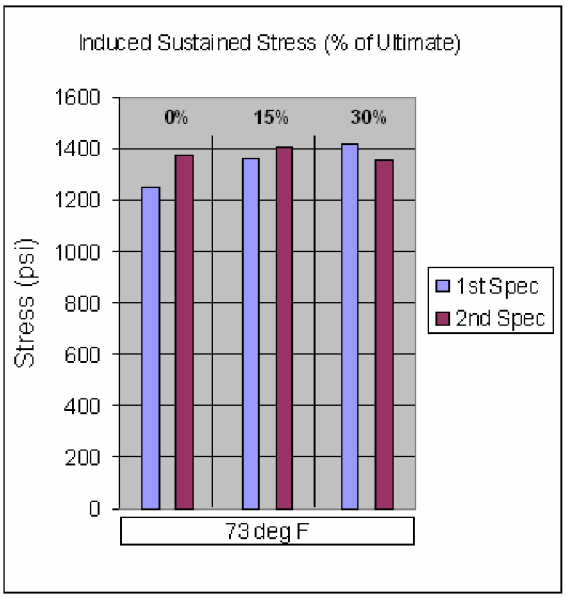

Figure 4.41 – Test II-B Salt: Strength

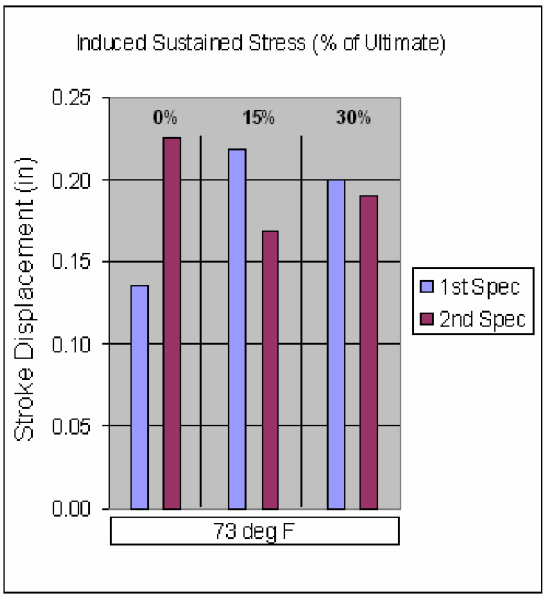

Figure 4.42 – Test II-B Salt: Displacement

4.4 Phase III: Thermal Strain Gradient

The behavior of the 4" by 8" small scale model of the proposed tank lining was investigated through a series of heated bath tests. It is strongly believed that basic material properties for the steel, CPVC, and adhesive are critical to the development of the thermal gradient strain results. Therefore the first phase of the thermal strain gradient test procedures was to experimentally characterize the thermal expansion behavior of individual material used in the current study. Three tests were conducted for each of the steel and CPVC plates to measure their coefficients of thermal expansion in both the long and short directions. Each test was repeated three times and the CTE was calculated based on the average of all tests. The steel plates were then bonded to the CPVC plates using adhesive thicknesses of 30, 50, and 80 mils. Verification of the measured data with a finite element model was performed on the bonded specimens with 80 mils adhesive thickness.

4.4.1 Coefficient of Thermal Expansion

Since the strain gages selected in the testing program were temperature-compensated for steel, they were not affected by accelerating the temperature, which was varied from 73°F to 180°F. The strain gages were used to measure the strain due to expansion of the steel produced by the applied temperature range. To determine the actual strain, a baseline set of data for the strain gages must be determined using a reference material with a known coefficient of thermal expansion. The simplest approach to accumulating baseline data is by testing a material with a negligible coefficient of thermal expansion. Titanium silicate was selected in the current testing program as an excellent reference material since it has an extremely small CTE (Vishay Tech Note 513). This glass material possesses a CTE of

almost zero value when subjected to the temperature range considered in the test program. As shown previously in Figure 2.3, the largest magnitude strain is almost -2 ppm/^{o}F, which occurs at 100°F. At any temperature, the tensile strain in the steel, adhesive, and CPVC materials were adjusted using the strain measurements produced by the titanium silicate. The following equation describes the adjustment:

$$\varepsilon_{adj} = \varepsilon_{measured} - \varepsilon_{ts} \quad (4.1)$$

where ε_{adj} is the adjusted strain in the steel, adhesive, and CPVC, $\varepsilon_{measured}$ is the measured strain in these materials, and ε_{ts} is the strain in the titanium silicate at a certain temperature. The following section attempts to develop a strain-temperature relationship for the titanium silicate. The proposed relationship will be verified for a wide range of temperatures and will be used to adjust the strain measurements in the steel, adhesive, and CPVC.

4.4.1.1 Titanium Silicate Adjustment

To achieve an accurate strain-temperature relationship for the titanium silicate, six tests were performed. Three tests were performed in the precision oven and three tests were performed using the test bath. Strain-temperature behavior for both the oven and bath data are plotted and shown in Figure 4.43. Regression analysis clearly showed that the behavior can be approximated using a linear relationship of the strain and the temperature. Though some values fall slightly off from best-fitting line, especially those of the bath tests, the best-fitting line using the two groups of tests indicate good agreement. Figure 4.44 shows the combined data, with the best fitting line encompassing all six tests comprising of 5040 data points. Based on the linear regression analysis, the

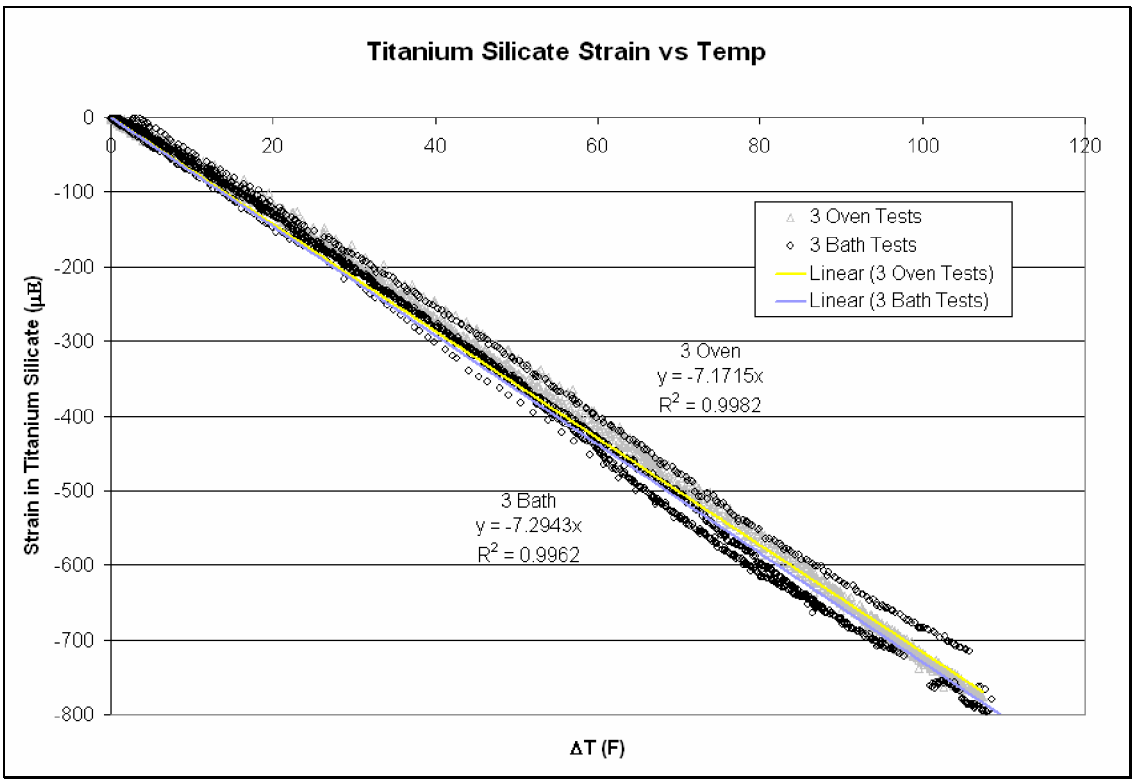

Figure 4.43 – Titanium Silicate Oven and Bath Data

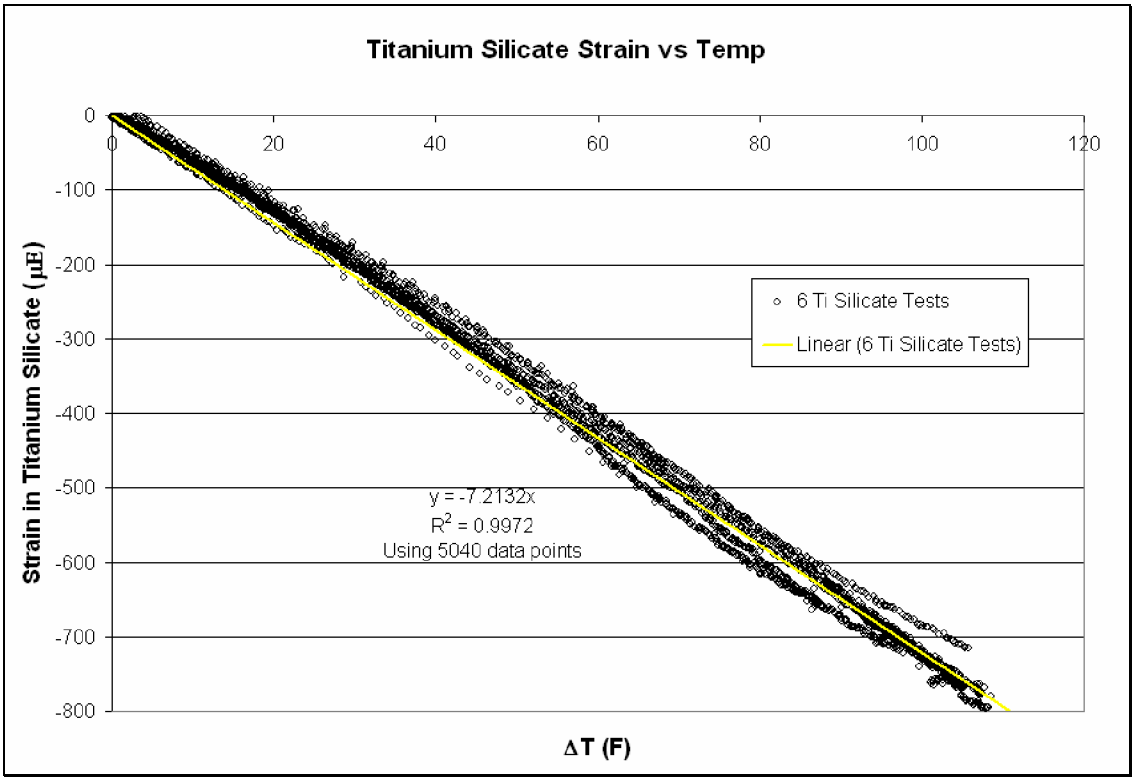

Figure 4.44 – Titanium Silicate Combined Data

strain in the titanium silicate, ε_{ts}, can be expressed by the following equation:

$$\varepsilon_{ts} = -7.2132*\Delta T \quad (4.2)$$

where ε_{ts} is the strain in the titanium silicate and ΔT is the temperature range. This proposed equation was used to adjust the strain recordings for all strain data accumulated throughout this test phase.

4.4.1.2 Steel

After applying the proposed equation (4.2) to the steel plate specimen, results were verified by matching the measured CTE with well-known published steel CTE data. The CTE average the oven test setup was 6.61 ppm/^{o}F, which matches closely with the widely accepted 6.5 ppm/^{o}F value for steel. It should be noted that strain measurements using the oven setup were recoded after maintaining the temperature for a period of at least thirty minutes. This allowed temperatures and strains to reach steady state conditions, which is especially needed for steel since its thermal conductivity is relatively high. It was observed that steel takes much longer to absorb or dissipate heat than other materials used in the testing program. Test results showed that the CTE found by averaging the three bath and three oven tests under continuously increasing temperature was 6.94ppm/^{o}F as shown in Figure 4.45. CTE averages were made for ΔT values greater than 20°F due to the observed inconsistent behavior at low temperatures. Test results showed that the measured CTE for steel is influenced by the rate of temperature increase. Increasing the rate of temperature increases the measured CTE.

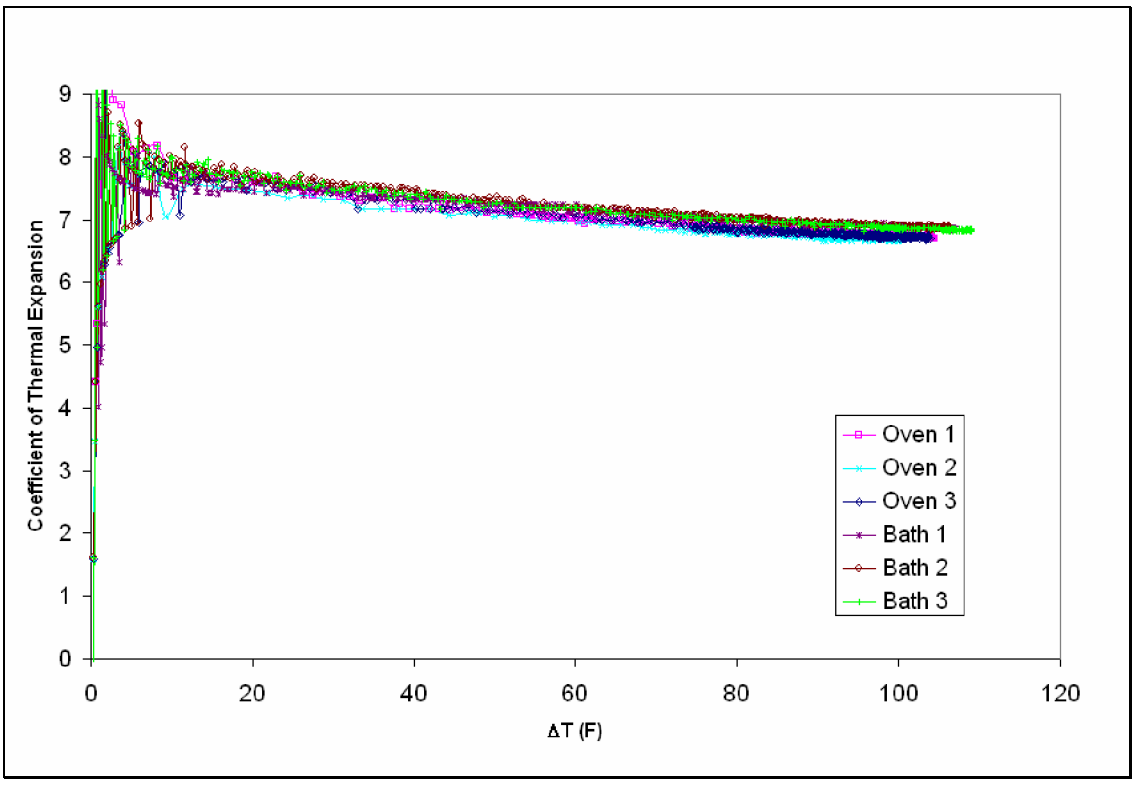

Figure 4.45 – Coefficient of Thermal Expansion of Steel

Prior to bonding with the CPVC, the bottom of the steel specimen was subjected to a temperature range of 73°F to 180°F in the test bath. Four strain gages, two attached to the top surface and two to the bottom surface in the short (y) and long (x) directions, were installed to monitor the thermal expansions during the temperature cycling. Two thermocouples, one on each side, were used to measure the temperature gradient. Three steel plate specimens were each tested three times to ensure repeatability and accuracy of strain readings. Strain results with titanium silicate adjustment for a typical steel plate specimen are given in Figure 4.46. Test results clearly show the isotropic nature of steel, indicated by the four lines being nearly identical. Results show good agreement with the reported CTE.

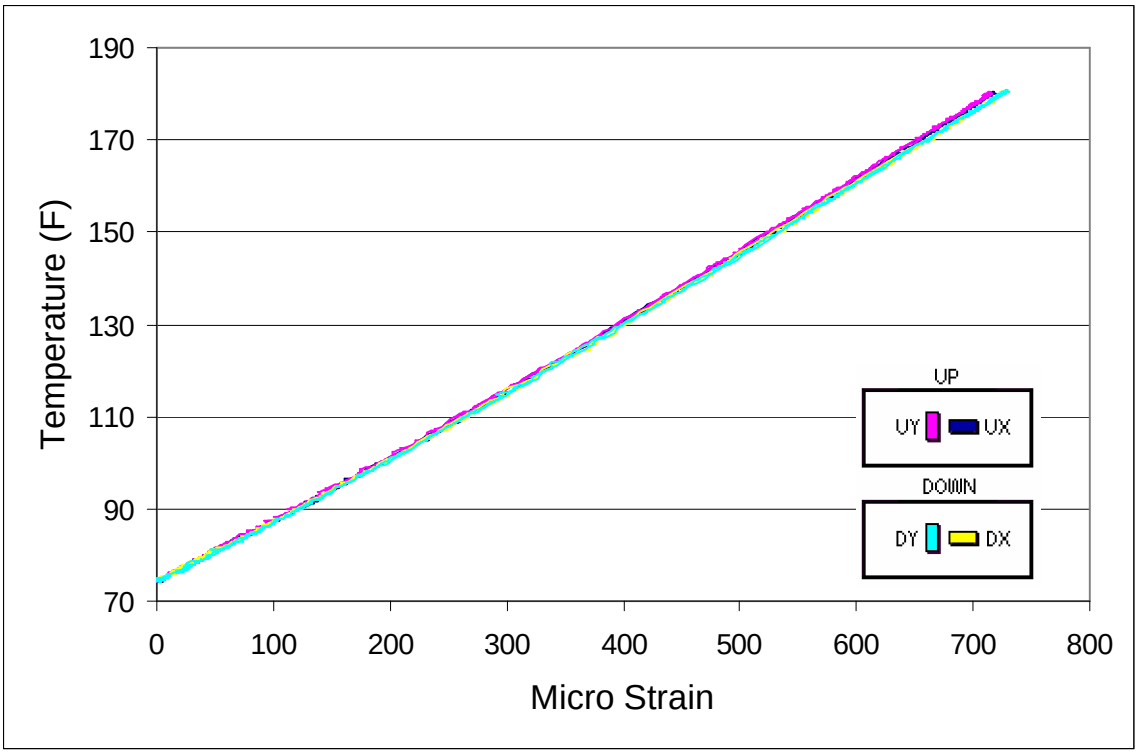

Figure 4.46 – Typical Steel Plate Thermal Expansions

4.4.1.3 CPVC

The CVPC plate was subjected to a temperature range of 73°F to 180°F. The test was repeated four times using the oven and the heat bath test setups. Two strain gages in both the short and long directions were installed to measure the CTE of the material in both directions. The measured CTE in both the short (y) and long (x) directions are shown in Figures 4.48 and 4.47, respectively. The results suggest an anisotropic behavior of the CPVC material. The measured CTE in the long direction of the plate was 44.2 ppm/^{o}F. The measured CTE in the short direction of the plate was 55.6 ppm/^{o}F, which s 27 percent higher than that measured in the long direction. Unlike the results for the steel, a close CTE correlation was observed using the oven and the heat bath setups. This is attributed to the following two reasons: First, the thermal conductivity of CPVC is 1/300th less than that of steel (Corzan n.d.-c). Secondly, the thickness of the CPVC was

1/8” compared to 1/4” for steel. The thinner the material, the easier it is to produce a uniform temperature change through the thickness. The average CTE values in the short and long directions were calculated using ΔT values greater than 20°F to eliminate the observed noise at low temperatures. Both graphs indicate CTE divergence at higher temperatures. Such a behavior could be attributed to different material characteristics of the samples used in testing. Despite the specimens being cut from the same sheet, these differences are likely attributed to the inconsistent thermal characteristics of the CPVC, which is common for many plastic materials.

Prior to bonding with the steel, the bottom of the CPVC specimen was subjected to a temperature range of 85°F to 180°F in the test bath. The starting ambient temperature for the repeated tests never reached the mid 70’s, as it did for steel. This observation,

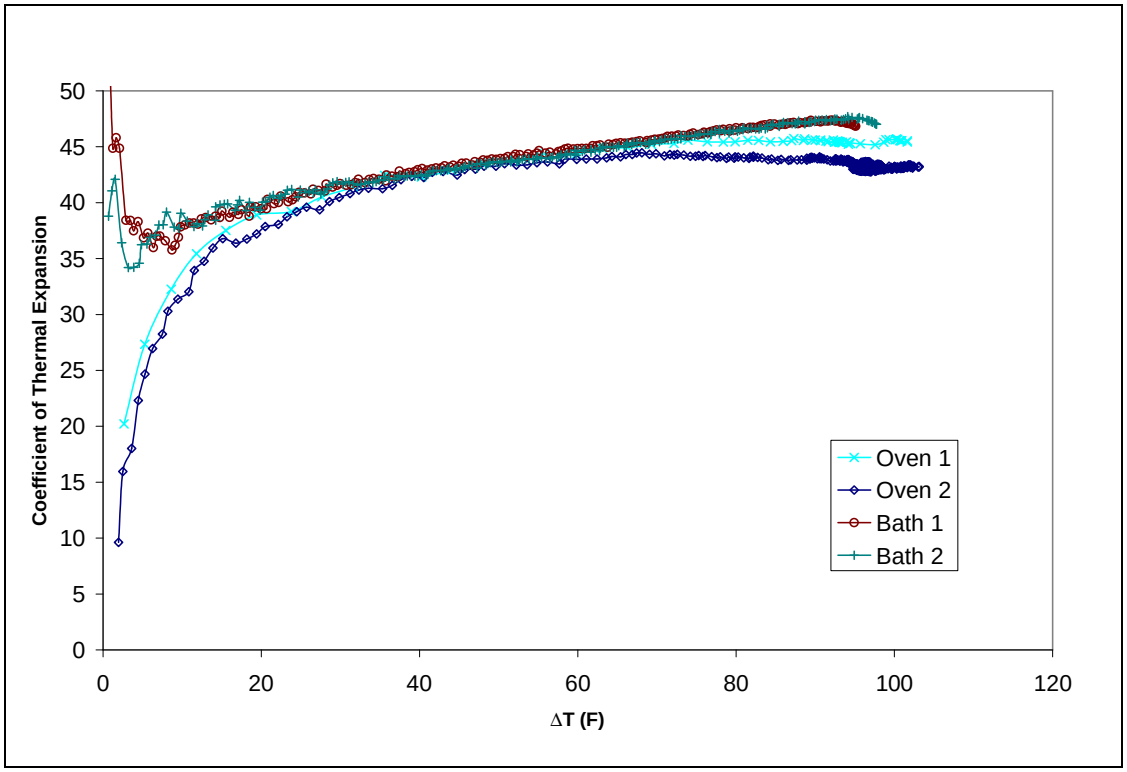

Figure 4.47 – Coefficient of Thermal Expansion of CPVC in the X-Direction

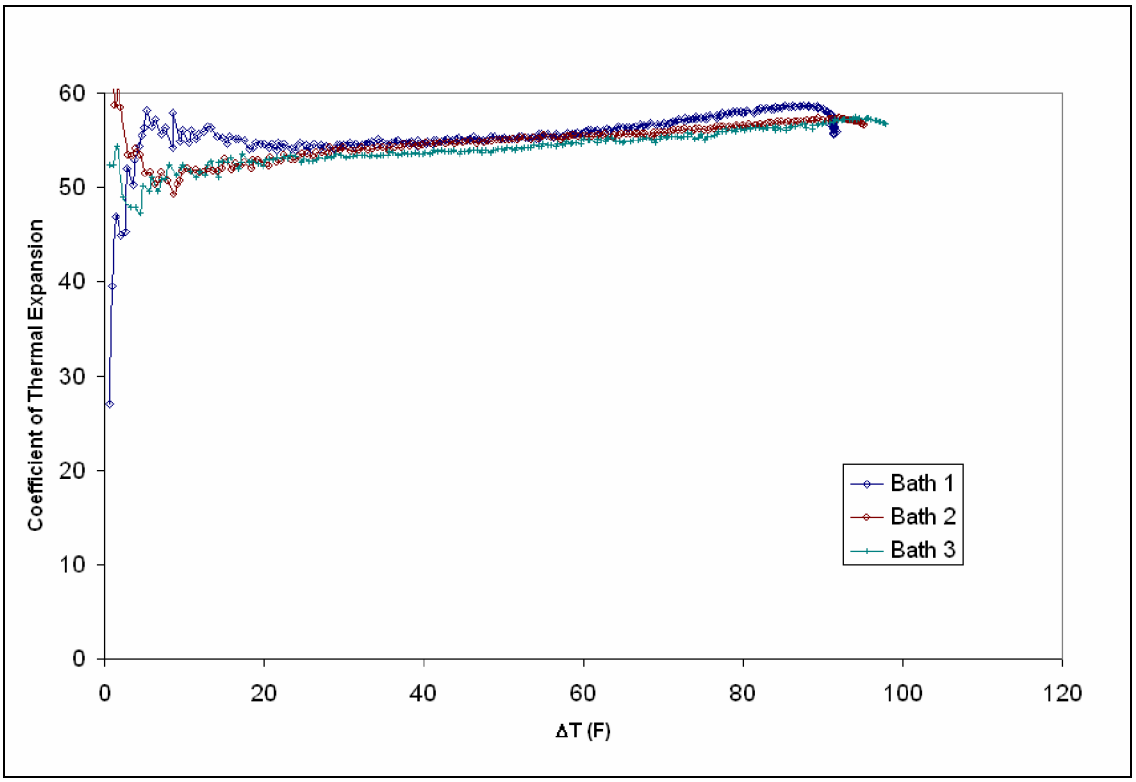

Figure 4.48 – Coefficient of Thermal Expansion of CPVC in the Y-Direction

however, does not affect the results of the test, since ΔT relationships are applied just as with steel. Two thermocouples, one on each side, were used to measure the temperature gradient. Three CPVC plate specimens were each tested three times to ensure repeatability and accuracy of strain readings. Strain results with titanium silicate adjustment for a typical steel plate specimen are given in Figure 4.49. Results clearly show the anisotropic nature of the CPVC material. The measured strains in the short direction were significantly higher than those measured in the long direction at all temperatures. Results show agreement with the measured CTE in both directions.

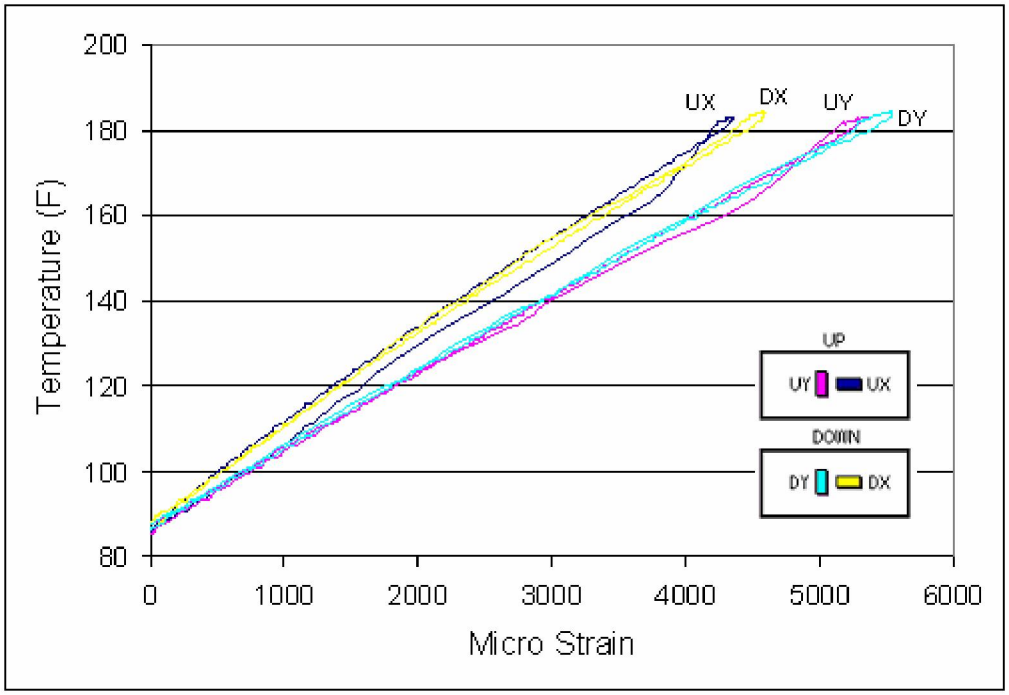

Figure 4.49 – Typical CPVC Plate Thermal Expansions

4.2.1.4 Adhesive CTE

Three oven tests were performed on an adhesive sample measuring 2" in the long direction and 1" in the short direction. Isotropic behavior for the adhesive was observed in all three tests. Figure 4.50 shows the three tests performed on the adhesive sample. Strain data was adjusted by the titanium silicate equation (4.2). The CTE slopes for each test are represented by the slope of the best fitting line for each of the three tests. Regression analysis showed that the CTE increased for each following test. However, it was noted during testing that a warping effect took place and seemed to have a greater influence at higher temperatures. This influence is clear on the results of Tests 2 and 3 at ΔT greater than $80^{o}F$. Therefore, the CTE of the adhesive would be best representative using the results of Test 1, since the data points remained the most linear throughout the test. Test 1 produced a CTE of 39 ppm/^{o}F, which was used in later stages of analysis.

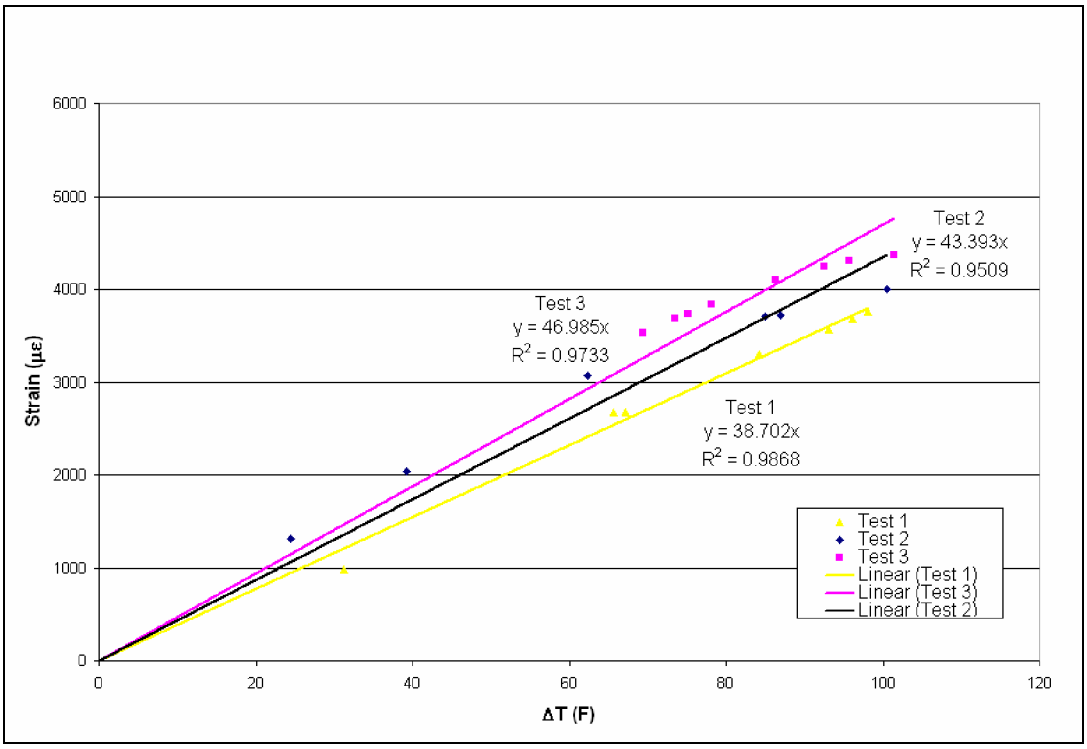

Figure 4.50 – Coefficient of Thermal Expansion of SS340 Adhesive

4.4.2 Bonded Specimens

To study the influence of thermal gradient on the bond strength of the proposed tank lining, three small scale models were constructed and tested at the Constructed Facilities Laboratory at NC State University. Each model consisted of steel and CPVC plates bonded together using SS340 adhesive. The adhesive thickness was varied from 30 to 80 mils to investigate its effect on the induced shear stresses within the adhesive layer. Detailed description of the experimental program and test setup are presented in Section 3.5. As shown in Figure 3.29, the bottom surface of the CPVC was directly exposed to the heated bath and subjected to a temperature range of 73°F to 180°F. Strain gages and thermocouples were attached to the top and bottom of the steel and CPVC materials. All the data was continuously recorded using a data acquisition system. The following sections describe in detail the observed behavior for the three specimens tested in the

current study. A finite element model was developed and validated using test results. The analysis was extended to investigate the influence of the restraint conditions and specimen dimensions on the overall behavior.

4.4.2.1 Specimen 1 (Adhesive thickness of 80 mils)

Three bath tests were conducted on specimen 1 with a nominal adhesive thickness of 80 mils. A typical temperature gradient plotted versus time is shown in Figure 4.51. As expected, the maximum temperature occurs on the bottom of the CPVC, which is directly exposed to the heat and moisture generated by the water bath. The adhesive temperature line maintains a 0-4°F temperature difference between the top of the steel plate throughout the test. When the insulating top cover is removed to allow for cooling of the specimen, it was observed that the adhesive layer maintains a slightly higher temperature than the steel and CPVC surfaces. Such a phenomenon occurs because the steel top and CPVC bottom are exposed to ambient air, while the adhesive is insulated from direct

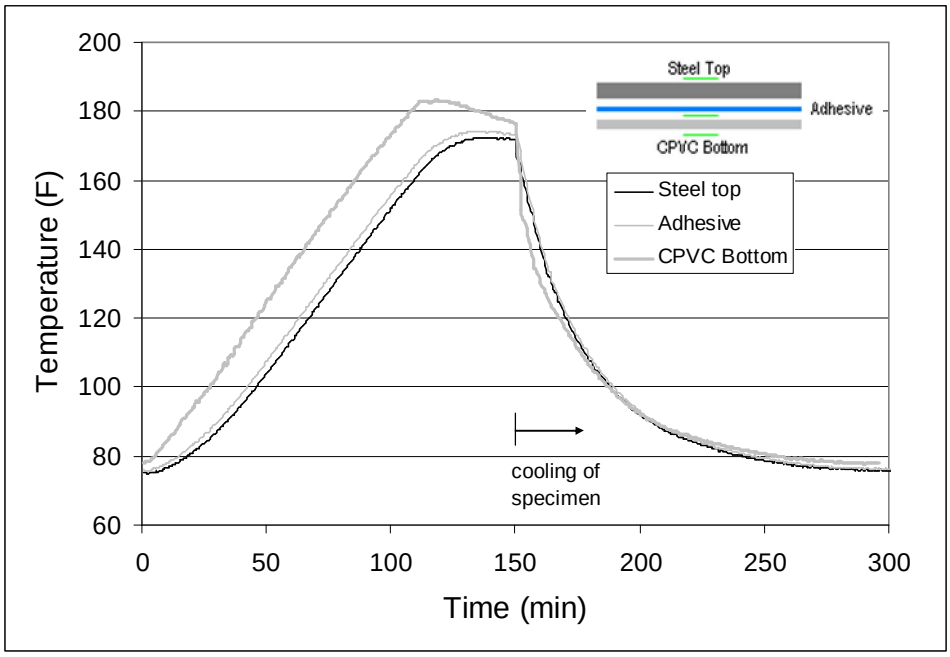

Figure 4.51 – Typical Temperature Gradient

exposure by the two materials. For most of the heating process, the steel and adhesive temperatures increase at the same rate as the CVPC bottom. However, the top steel surface maintains a temperature of about 20°F less than the CPVC surface. Once the CVPC reaches 180°F and is essentially maintained for a period of 30 minutes, the steel and adhesive layers begin to close the temperature gap and achieve a minimum ΔT of around 5°F. Typical steel strain-temperature behavior is shown in Figure 4.52. The figure includes the heating and cooling phases of the specimen as was described in Figure 4.51. Strain gages mounted on the top surface of the steel plates in the short (y) and long (x) directions are denoted as UY and UX, respectively. Similarly, strain gages mounted to the bottom surface are denoted as DY and DX. Figure 4.53 depicts the results of the four strain gages located in the x and y-directions on the CPVC plate. Test results showed linear strain behavior for both the heating and cooling phases at the top and

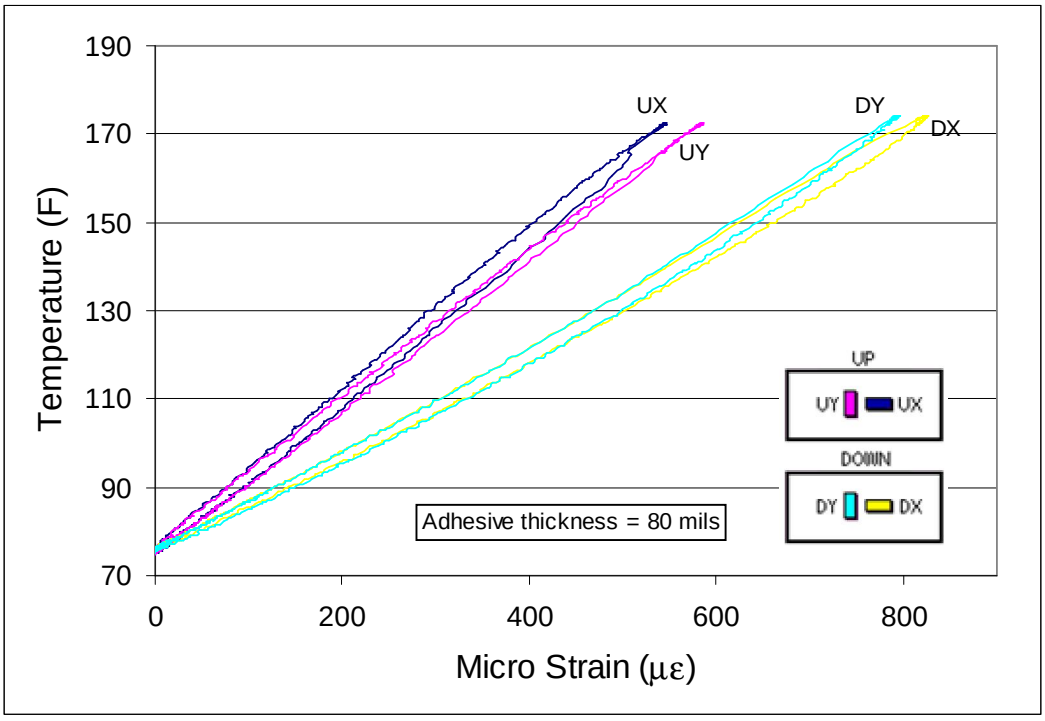

Figure 4.52 – Measured Steel Strain of Specimen 1

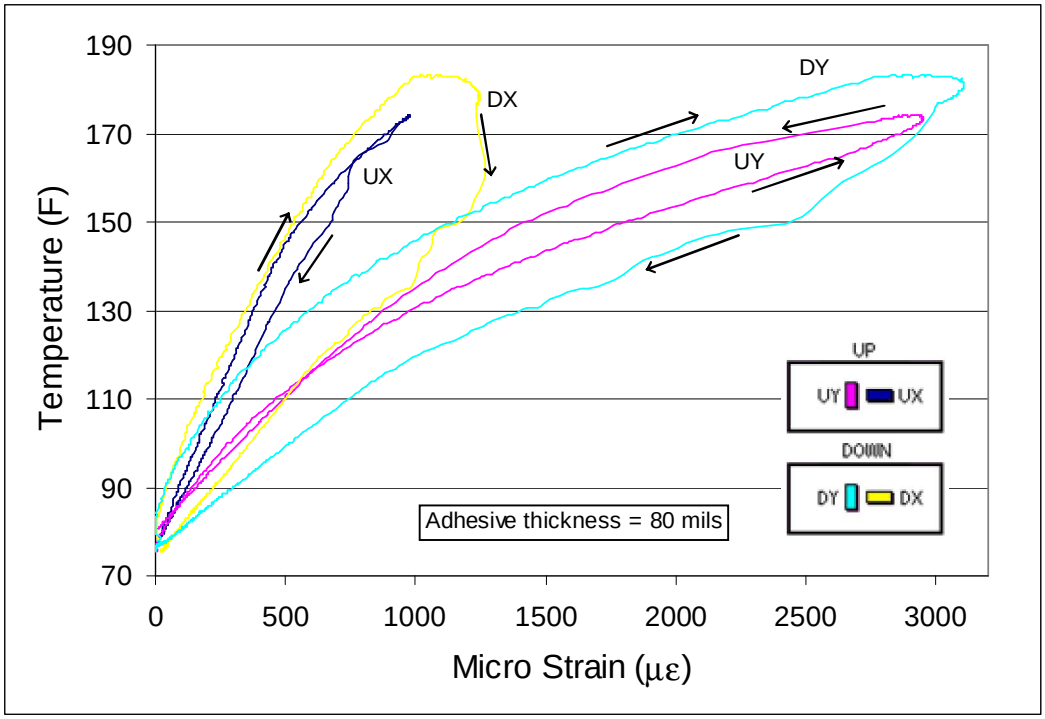

Figure 4.53 – Measured CPVC Strain of Specimen 1

bottom of the steel plate. Only a slight offset occurs between the two phases. Conversely, a non-linear behavior was observed for the CPVC during the heating and cooling phases, especially in the y-direction. Results also highlight the influence of the heating and cooling phases on the strain distribution at the bottom surface of the CPVC plate. Arrows are drawn in Figure 4.53 to specify heating and cooling phases. The measured strains at the CPVC-adhesive layer interface (UX and UY) exhibit a minimal effect from the heat cycling. It is strongly believed that the bond of the adhesive to the steel provides a stiffening effect to the top side of the CPVC. The bottom surface of the CPVC is relatively unconstrained through the thickness, thus it behaves more freely. The large variation in the heating and cooling phase for the CPVC bottom surface is likely attributed to the fast cooling of the materials. Typical behavior was observed for all bonded specimens (Similar heating and cooling phase graphs for Specimens 2 and 3 are

found in Appendix C.). Therefore, further discussions of the specimens' behavior will focus only on the heating phase prior to removal of the insulating top cover. The strain behavior in both the x and y-directions during the heating phase of specimen 1 is shown in Figures 4.54 and 4.55, respectively. The figure clearly shows the interaction between the steel and CPVC. Results indicate an immediate distinction in the dissimilar behavior of CPVC in the short and long-directions. Steel, however, remains linear and behaves as expected with the bottom surface expanding more than the top surface. By comparing the steel strains in these figures with the free thermal expansion results in Figure 4.46, it was observed that the bottom surface of the steel expanded at a faster rate than the baseline measurement, while the top surface expanded at a lower rate. As a result, bending moments were induced, where the bottom steel surface acts in tension and the top steel surface acts in compression. Results also indicate that the magnitude of the steel bottom strain is greater in the x-direction than the y-direction. A nonlinear behavior was observed in the strain-temperature relationship of the CPVC material. The nonlinearity was highly pronounced in the y-direction as shown in Figures 4.54 and 4.55. There are two main factors that contribute to the differences in the x and y-directions. The first factor is the anisotropic nature of CPVC. The measured CTE in the y-direction was 27 percent higher than that measured in the x-direction. The second factor is the rectangularity of the specimens ($l_{long}/l_{short} = 2.0$), which is influenced by the boundary conditions. Negating friction effects from the Styrofoam cover, the specimen was primarily restrained in the vertical direction along the bottom perimeter of the CPVC.

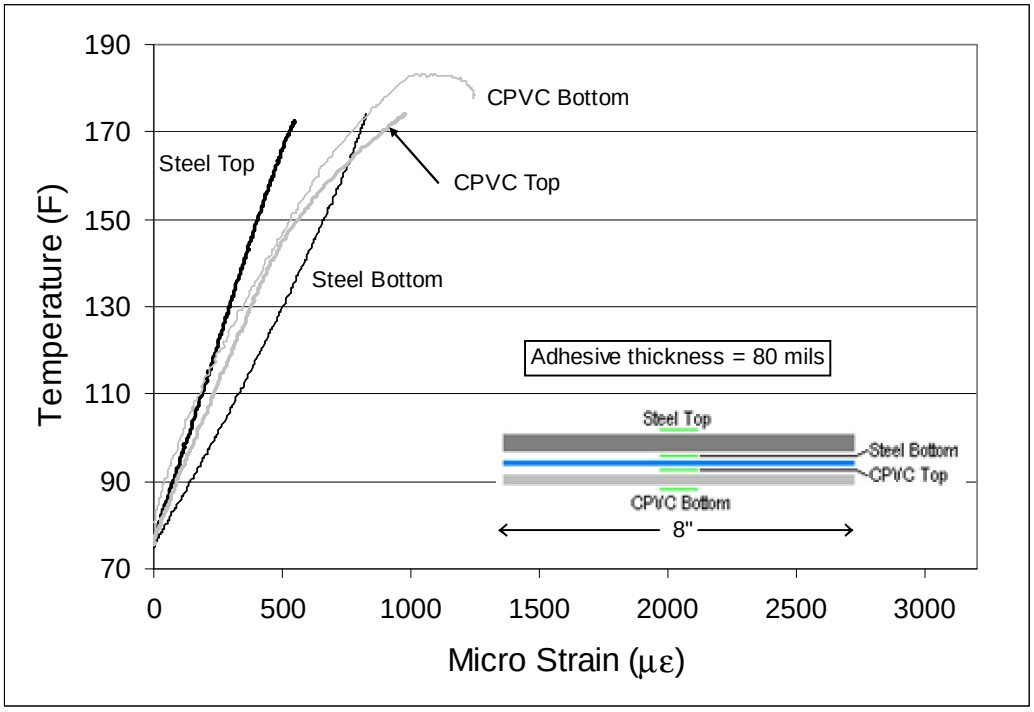

Figure 4.54 – Strain Behavior of Specimen 1 in X-Direction

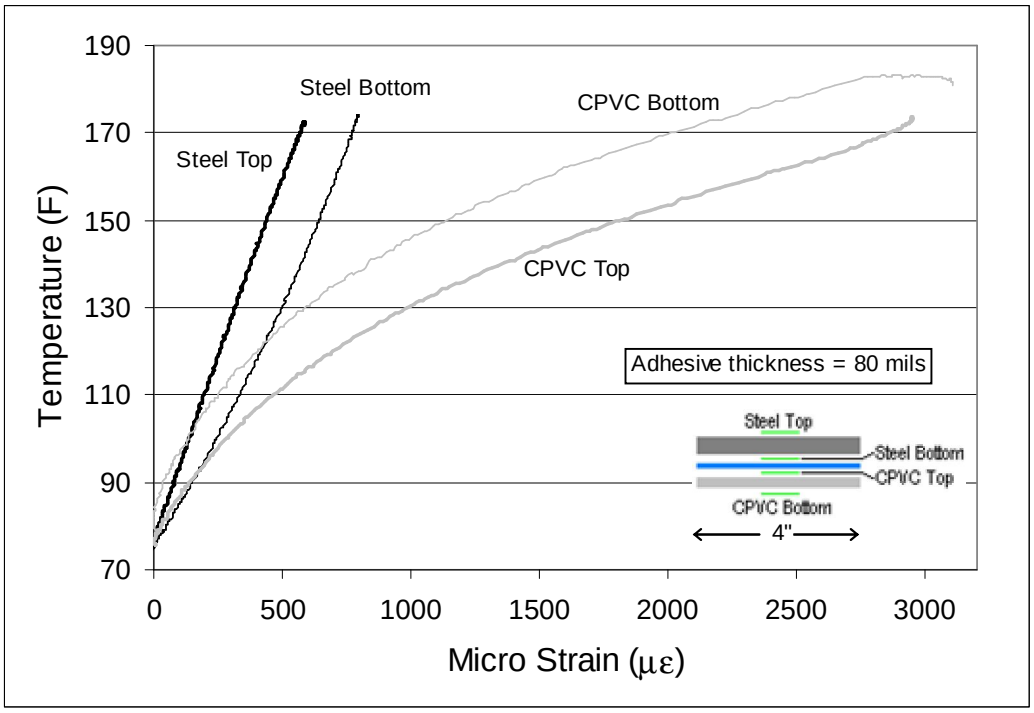

Figure 4.55 – Strain Behavior of Specimen 1 in Y-Direction

Therefore the specimens are not permitted to expand as freely in the x-direction. Finite element analysis confirmed the above observation, as will be discussed later in this chapter. Results clearly indicate that as temperature increases the bond between the steel and CPVC deteriorates significantly. Such a phenomenon was evidenced by the highly nonlinear behavior of the CPVC material shown in Figure 4.55. Consequently, the CPVC is allowed to expand more freely at these high temperatures, preventing the full composite action. According to initial CPVC strain tests, the maximum strains achieved in the short direction for a temperature of 180°F were in the vicinity of 6000 micro strain. This suggests that the adhesive, though much less effective at high temperatures, still has a restraining effect. Results in the short direction may suggest a possible decay in bond strength over time leading to an adhesive shear failure. Further analysis would have to be performed to determine the possibility of such failures.

Cross sectional snapshots of the temperature and strain gradients selected at various times during the heating cycle are shown in Figures 4.56 through 4.63. Even numbered figures represent the behavior in the x-direction and odd numbered figures represent the behavior in the y-direction. Figure 4.51 corresponds to the temperature gradient of the various selected time steps. The interface temperatures and the corresponding strains along the interface line at a time of 40 minutes are shown in Figure 4.56 and 4.57. It should be noted that a time of 40 minutes corresponds to a temperature of 112°F at the bottom surface of the CPVC. At such low temperature, minimal strains exist in both the x and y-directions. Both figures show that the bottom sides of the steel and the CPVC materials have greater strains than their corresponding top sides. Figures 4.58 and 4.59 show a

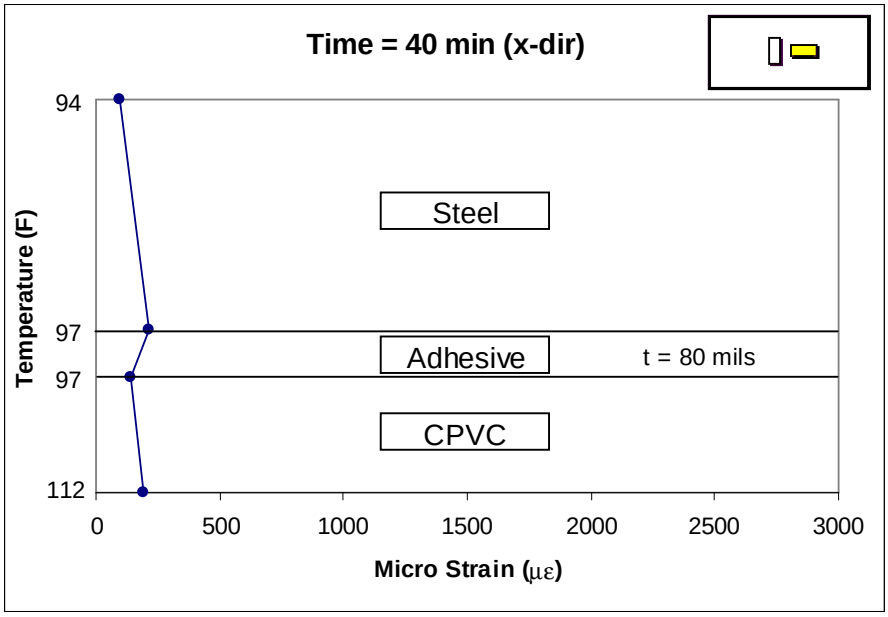

Figure 4.56 – Strain Profile for Specimen 1 at 40 min in the X-Direction

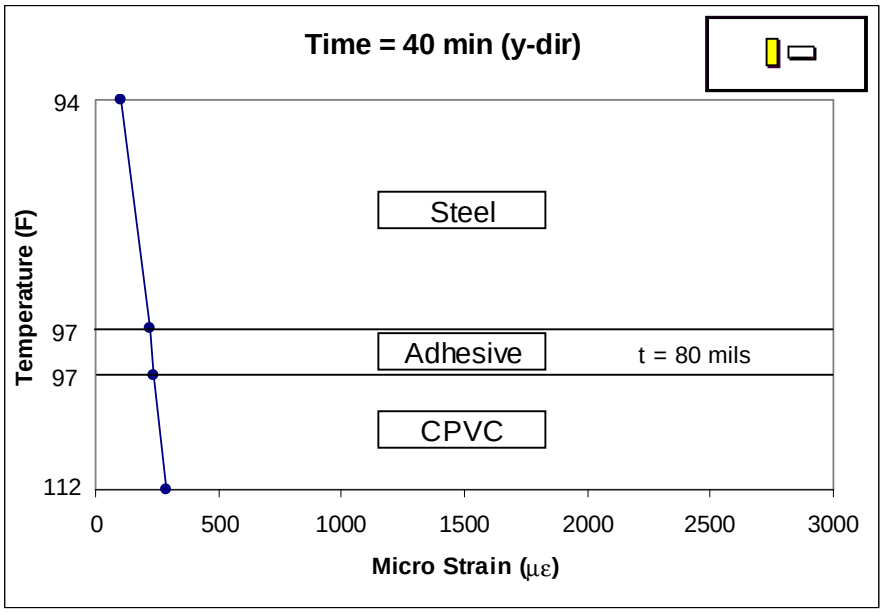

Figure 4.57 – Strain Profile for Specimen 1 at 40 min in the Y-Direction

considerable increase in the strains and temperatures at a time of 80 minutes due to the corresponding increase in temperature. The measured strains were almost double the measured values at a time of 40 minutes. The tensile strains at the top and bottom of the steel plate were almost identical in the x and y-directions. However, the measured strains

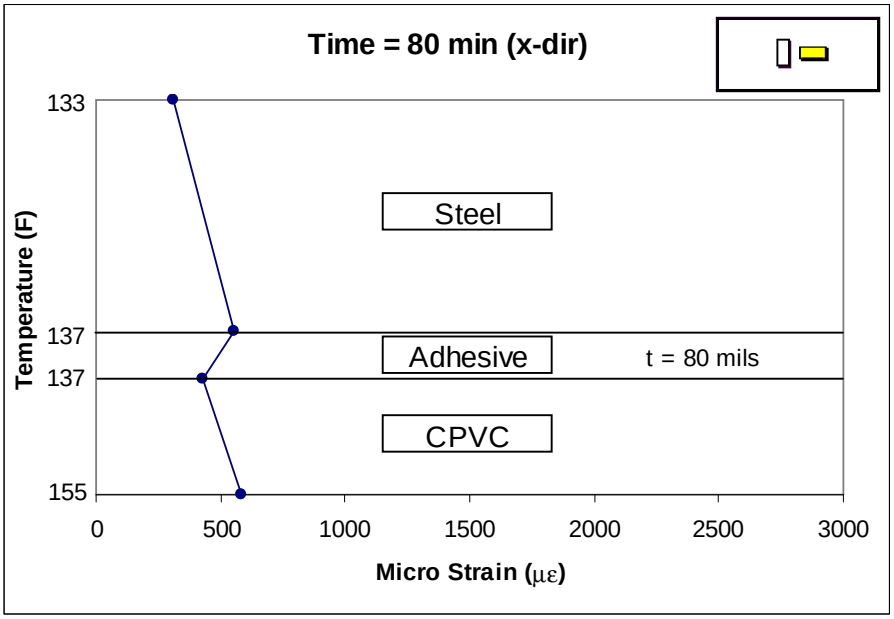

Figure 4.58 – Strain Profile for Specimen 1 at 80 min in the X-Direction

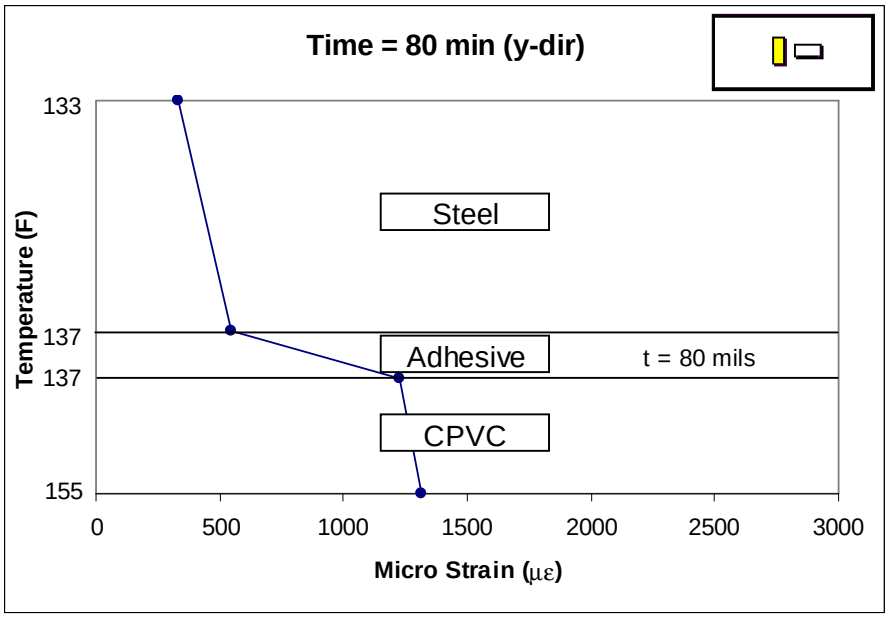

Figure 4.59 – Strain Profile for Specimen 1 at 80 min in the Y-Direction

in the CPVC were much higher in the y-direction compared to the x-direction. Figures 4.60 and 4.61 show the strain and temperature results at a time of 100 minutes, which corresponds to a temperature of 173°F at the bottom of the CPVC material. These figures show similar behavior as that observed at 80 minutes, where the CPVC tensile strains in

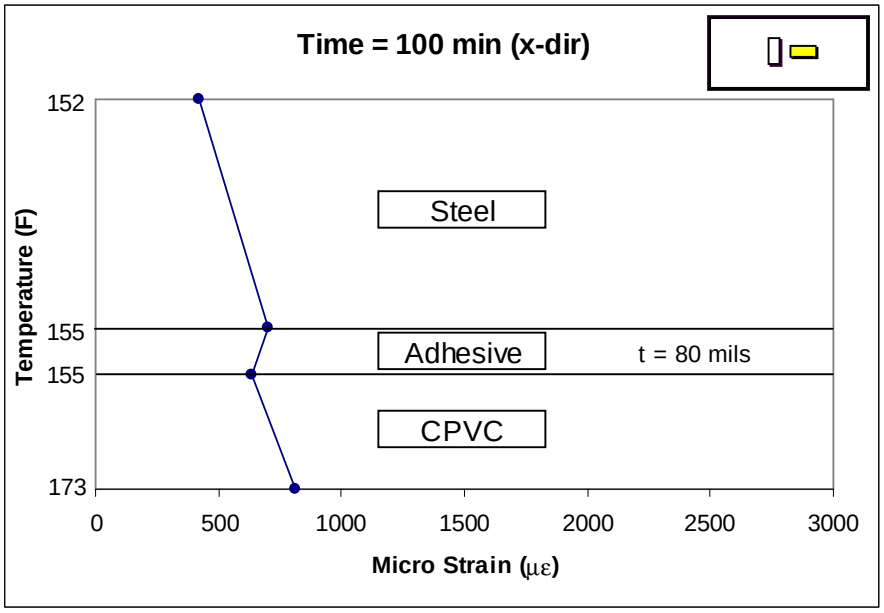

Figure 4.60 – Strain Profile for Specimen 1 at 100 min in the X-Direction

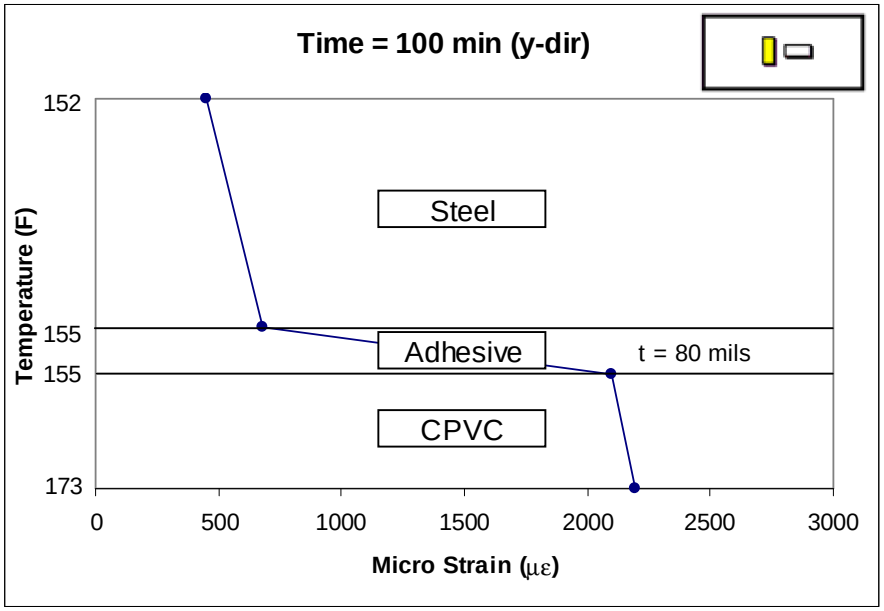

Figure 4.61 – Strain Profile for Specimen 1 at 100 min in the Y-Direction

the y-direction were almost doubled the measured values at 80 minutes. Figures 4.62 and 4.63 show strain and temperature results at a time of 120 minutes, which corresponds to a temperature of 183°F at the bottom of the CPVC material. The strains in the x-direction are linearly increasing along the adhesive layer, while strains in the y-direction continue

to reflect the nonlinear behavior of the CPVC and an increased shear strain value within the adhesive layer as will be discussed later in this chapter. For snapshot results at any time, graphs showing strain versus time across the heating cycle are included in Appendix C.

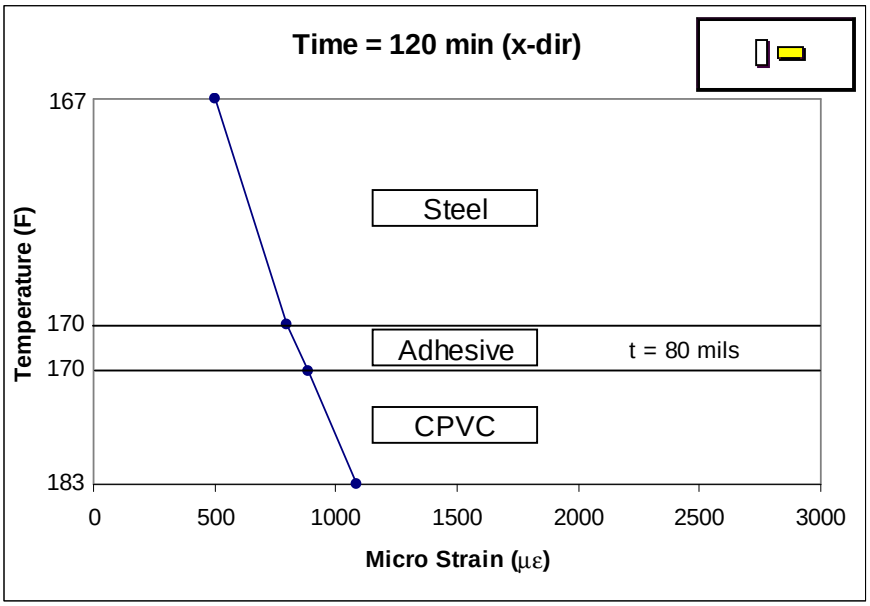

Figure 4.62 – Strain Profile for Specimen 1 at 120 min in the X-Direction

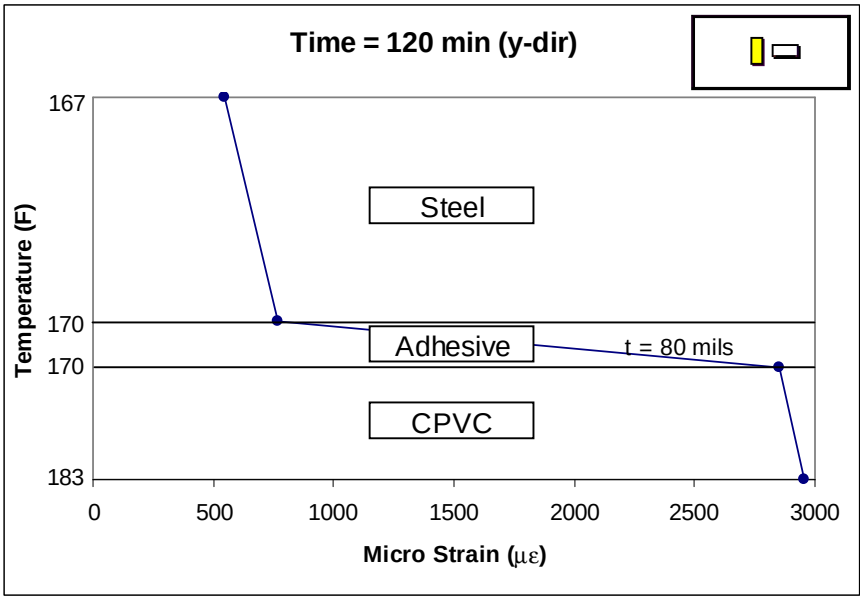

Figure 4.63 – Strain Profile for Specimen 1 at 120 min in the Y-Direction

4.4.2.2 Influence of Boundary Condition

Due to the dissimilar behavior of the CPVC in the short and long-directions, test bath boundary conditions were scrutinized. An alternate test method was created where the bonded specimen was rested on rollers instead of being supported by the insulated cover along the perimeter of the CPVC. This typical support could have caused undesirable lateral friction effects. The rollers supported the corners of the specimen, are shown in Figure 3.37. Oil was added to the rollers to minimize the friction as much as possible. The measured tensile strains in the steel and the CPVC for both x and y-directions are shown in Figures 4.65 and 4.66, respectively. These figures should be compared with original test results displayed previously in Figures 4.54 and 4.55. Results suggest that the addition of the rollers had no effect on the performance of the specimen. Steel strains in both directions were nearly identical, with the only difference being the maximum

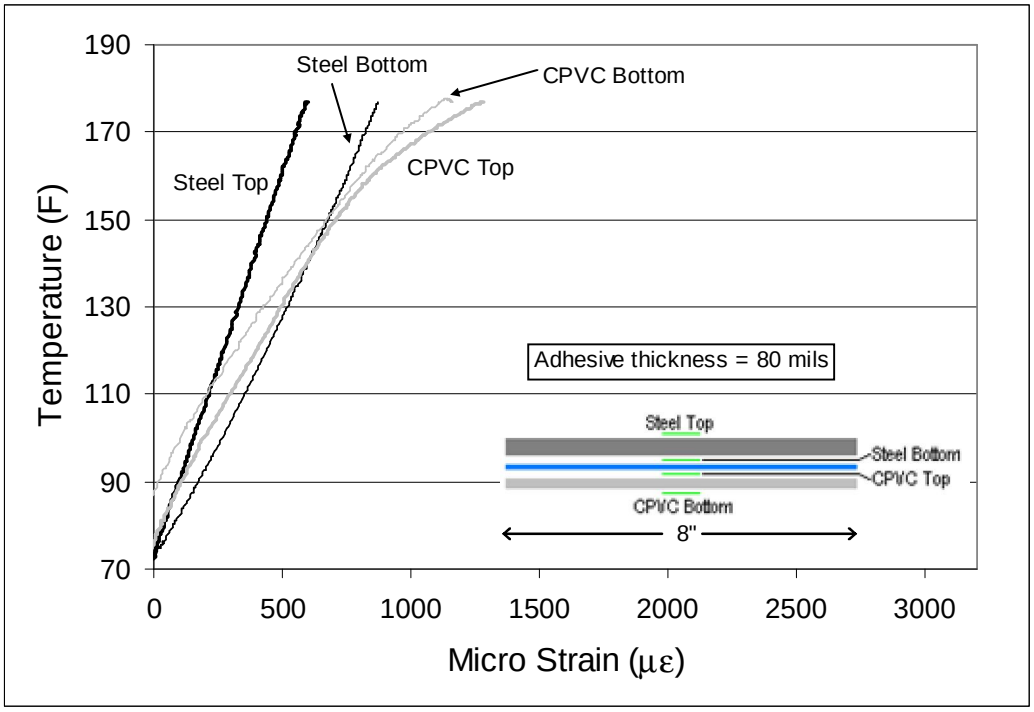

Figure 4.65 – Strain Behavior of Specimen 1 in the X-Direction using the Roller Supports

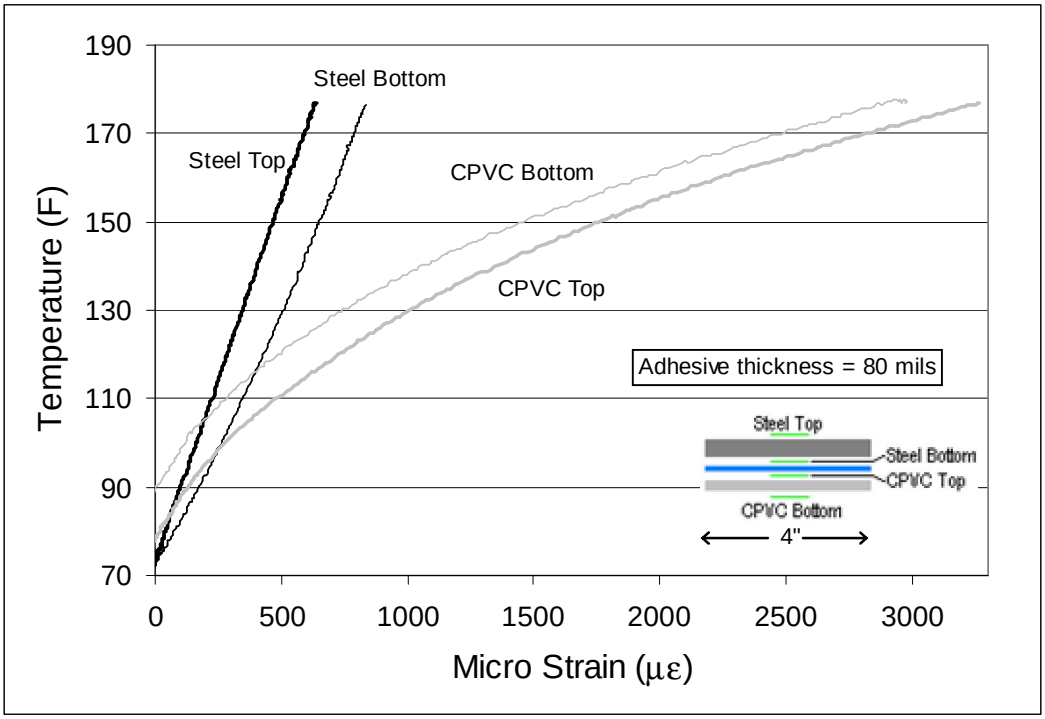

Figure 4.66 – Strain Behavior of Specimen 1 in the Y-Direction using the Roller Supports

temperature achieved was slightly higher for the roller case. Therefore strains were slightly higher. CPVC material performed similarly to the original test, where the nonlinear behavior was observed to correspond for both tests. The roller test helped to validate previous results.

4.4.2.3 Development of a Finite Element Model

To achieve greater understanding of test results, finite element analysis of the specimen behavior was conducted. The independent results for the linear elastic finite element analysis were performed using a general-purpose finite element program, Straus7, version 2.2.3, 2003. Like most FE analysis programs, it employs a system consisting of pre-processor, solvers, and post-processor. The graphical environment of Straus7 is highly advanced and simplifies many of the design tasks such as the application of loading, boundary conditions, and mesh generation. The analysis system can utilize a number of

solvers, including basic linear static, non-linear static and dynamic, as well as steady state and transient heat solvers. The 3-D analytical model was created using 10,368 8-node brick elements, each node has 3 translational degrees of freedom. Three layers were used within the thickness of the steel, adhesive and CPVC material. Several mesh designs were studied to provide optimum results. The mesh was chosen to provide adequate aspect ratio for all elements. The material properties used in the analysis are listed in Table 4.10. Well documented values for the elastic modulus and Poisson's ratio were used for the steel. For the CPVC material and SS340 adhesive, the elastic modulus was selected according to the individual material data sheets. It must be noted that the elastic modulus selected for both the CPVC and adhesive are under room temperature conditions. The application of heat will significantly reduce the elastic moduli. Test results by other researchers showed that the elastic modulus of the CPVC could decrease to 270 psi at a temperature of 180°F. The Poisson's ratio for the CPVC was set to 0.36 as recommended by the manufacturer. For the adhesive, an estimate of 0.4 for the Poisson's Ratio was used, which is a common value in many plastic materials. The shear moduli was calculated for each material according to the following equation:

$$G = \frac{E}{2(1+\upsilon)} \tag{4.3}$$

where G is the shear modulus, E is the modulus of elasticity, and υ is the Poisson's ratio. CTE values were used from previously discussed coefficient of thermal expansion tests. The CPVC was modeled using an orthotropic material. Both long (x) and short (y) directional properties were used in the program. Figure 4.67 displays the model with the three materials, steel, adhesive, and CPVC.

Table 4.10 – Material Properties used in the Finite Element Model

Property	Steel	CPVC x-dir	CPVC y-dir	Adhesive
Elastic Modulus, E (ksi)	29,000	350	350	35
Poisson's Ratio, υ	0.30	0.36	0.36	0.40
Shear Modulus, G (ksi)	11,154	129	129	13
CTE, a (ppm/^{o}F)	6.94	44	56	39

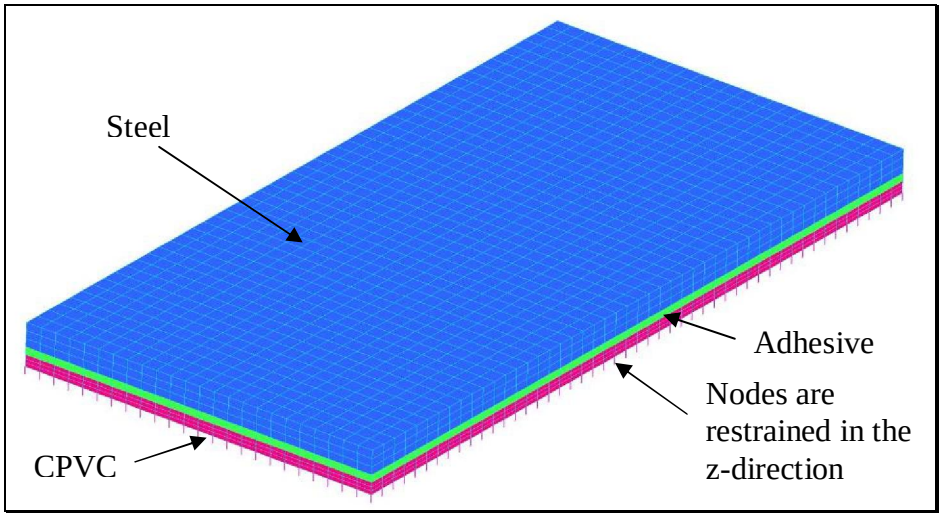

Figure 4.67 – Finite Element 3-D Model

Restraints for the member were applied only in the vertical (z) direction at points along the bottom of the CPVC perimeter, thus allowing free expansion in the horizontal plane. The temperature gradient of specimen 1 snapshots at 120 minutes (shown in Figures 4.62 and 4.63) was selected as the model thermal inputs. The selected thermal gradient represents high temperature conditions and an overall ΔT of 16.3^{o}F from the bottom of the CPVC surface to the top of the steel surface. Based on the actual initial starting temperature of 75°F, the ΔT's used in the model were calculated by subtracting 75°F

from the measured temperatures at each interface. The thermal input used in the model as well as the actual interface temperatures for specimen 1 at 120 minutes are listed in Table 4.11. The resulting deformed shape is shown in Figure 4.68. The model shows that the CPVC material expands at a higher rate than the steel, resulting in warping of the composite section. The resulting surface strain distributions from the output of the model are displayed in Figures 4.69 through 4.76. These eight figures represent the strain distributions for top and bottom surfaces of the steel and CPVC in both the long and short directions. Continuous decay in the bond between the steel and CPVC was not considered in the analysis. The analysis indicated that the general behavior of the composite section can be predicted using finite element analysis. The bottom surface of the steel in the x and y-directions expands slightly larger than the top surface. Comparing

Table 4.11 – Finite Element Model Input Surface Temperatures

Model $T_{Measured}$ and ΔT and at Each Interface	Steel		CPVC	
	top	bottom	top	bottom
T measured (F)	166.7	169.8		183.0
Model Input ΔT (F)	91.7	94.8		108.0

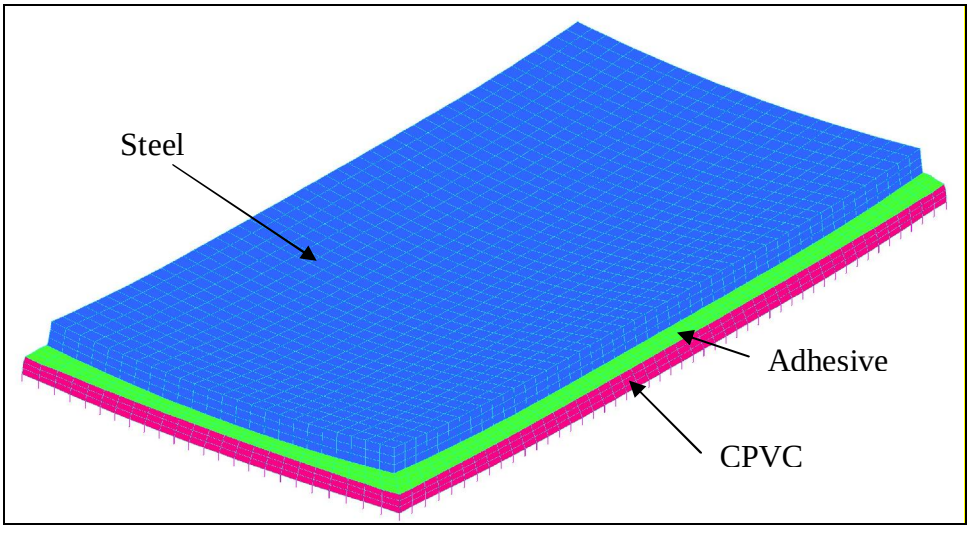

Figure 4.68 – Deformed Shape of FE Model

the strain distribution in steel bottom surface with the CPVC top surface, higher shear strains were predicted within the adhesive layer in the y-direction than the x-direction, which matched the observed behavior during testing. The figures clearly show that the tensile strains on the bottom surface for the steel are almost half of the tensile strains on the top surface of the CPVC. For CPVC top and bottom surfaces, the strain distributions in the short direction are significantly higher than those in the long direction, which shows good agreement with the measured values. This behavior could be attributed to the rectangularity effects, boundary conditions, and orthotropic nature of CPVC. Additional models will be discussed in a later section to investigate boundary conditions and the rectangularity effects on the strain behavior of the specimen.

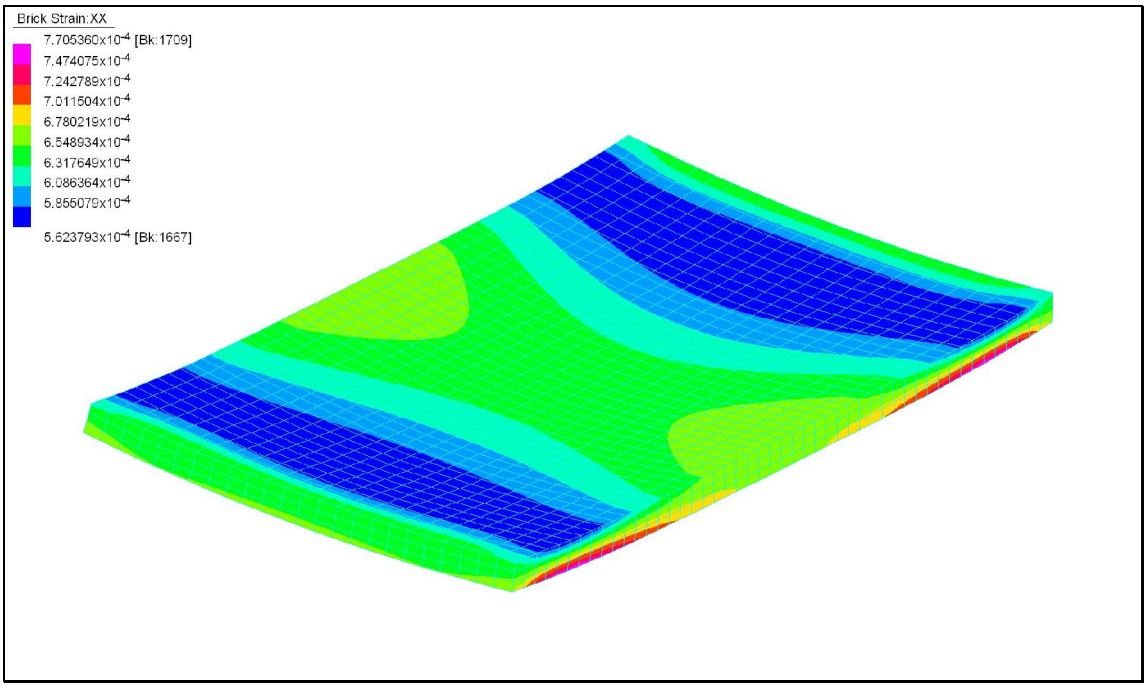

Figure 4.69 – FEM Strain Distribution for Steel Top in Long Direction

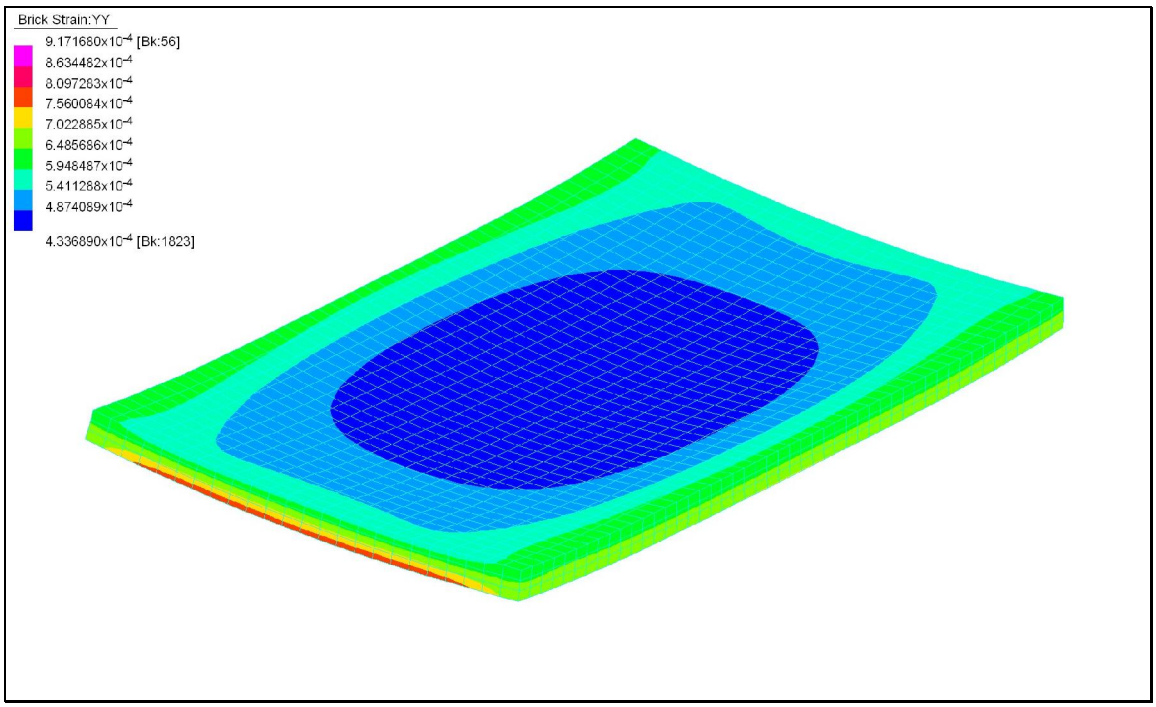

Figure 4.70 – FEM Strain Distribution for Steel Top in Short Direction

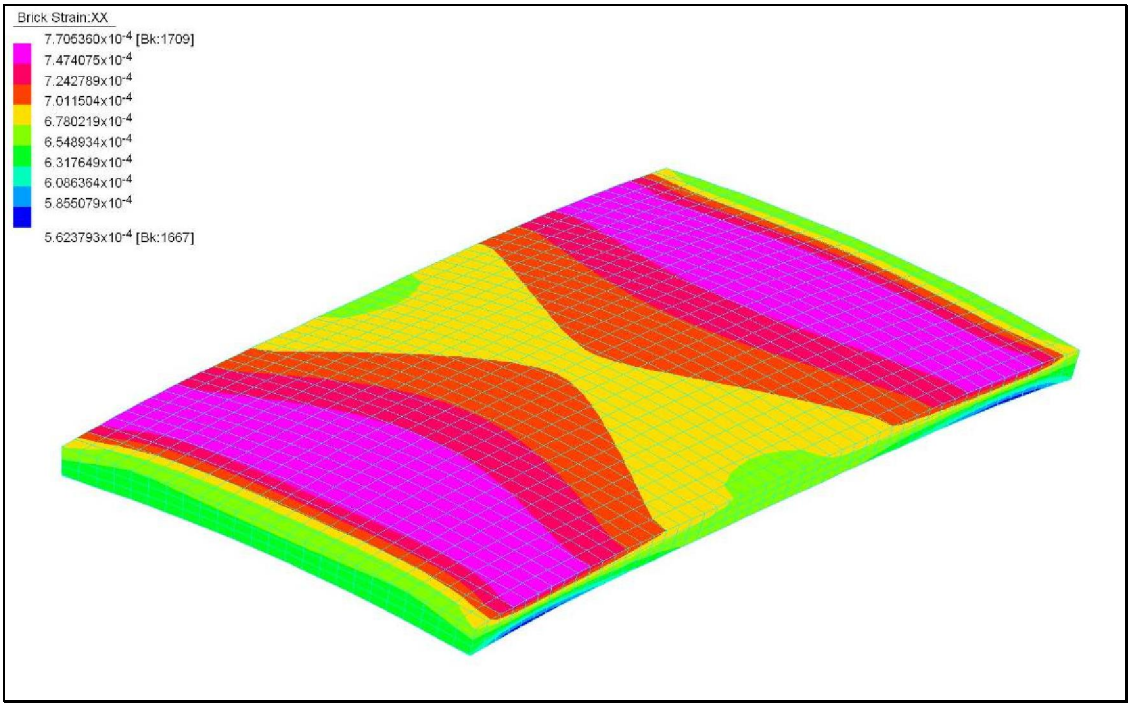

Figure 4.71 – FEM Strain Distribution for Steel Bottom in Long Direction

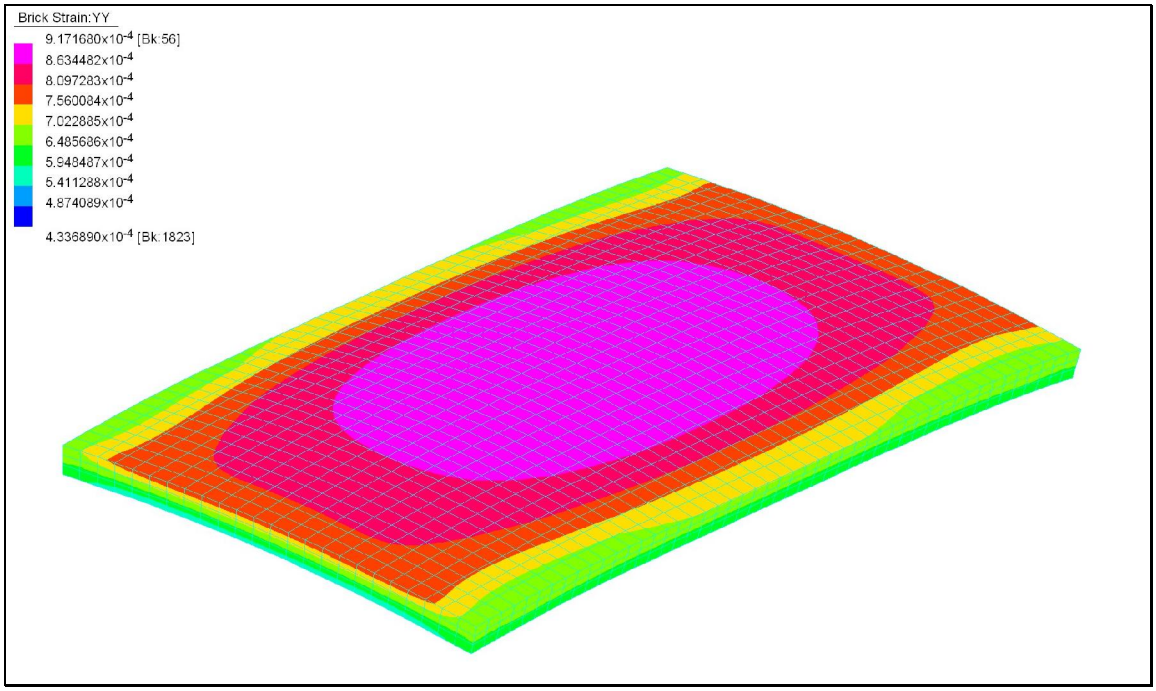

Figure 4.72 – FEM Strain Distribution for Steel Bottom in Short Direction

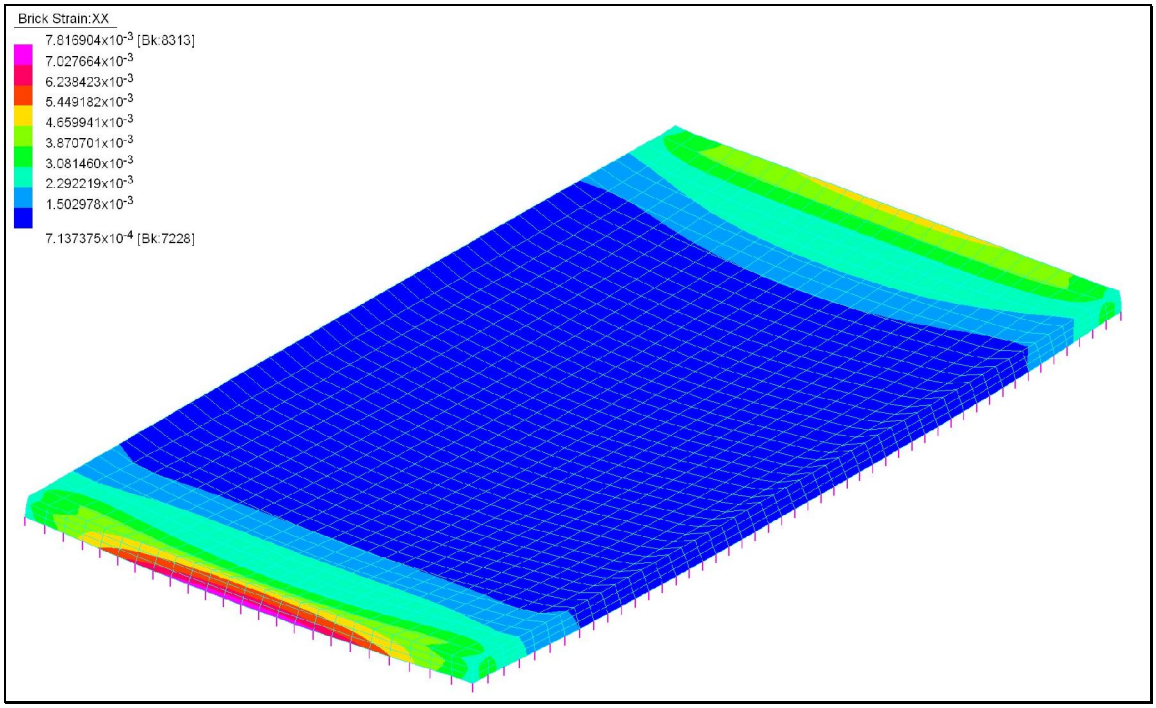

Figure 4.73 – FEM Strain Distribution for CPVC Top in Long Direction

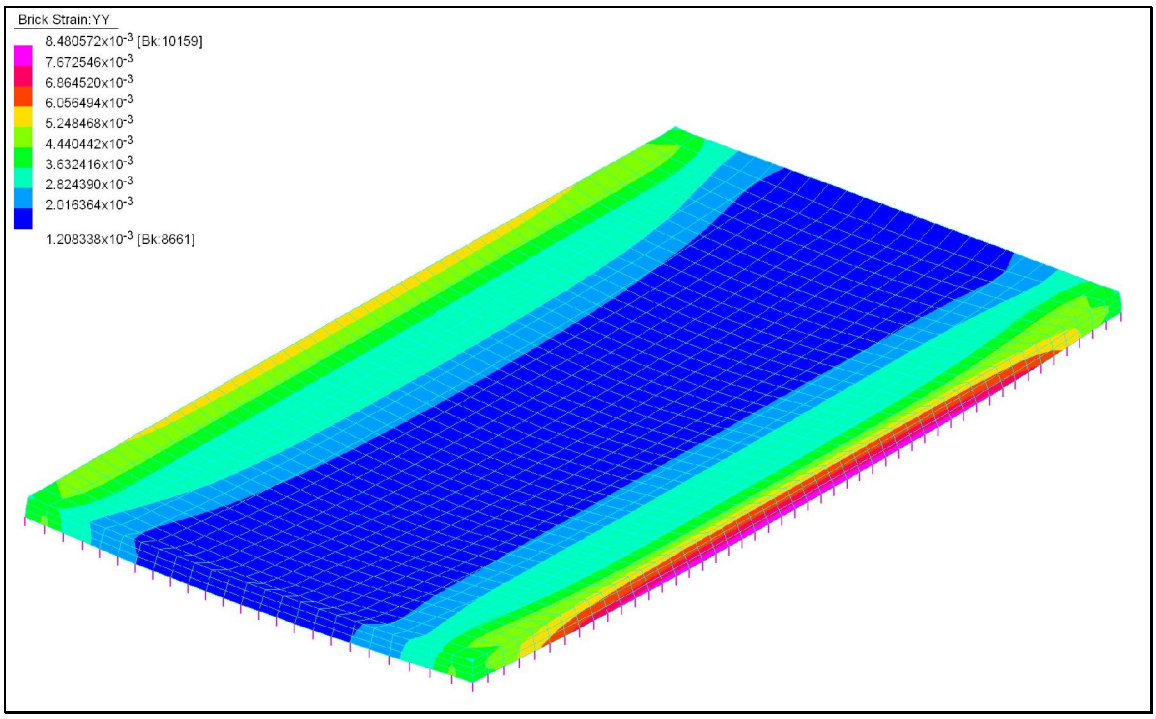

Figure 4.74 – FEM Strain Distribution for CPVC Top in Short Direction

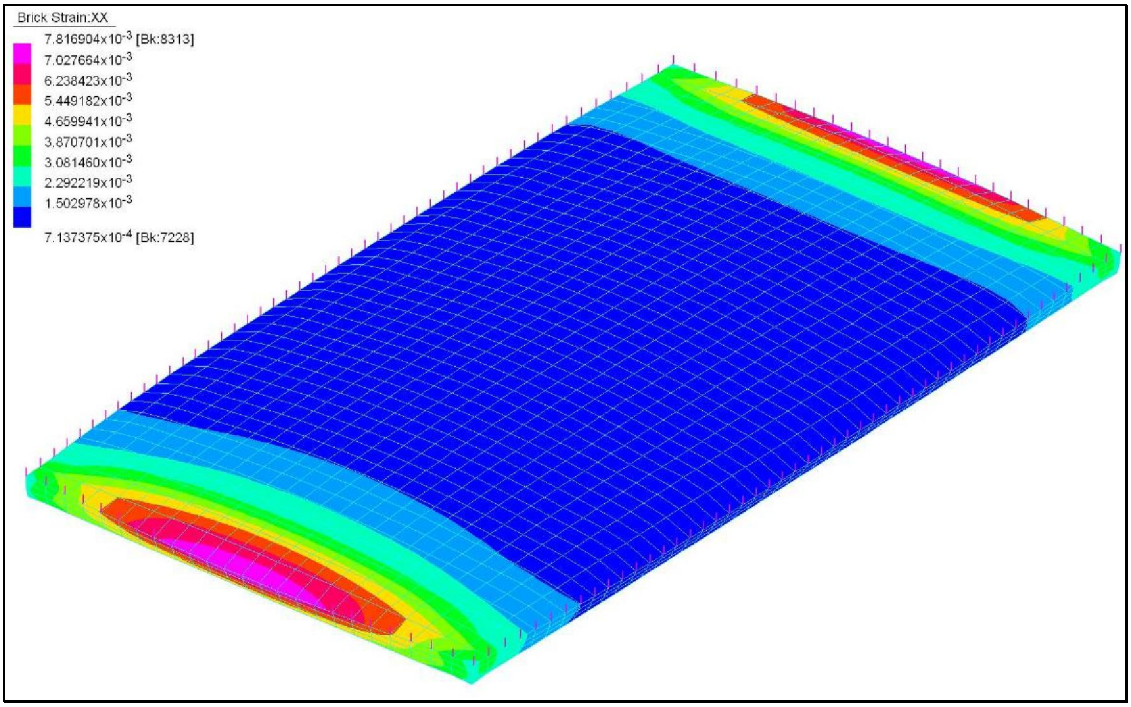

Figure 4.75 – FEM Strain Distribution for CPVC Bottom in Long Direction

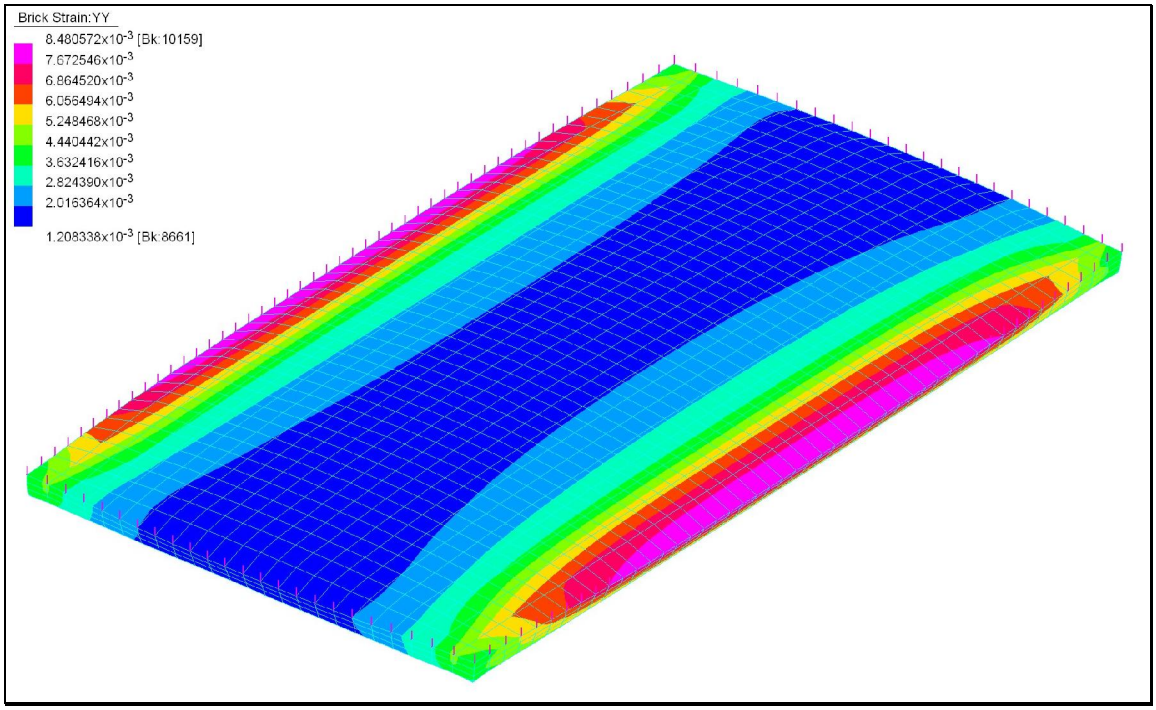

Figure 4.76 – FEM Strain Distribution for CPVC Bottom in Short Direction

Strain results from the finite element model are listed in Table 4.12. The strain values were retrieved from the centroid locations of the steel and CPVC surfaces. These values are plotted linearly in Figures 4.77 through 4.80 using initial temperatures of 75°F. The figures also include the corresponding measured results from specimen 1 for comparison. The first two figures represent the steel specimen in the short (y) and long (x) directions while the second two figures represent the CPVC specimen in both directions. The predicted results indicate a reasonable correlation for the actual behavior. Due to the assumed linear elastic behavior of the materials, the finite element results for the steel and CPVC were inherently linear. The predicted tensile strains for the CPVC material,

Table 4.12 – Strain Results of Finite Element Model

Strain Results of Finite Element Model	Steel				CPVC			
	top		bottom		top		bottom	
	x	y	x	y	x	y	x	y
Model 1 (με)	654	514	691	836	737	1479	757	1661

shown in Figures 4.79 and 4.80, indicate less agreement to the measured data. This is attributed the nonlinear behavior of the CPVC, which cannot be modeled in a linear

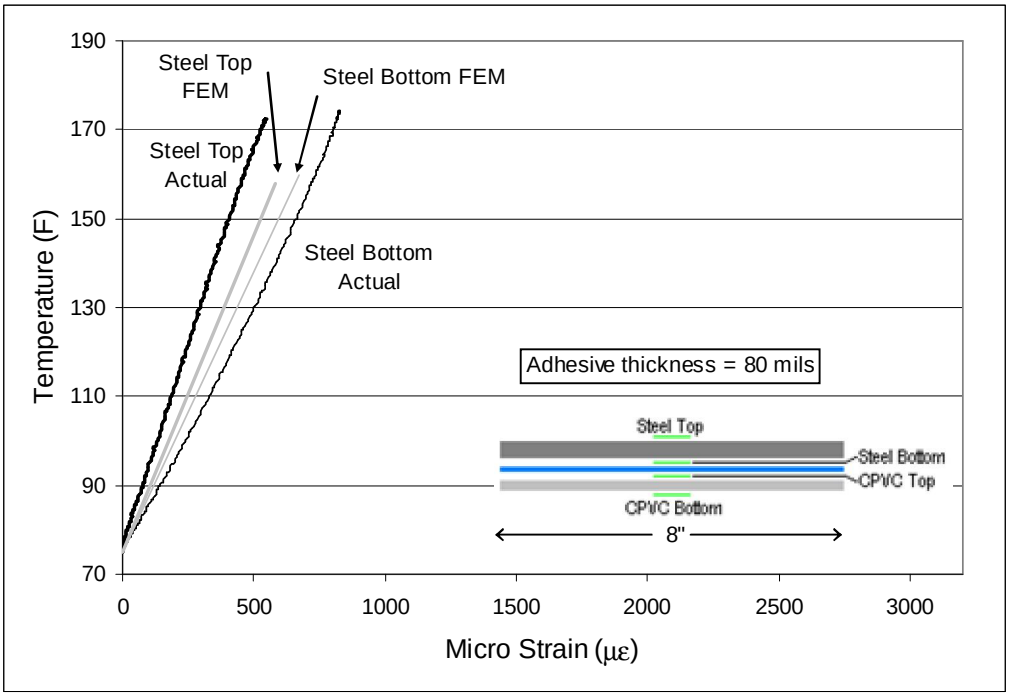

Figure 4.77 – Steel Strain Behavior of Specimen 1 in X-Direction

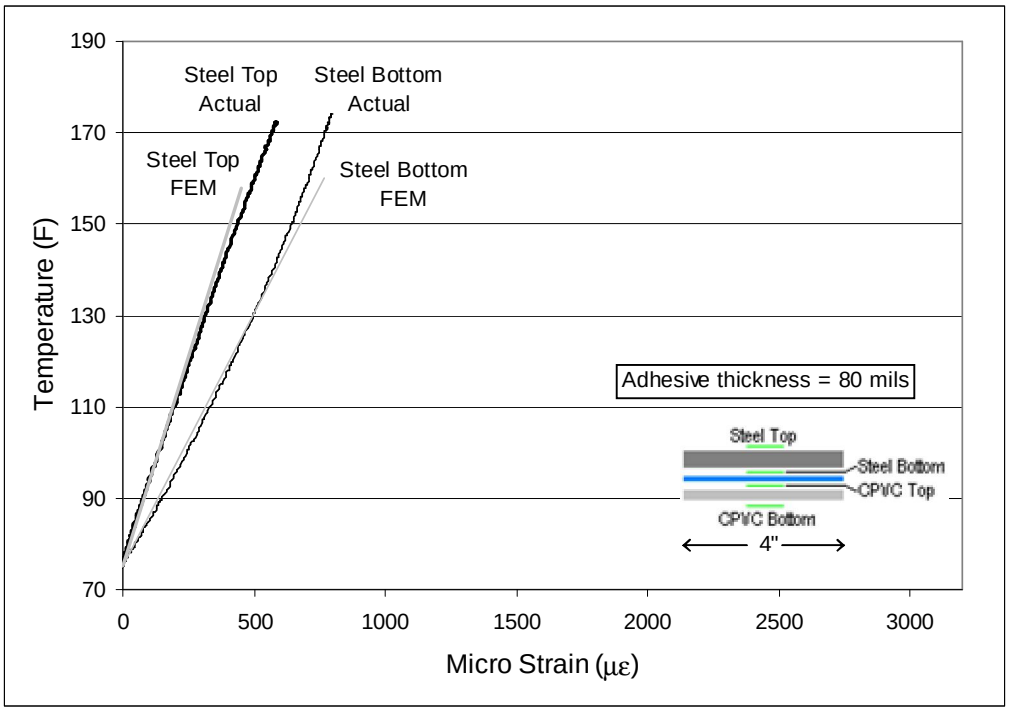

Figure 4.78 – Steel Strain Behavior of Specimen 1 in Y-Direction

elastic finite element model. The model predicts accurate behavior for the CPVC material in the long direction up to a temperature of about 150°F, where the nonlinear

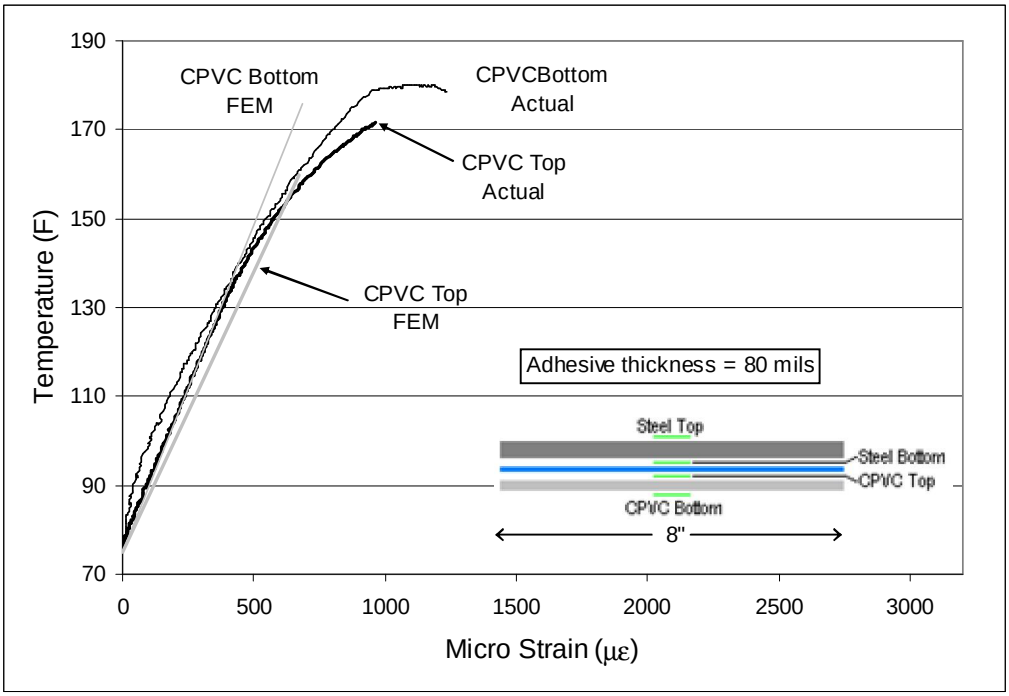

Figure 4.79 – CPVC Strain Behavior of Specimen 1 in X-Direction

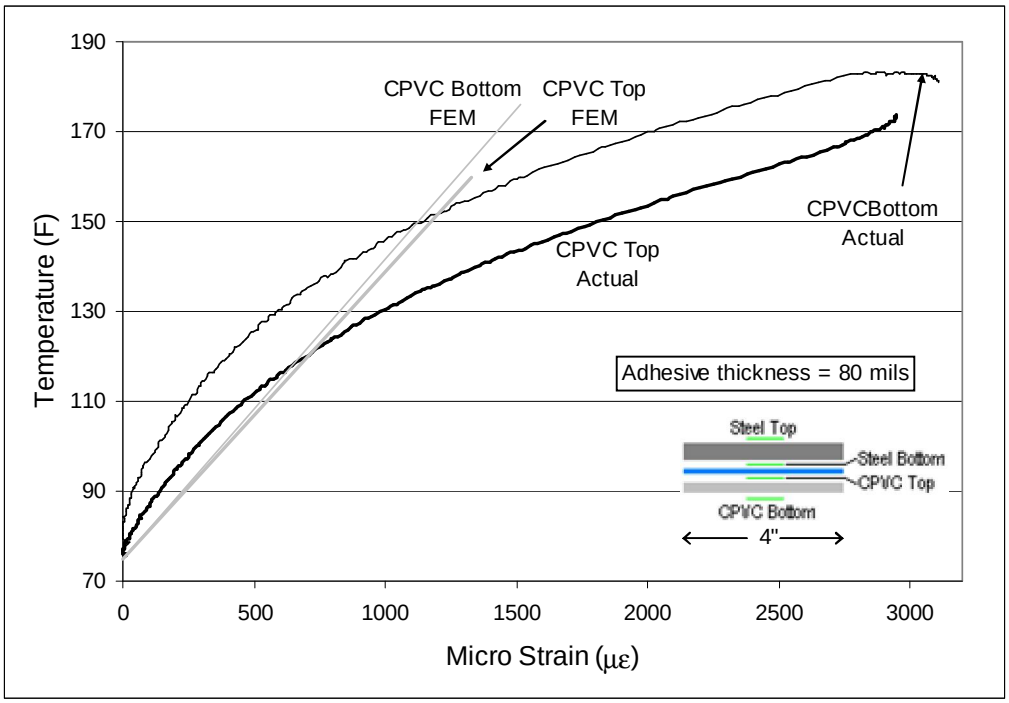

Figure 4.80 – CPVC Strain Behavior of Specimen 1 in Y-Direction

behavior begins. In the short direction, finite element results are clearly not good indicators of the nonlinear behavior. However, the modeled results remain in the same order of magnitude since the initial slope was predicted, which indicates overall agreement with the behavior observed in specimen 1.

4.4.2.4 Influence of End Restraints and Plate Geometry

Additional finite element models were used to study the influence of vertical restraints and the plate geometry on the behavior of the specimen. To study the influence of the vertical restraints used in the original model, the restraints were removed from the perimeter of the CPVC bottom surface. Therefore, the model was allowed to expand freely with no effect from the boundary conditions. All other design considerations remained the same as the original model. Strain results are summarized in Table 4.13 as Model 2. A comparison of these results with Model 1 shows significant changes in the strain profile along the thickness of the specimen model. The strains at the top and bottom surfaces of the CPVC in the x-direction were increased by 31 and 42 percent, respectively. Conversely, the strains for both CPVC surfaces in the y-direction were decreased. As previously found in Model 1, the large difference for CPVC strains in the x and y-directions was diminished. Still, the overall behavior of the CPVC was unchanged. At the steel surfaces, the changes in the tensile strains were less pronounced. By removing the vertical restraints along the perimeter of the CPVC bottom surface, overall results indicate that the specimen produces increased thermal expansions in the long direction, which in turn reduces the predicted strains in the short direction. Figure 4.81 displays the deformed shape.

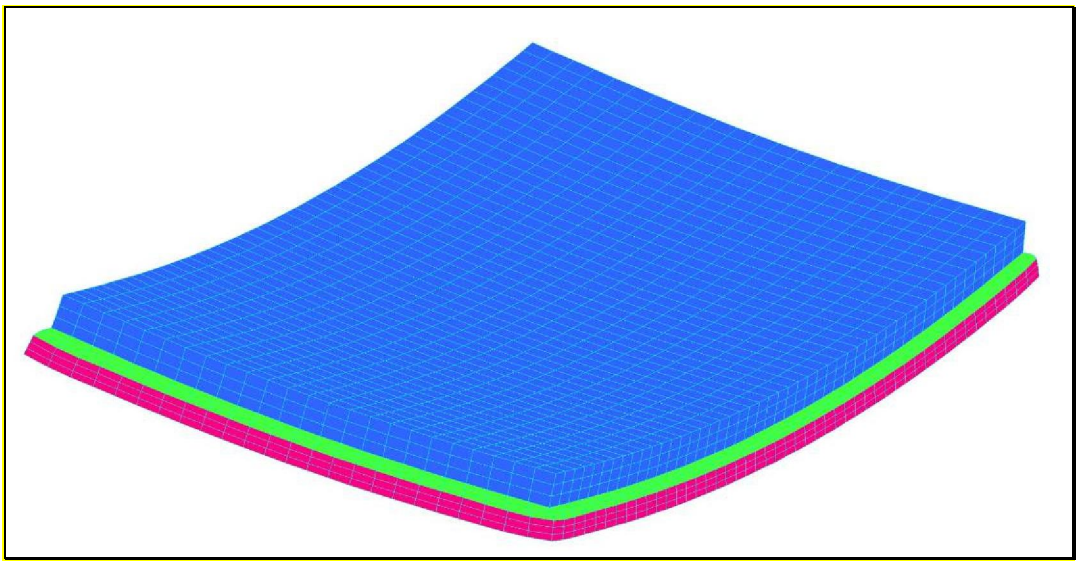

Figure 4.81 – Deformed Shape of Finite Element Model 2

To study the influence of the rectangularity of the test specimen, the model was cut in half. The resulting square model has overall dimensions of 4" x 4" and was modeled using 5,184 8-node brick elements. All other design considerations remained the same as Model 2. Strain results are summarized in Table 4.13 as Model 3. A comparison of these results with Model 2 shows significant changes only in the CPVC material. Results indicate that strains in the long (x) direction continue to increase from the previous model. The tensile strains in the x-direction at the top and bottom surfaces of the CPVC increased by 28 and 26 percent, respectively. Resulting steel strains showed relatively no change due to the change in the specimen aspect ratio. Results for Model 3 suggest that

Table 4.13 – Strain Results of 3 Finite Element Models

Strain Comparison of 3 Finite Element Models	Steel				CPVC			
	top		bottom		top		bottom	
	x	y	x	y	x	y	x	y
Model 1 (με)	654	514	691	836	737	1479	757	1661
Model 2 (με)	564	547	778	804	968	1393	1076	1574
Model 3 (με)	568	548	770	803	1243	1377	1361	1515

*Model 1 - original, Model 2 - no restraints, Model 3 - square with no restraints

the rectangularity only affects the induced strains in the CPVC material. The differences in the x and y-directions at each surface location are attributed to the orthotropic behavior of the CPVC. Figure 4.82 represents the deformed shape for the square model.

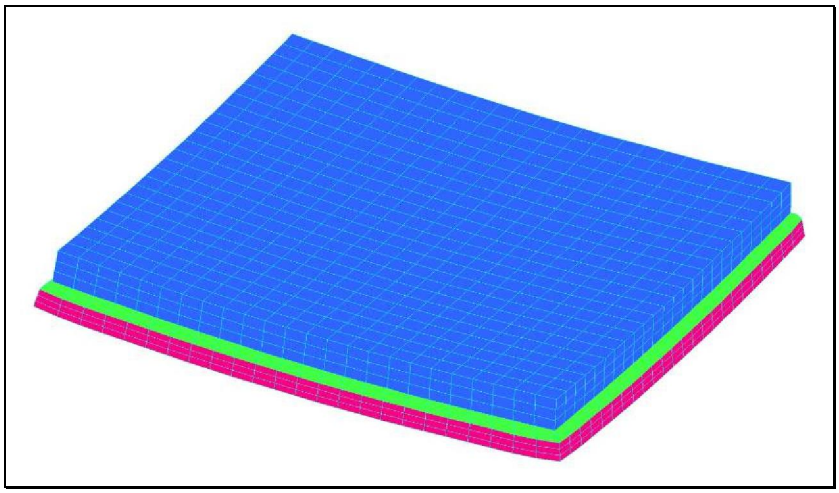

Figure 4.82 – Deformed Shape of Finite Element Model 3

4.4.2.5 Specimen 2 (Adhesive thickness of 50 mils)

Three bath tests were conducted on specimen 2 with a nominal adhesive thickness of 50 mils. Test setup, temperature control of the heating and cooling phases, and resulting temperature gradient behavior was similar to that of specimen 1. A typical temperature gradient plotted versus time is shown in Figure 4.51. The strain behavior in both the x and y-directions during the heating phase of specimen 2 is shown in Figures 4.83 and 4.84, respectively. Testing of specimen 2 resulted in similar behavior as that of specimen 1, which is shown in Figures 4.54 and 4.55. The figures for specimen 2 clearly shows the interaction between the steel and CPVC. Results indicate an immediate distinction in the dissimilar behavior of CPVC in the short (y) and long (x) directions. Steel strains remain linear with the bottom surface expanding more than the top surface. The bottom steel is bonded to the adhesive layer; therefore, it expands at a higher rate than normal due to the

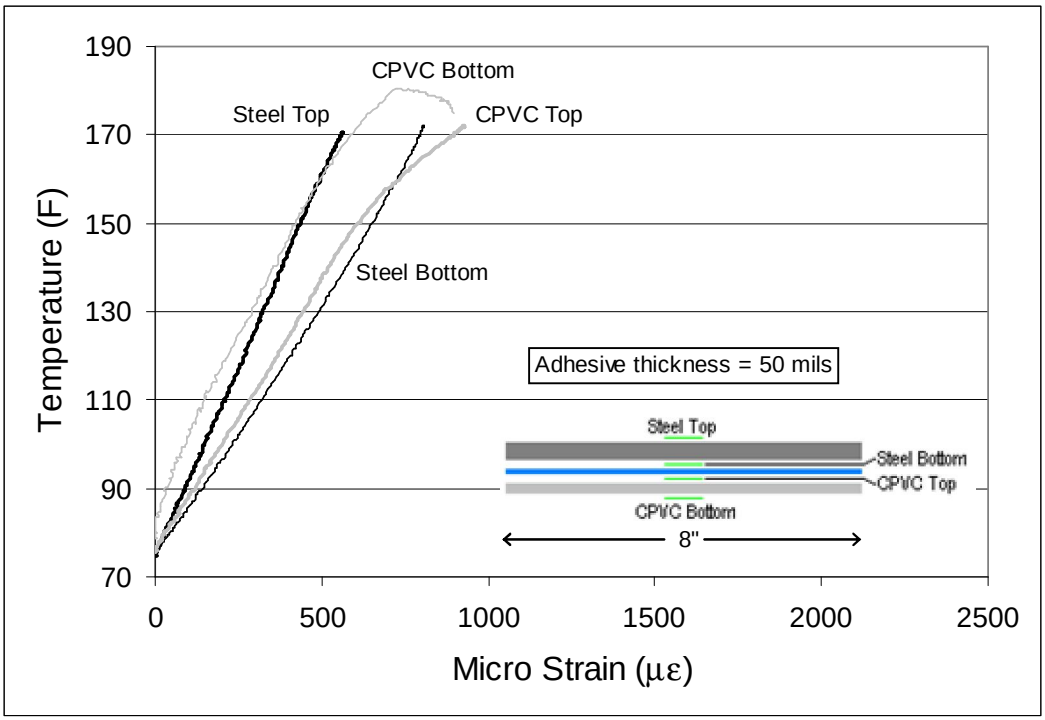

Figure 4.83 – Strain Behavior of Specimen 2 in X-Direction

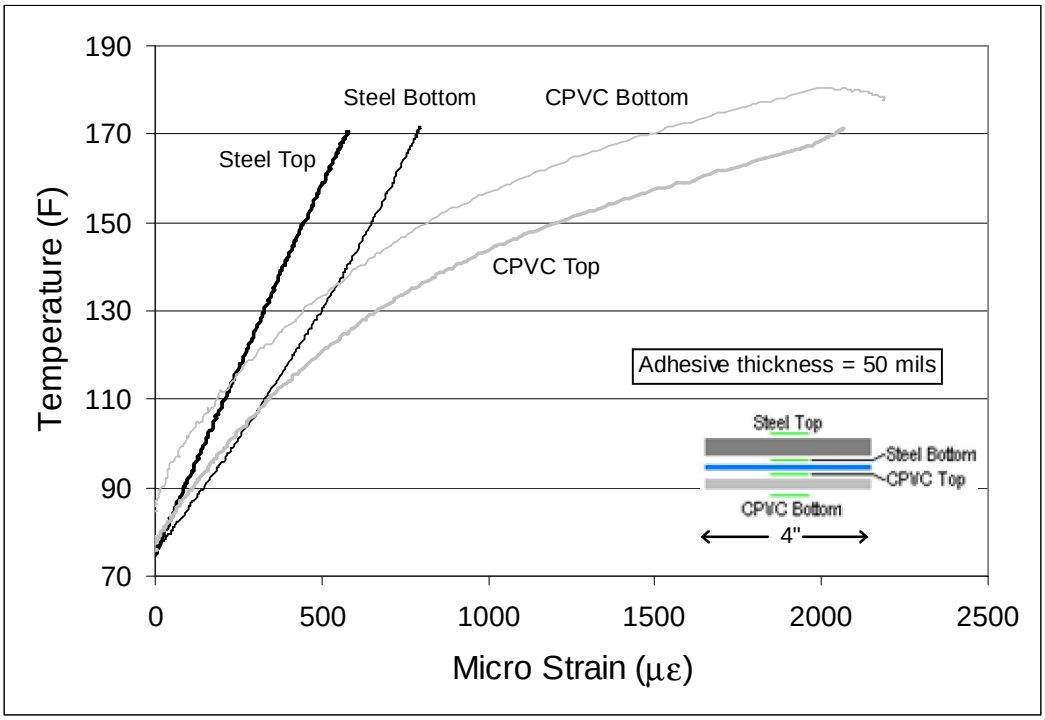

Figure 4.84 – Strain Behavior of Specimen 2 in Y-Direction

influence of the CPVC and adhesive expansion. At the same time the steel provides a restraining effect to the CPVC plate. Test results show that the measured strain in the short direction of the CPVC is almost twice that in the long direction. This could be attributed to the different CTE for the CPVC in the long and short directions in addition to the effect of boundary conditions, which were discussed previously for specimen 1. Test results showed that the adhesive thickness does affect the performance of the specimen. Although the behavior of the steel plate was not considerably affected, the magnitude of the strains induced in the CPVC were 20 to 30 percent less than those measured for the 80 mils specimen. This behavior was observed in both the long and short directions. These results suggest using a thinner adhesive layer for a more effective bond, but further comparisons using shear strain will provide a more accurate conclusion, as will be discussed in the final section. Figure 4.83 shows a nonlinear strain behavior of the CPVC in long direction begins at 150°F, which is slightly higher than that observed for specimen 1. A highly nonlinear behavior of the CPVC strain in short direction was observed at 110°F compared to the range of 100 to 110°F indicated for specimen 1. Results clearly show that as temperature increases, the bond between the steel and CPVC deteriorates significantly, as evidenced by the highly nonlinear behavior of the CPVC. As the bond deteriorates the CPVC is allowed to expand more freely at the high temperature resulting in a nonlinear strain behavior. Though adhesive performance has deteriorated, it still has a restraining effect. In the long direction of the CPVC, the maximum strains are five times less compared to measured strains for the CPVC material acting alone, shown in Figure 4.49. In the short direction, the maximum strains are about two and a half times less than the strains for the CPVC material acting alone.

Snapshots of the temperature and strain gradients selected at various times are shown in Figures 4.85 through 4.92 for specimen 2 with an adhesive thickness of 50 mils. Even numbered figures represent the behavior in the long (x) direction and odd numbered figures represent the behavior in the short (y) direction. The interface temperatures and the corresponding strains along the interface line at a time of 40 minutes are shown in Figure 4.85 and 4.86. It should be noted that a time of 40 minutes corresponds to a temperature of 112°F at the bottom surface of the CPVC. At such low temperature, minimal strains exist in both the x and y-directions. Both figures show that the bottom side of the steel has greater strains than its corresponding top side. The CPVC material does not adhere to this same behavior since its top and bottom strains are fairly linear in their respective directions. Figures 4.87 and 4.88 show considerable increasing strains and temperatures at a time of 80 minutes (temperature = 153°F) due to the corresponding increase in temperature. The increasing strain behavior for the CPVC and steel surfaces

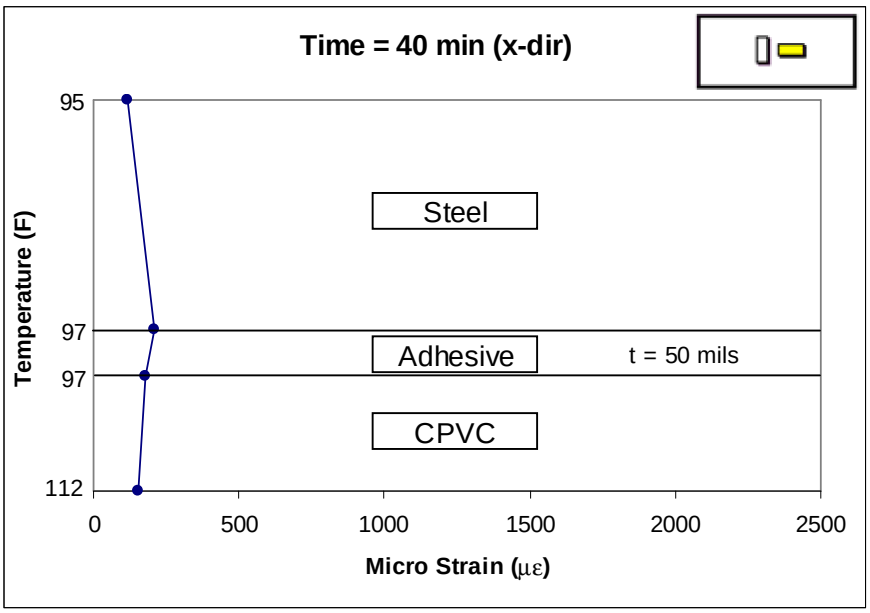

Figure 4.85 – Strain Profile for Specimen 2 at 40 min in the X-Direction

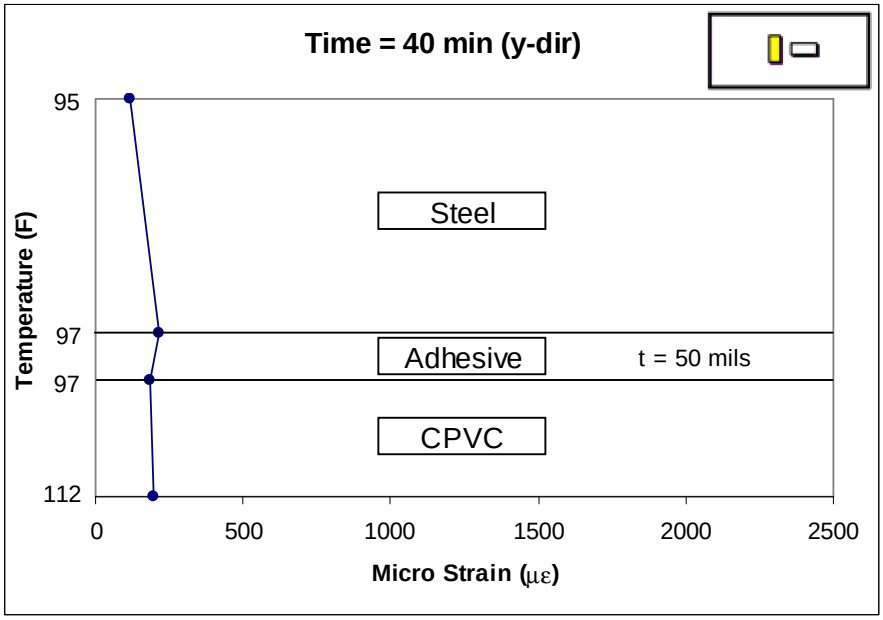

Figure 4.86 – Strain Profile for Specimen 2 at 40 min in the Y-Direction

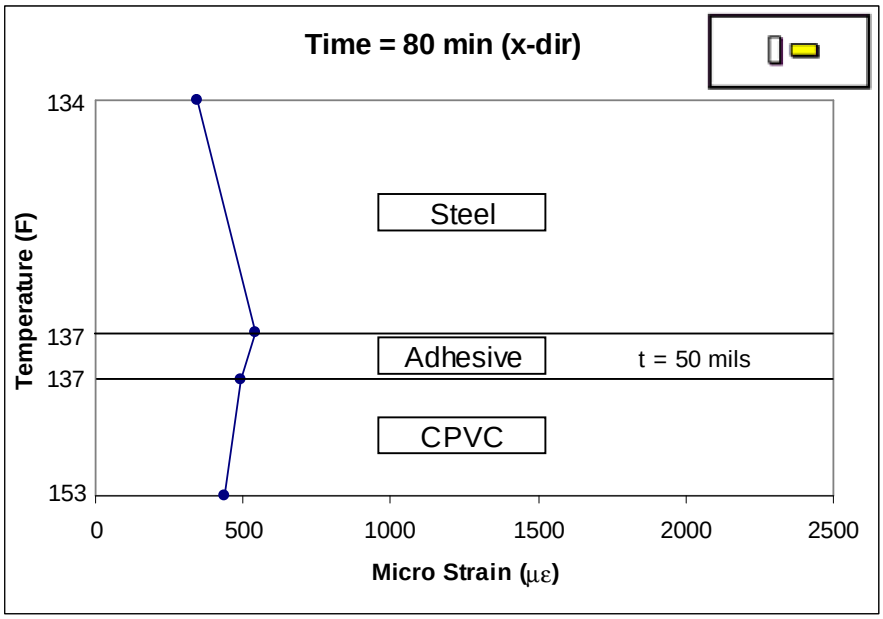

Figure 4.87 – Strain Profile for Specimen 2 at 80 min in the X-Direction

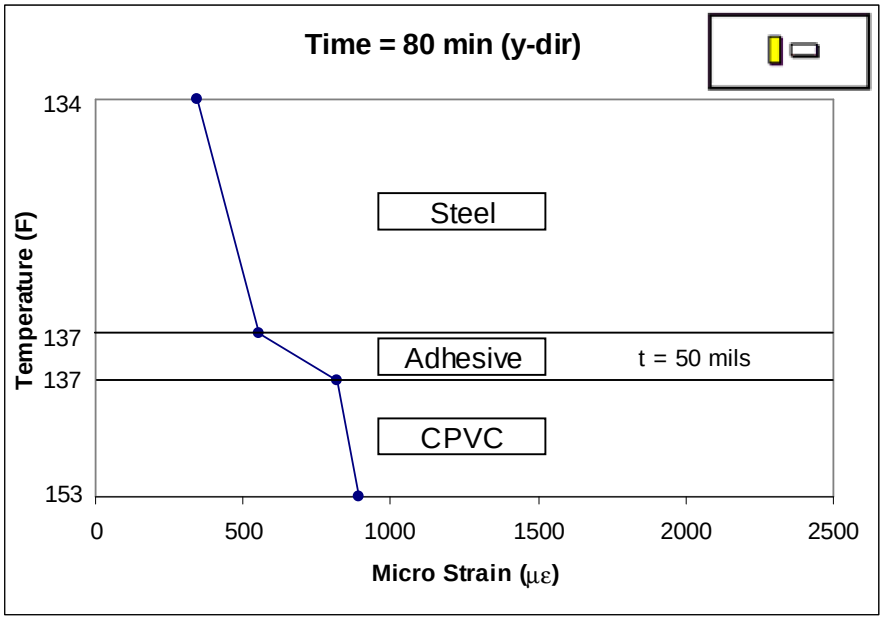

Figure 4.88 – Strain Profile for Specimen 2 at 80 min in the Y-Direction

was nearly tripled at points in the x-direction when compared to the measured values at 40 minutes. However, the measured CPVC strain in the y-direction dramatically increases by about four times the magnitude when compared the values at 40 minutes. Figures 4.89 and 4.90 represent strain and temperature results at a time of 100 minutes, which correspond to a temperature of 171°F at the bottom of the CPVC material. These figures show similar increasing strain behavior as that observed at 80 minutes, where the CPVC tensile strains in the y-direction were almost doubled from the measured values at 80 minutes. Figures 4.91 and 4.92 represent strain and temperature results at a time of 120 minutes, which correspond to a temperature of 179°F at the bottom of the CPVC material. The strains in the x-direction increase marginally, while increasing temperature in the CPVC continue to produce significant increases in strains for the y-direction. It was observed throughout the snapshots of specimen 2 that the measured strains on bottom surface of the CPVC in the x-direction were smaller than those on the top surface.

Other test results including snapshots at any time as well as graphs showing strain versus time across the heating and cooling cycles are included in Appendix C.

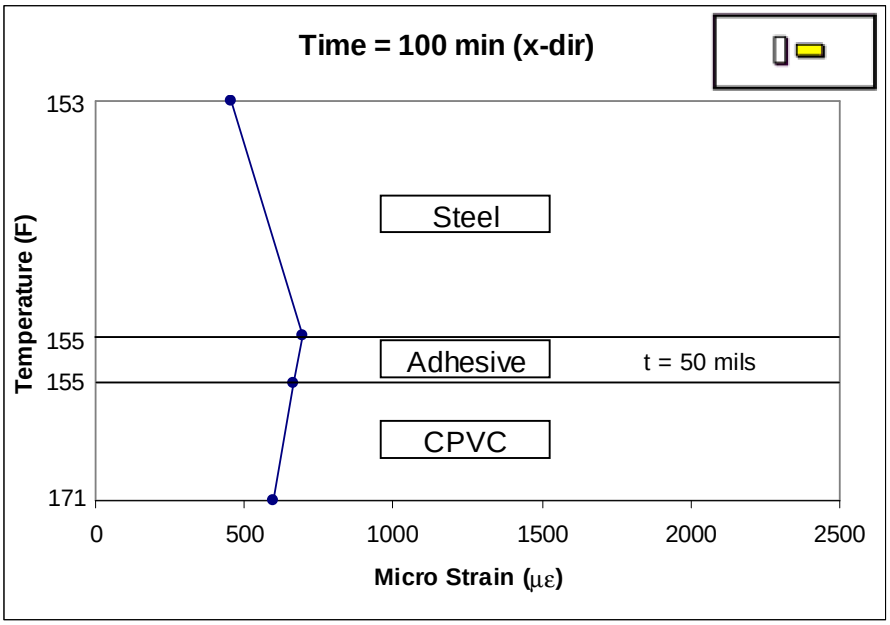

Figure 4.89 – Strain Profile for Specimen 2 at 100 min in the X-Direction

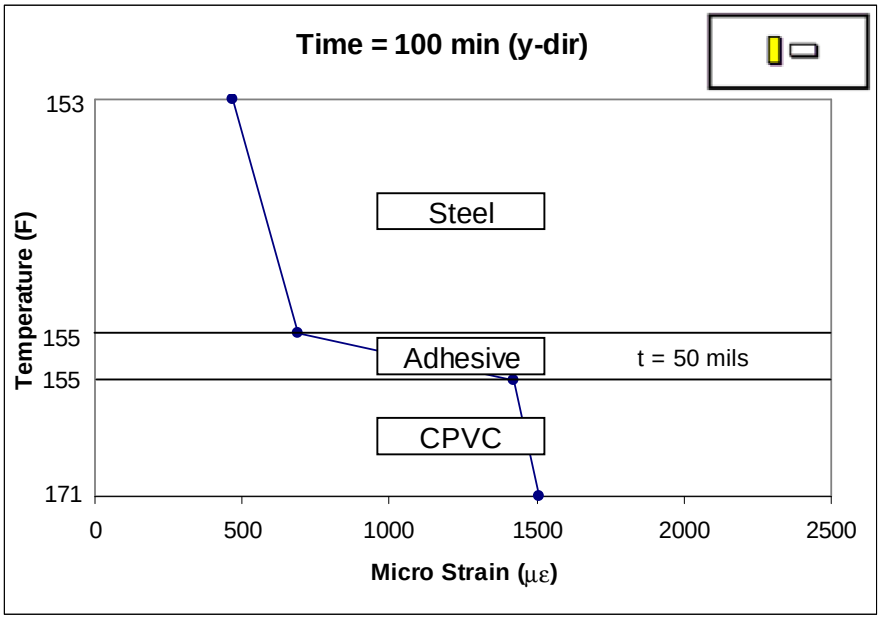

Figure 4.90 – Strain Profile for Specimen 2 at 100 min in the Y-Direction

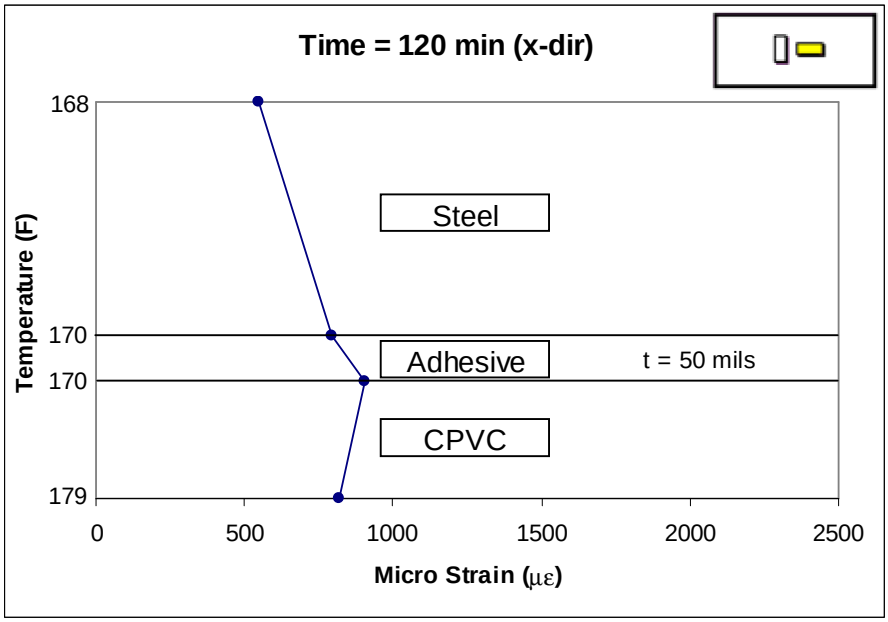

Figure 4.91 – Strain Profile for Specimen 2 at 120 min in the X-Direction

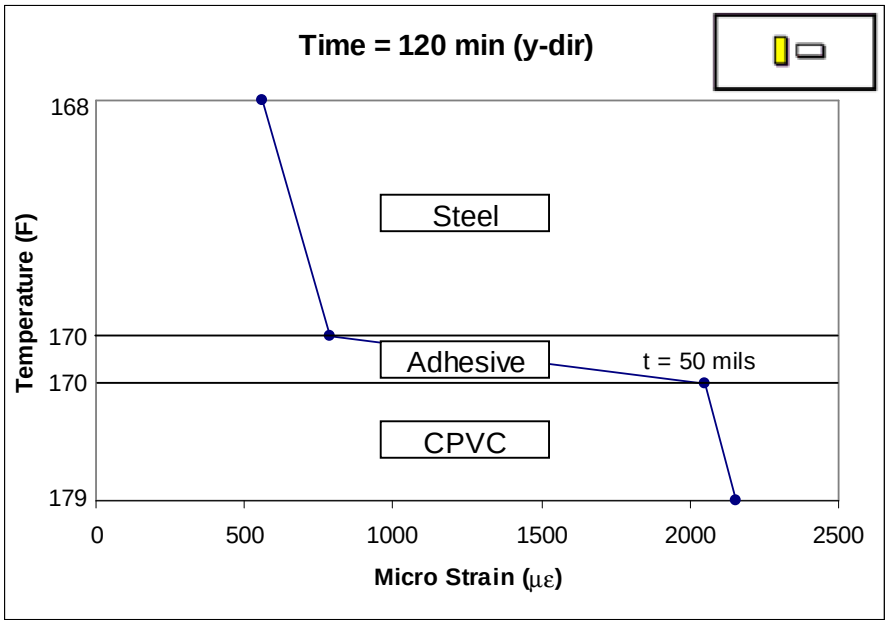

Figure 4.92 – Strain Profile for Specimen 2 at 120 min in the Y-Direction

4.4.2.6 Specimen 3 (Adhesive thickness of 30 mils)

Three bath tests were conducted on specimen 3 with a nominal adhesive thickness of 30 mils. Test setup, temperature control of heating and cooling phases, and resulting temperature gradient behavior was similar to that of specimens 1 and 2. The strain behavior in both the x and y-directions during the heating phase of specimen 3 is shown in Figures 4.93 and 4.94, respectively. Due to a mechanical failure of one of the strain gages in the adhesive layer, strain measurements for the top surface of the CPVC plate in the y-direction are not available. Testing of specimen 3 resulted in similar behavior from the previous test specimens. Figures 4.93 and 4.94 clearly show the interaction between the steel and CPVC. Results indicate an immediate distinction in the dissimilar behavior of CPVC in the short (y) and long (x) directions. Steel strains remain linear with the bottom surface expanding more than the top surface. The bottom steel is bonded to the adhesive layer; therefore, it expands at a higher rate than normal due to the influence of the CPVC to the adhesive expansion. At the same time the steel provides a restraining effect to the CPVC plate. Test results showed that the measured strain in the y-direction of the bottom CPVC surface is almost twice that in the x-direction. This could be attributed to the different CTE values for the CPVC in both the x and y-directions in addition to the effect of boundary conditions. Test results showed that the adhesive thickness affects the performance of the specimen. Again, the steel strains remained unchanged from previous test results. Although the behavior of the steel plate was not considerably affected, the magnitude of the strain induced in the y-direction of the CPVC bottom was 23 percent less than that measured for the 80 mils specimen. These results suggest using a thinner adhesive layer for a more effective bond. Measured CPVC strain

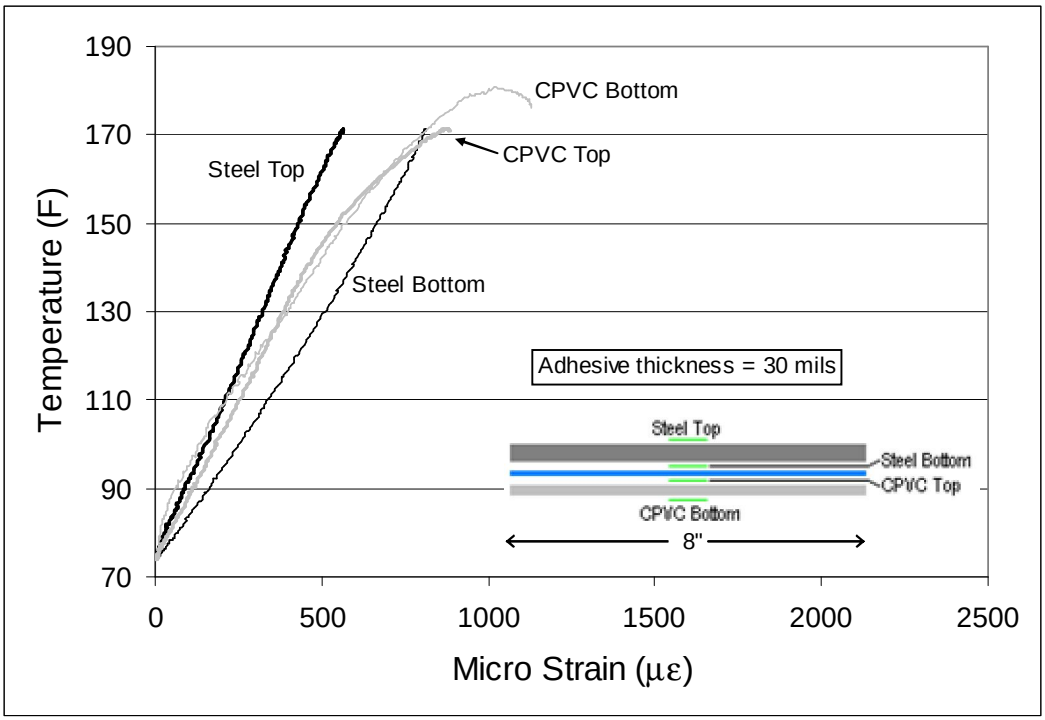

Figure 4.93 – Strain Behavior of Specimen 3 in X-Direction

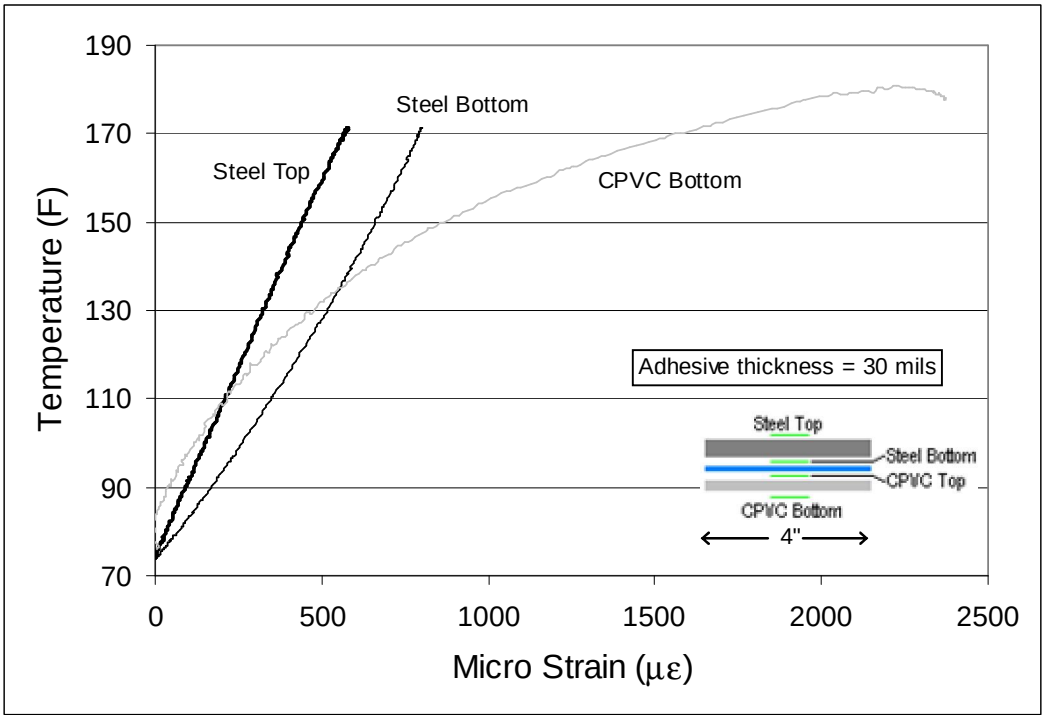

Figure 4.94 – Strain Behavior of Specimen 3 in Y-Direction

values showed more agreement with specimen 3 and the 50 mils specimen. Strain results in the x and y-directions of the CPVC plate were marginally greater than the strains from the 50 mils specimen. These results suggest that an adhesive thickness of 30 mils and 50 mils has no significant effect on the adhesive bond. Figure 4.93 show a nonlinear strain behavior of the CPVC in x-direction begins at 150°F, which is identical to the behavior observed for specimen 2. The highly nonlinear behavior of the strain in the y-direction of the CPVC, shown in Figure 4.94, was observed at 110°F, which is also similar to specimen 2. Results clearly indicate that as temperature increases, the adhesive bond between the steel and the CPVC surface deteriorates significantly as evidence by the highly nonlinear behavior of the CPVC. As the bond deteriorates the CPVC is allowed to expand more freely at the high temperature resulting in a nonlinear strain behavior. Though adhesive performance has deteriorated, it still has a restraining effect. In the long direction of the CPVC, the maximum strains are five times less compared to measured strains for the CPVC material acting alone. In the short direction, the maximum strains are about two and a half times less than the strains for the CPVC material acting alone.

Snapshots of the temperature and strain gradients selected at various times are shown in Figures 4.95 through 4.99 for specimen 3. Only figures showing strain profile behavior in the long (x) direction are presented in the following graphs since the CPVC strain gage in the adhesive layer sustained permanent damage. At time of 40 minutes, Figure 4.95 shows that only minimal strains exist in the long direction. Results indicate that strains are fairly linear throughout the thickness when the CPVC bottom surface temperature is 114°F. Figure 4.96 shows increasing strain and temperature results at a time of 80

minutes, which corresponds to a temperature of 154°F at the bottom of the CPVC material. The increasing strain behavior for both materials more than doubles when compared to the values at 40 minutes. Figure 4.97 represents strain and temperature results at a time of 100 minutes, where the bottom surface of the CPVC is 172°F. The

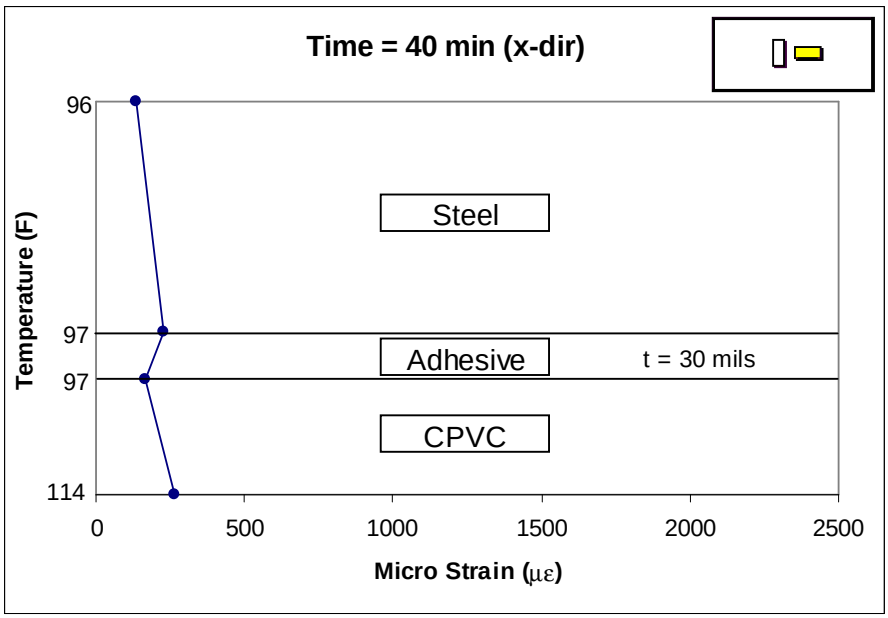

Figure 4.95 – Strain Profile for Specimen 3 at 40 min in the X-Direction

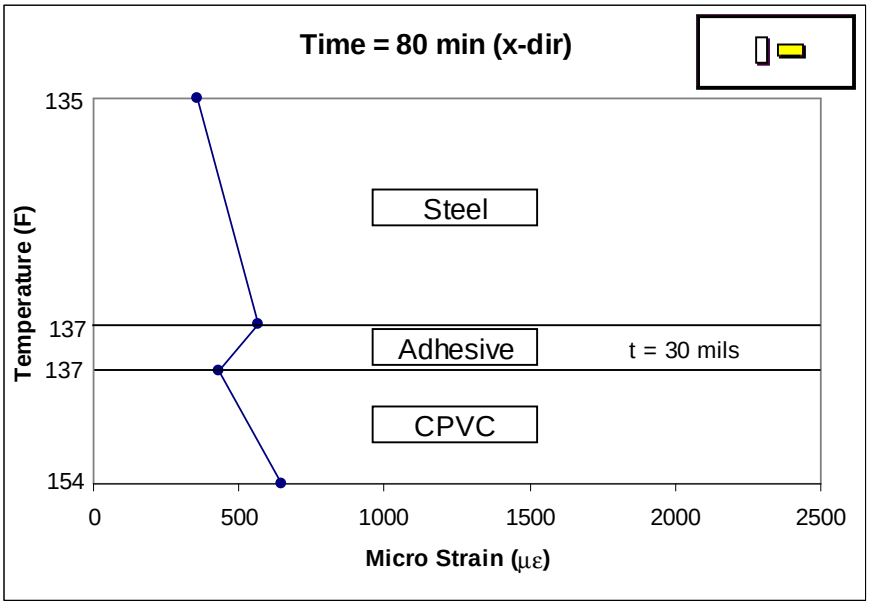

Figure 4.96 – Strain Profile for Specimen 3 at 80 min in the X-Direction

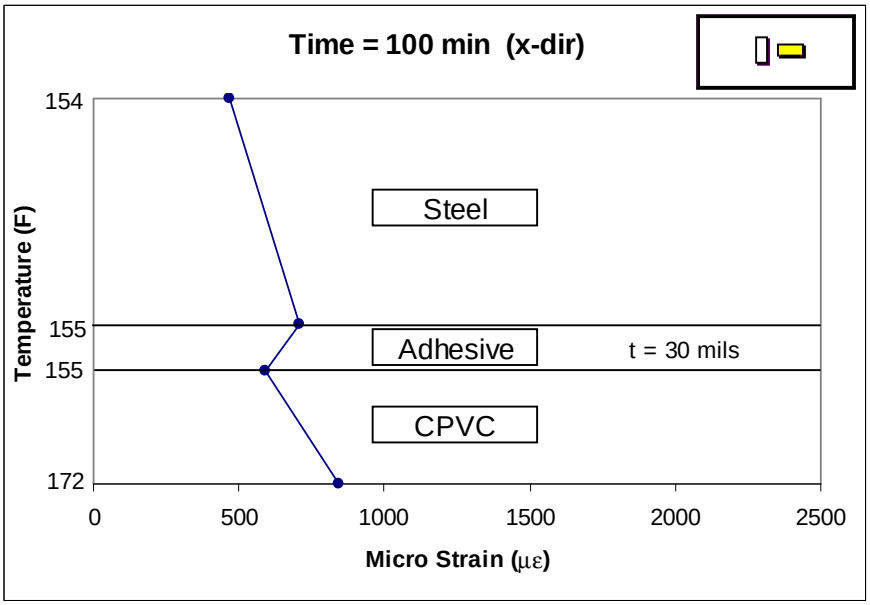

Figure 4.97 – Strain Profile for Specimen 3 at 100 min in the X-Direction

figure shows a similar increasing strain behavior as that observed at 80 minutes. The strain increase is most pronounced for the bottom surface of the CPVC than at the other surfaces. Results indicate no change in the strain differences between the top surface of the CPVC and the bottom surface of the steel from 80 minutes to 100 minutes. Figure 4.98 represents strain and temperature results at a time of 120 minutes which corresponds to a temperature of 178°F at the bottom of the CPVC material. Measured strains in the x-direction increase marginally for steel, and a substantial increase was observed in the CPVC. It was also observed that the measured strain at the bottom of the steel surface is the same as the strain at the top surface of the CPVC. This result suggests that the shear strain effects in the x-direction of the adhesive layer are minimized when the adhesive layer is 169°F. Other test results including snapshot results at different times as well as graphs showing strain versus time across the heating cycle can be found in Appendix C.

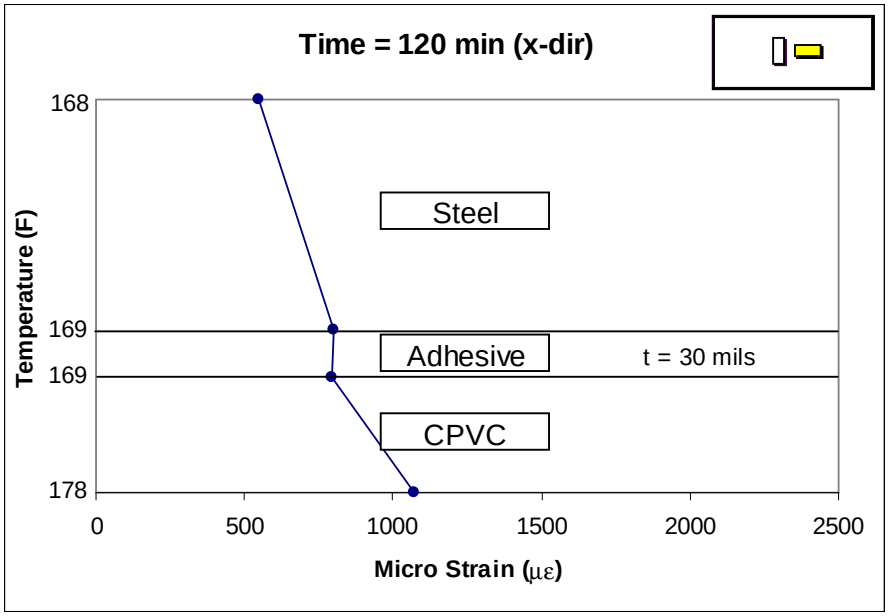

Figure 4.98 – Strain Profile for Specimen 3 at 120 min in the X-Direction

4.4.2.7 Effect of Adhesive Thickness

The effect of the adhesive thickness can be most easily displayed by comparing the snapshots of different specimens. Combined snapshots for different specimens are shown in Figures 4.99 through 4.106. Temperature gradients varied slightly from each of the corresponding time step results, so interface temperatures were averaged from the three specimens. As discussed earlier, the strain gage in the y-direction was mechanically damaged in the adhesive layer for the 30 mils thick specimen. To avoid confusion, results for the other three y-direction gages were not included. However, the behavior of the accumulated data from the three functioning gages was similar to that observed for the 50 mils specimen. Figures 4.99 and 4.100 compare strains at a time of 40 minutes for the short and long-directions, respectively. While similar behavior was observed for the steel in the x and y-directions for the three specimens, a considerable deviation existed for the measured CPVC strains. In the y-direction, the measured strains suggest an early

sign of severe variations within the adhesive thickness, indicating shear stress at the CPVC-adhesive interface. Figures 4.101 and 4.102 compare strains at a time of 80 minutes for the x and y-directions, respectively. Again, steel strains coincide for all

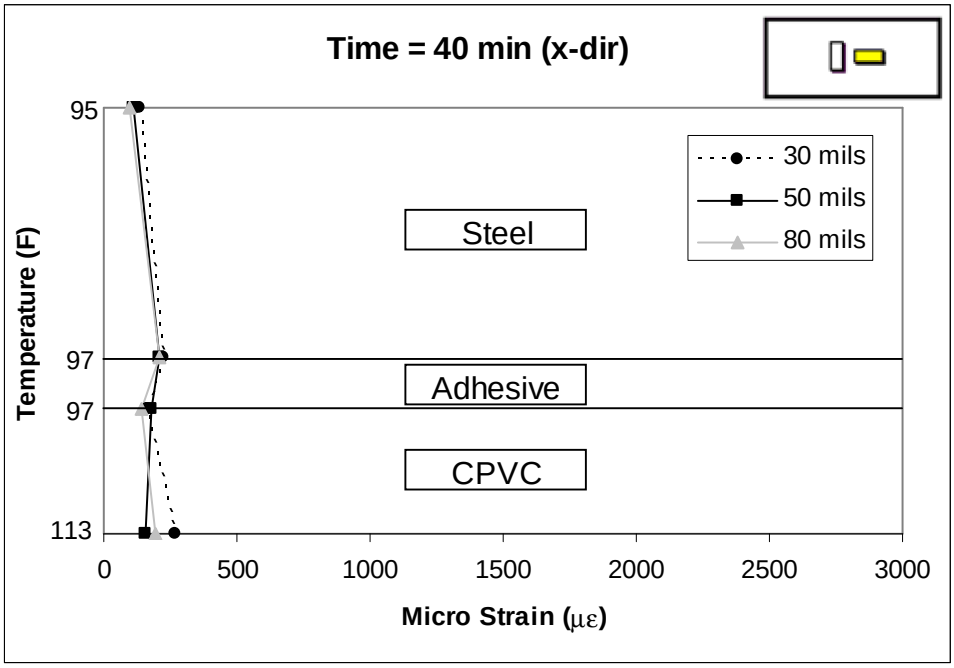

Figure 4.93 – Strain Profile for Specimens at 40 min in the X-Direction

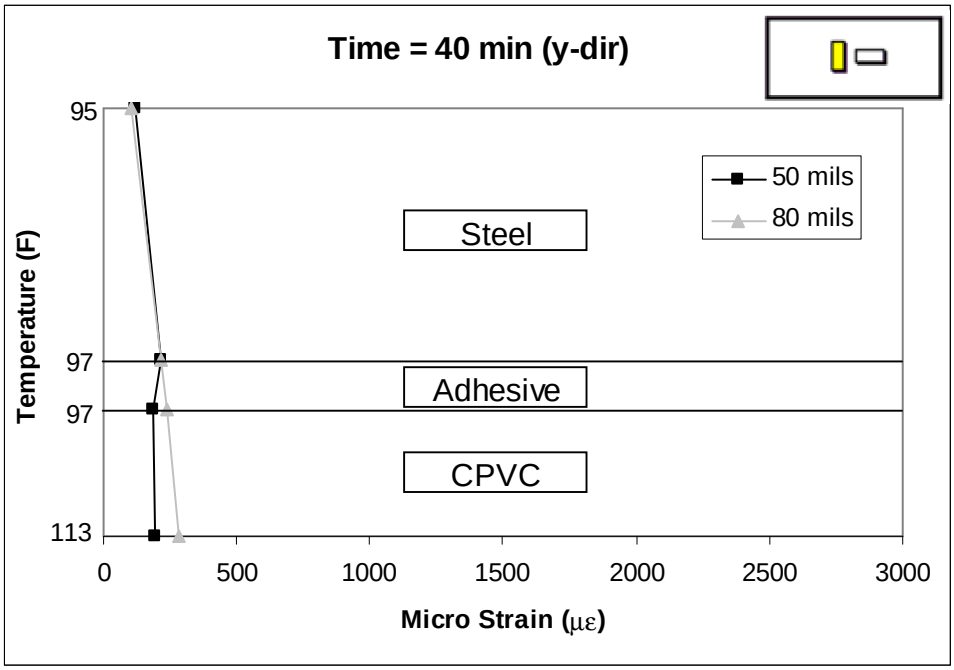

Figure 4.94 – Strain Profile for Specimens at 40 min in the Y-Direction

results. The measured strains in the CPVC x-direction match well for 30 and 80 mils thicknesses. The measured CPVC strains in the y-direction, shown in Figure 4.96, clearly demonstrate the presence of large shear strains within the 80 mil adhesive.

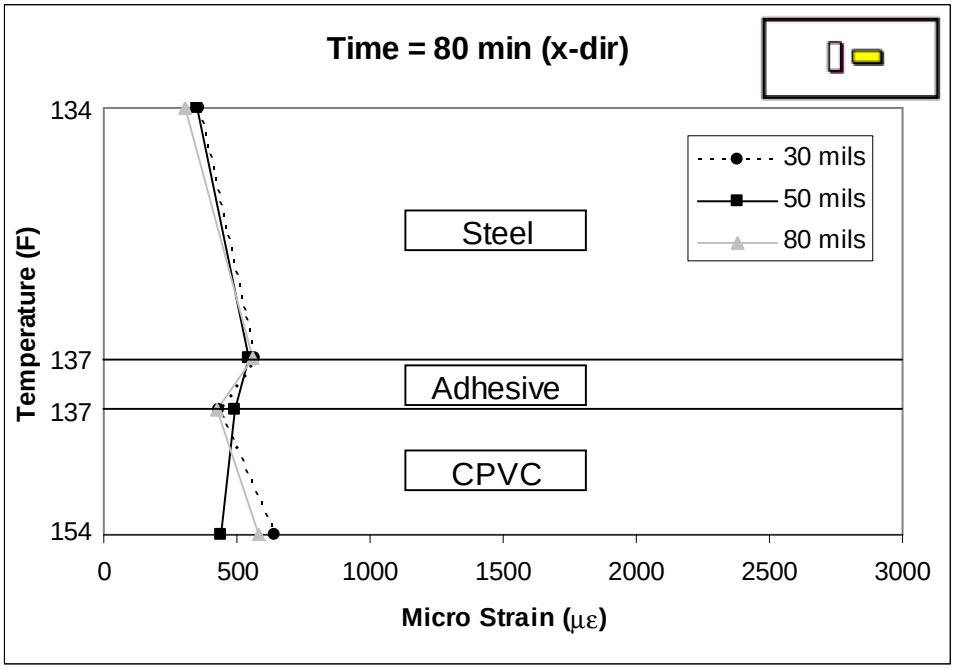

Figure 4.95 – Strain Profile for Specimens at 80 min in the X-Direction

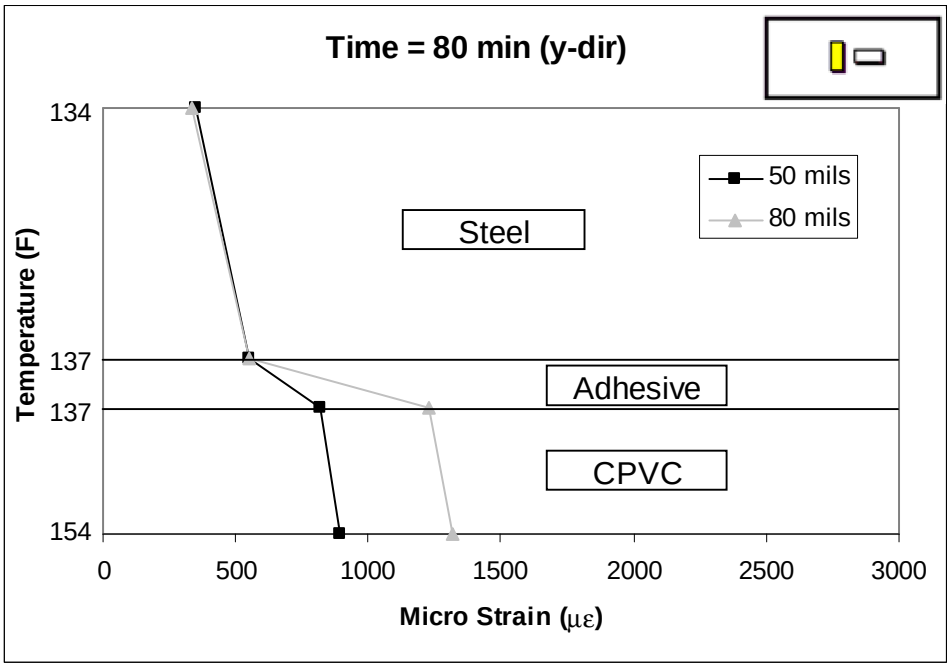

Figure 4.96 – Strain Profile for Specimens at 80 min in the Y-Direction

Figures 4.103 and 4.104 compare strains at a time of 100 minutes for the x and y-directions, respectively. Steel strains coincide for all results. Similar behavior was observed for the measured CPVC strains as for the 80 minute snapshots in the x and y-directions. However, the increased temperatures show a more significant effect in the divergence of the shear strains in the y-direction within the adhesive layer. Figures 4.105 and 4.106 compare strains at a time of 120 minutes for the x and short directions, respectively. The y-direction snapshot showing the adhesive layer strains further supports that increased temperatures result in a significantly higher shear strains within the adhesive layer. Since steel strains behave similarly for all specimens in both short and long directions at the various time steps, results suggest that the adhesive thickness does not contribute to steel performance. Essentially, the significantly higher modulus of steel dominates CPVC (approximately 80 times greater for steel) throughout the composite interaction. Corzan Industrial Systems indicates that for restrained

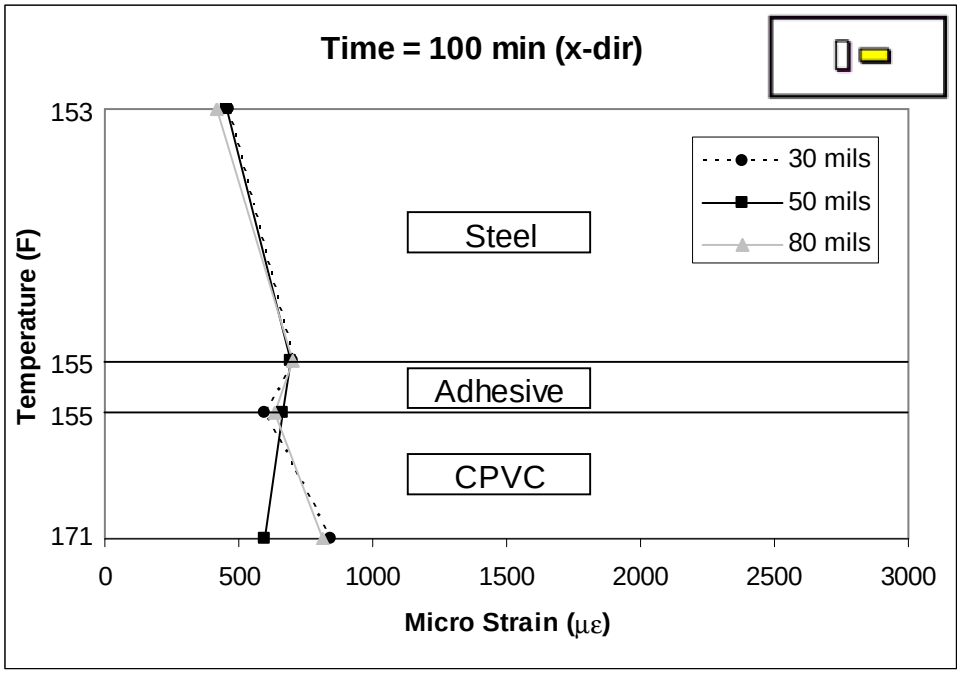

Figure 4.97 – Strain Profile for Specimens at 100 min in the X-Direction

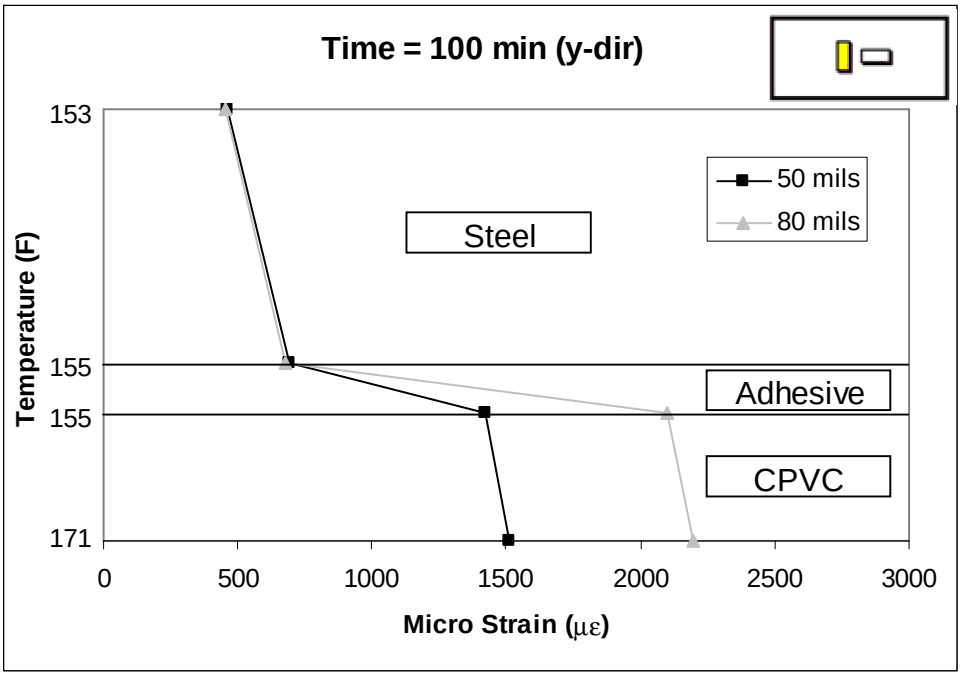

Figure 4.98 – Strain Profile for Specimens at 100 min in the Y-Direction

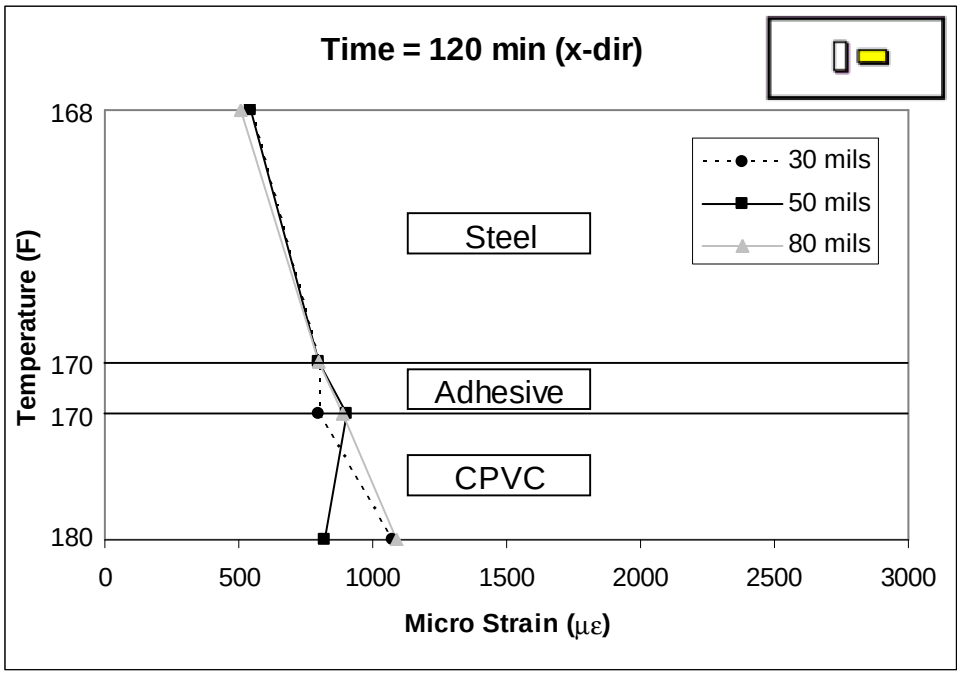

Figure 4.99 – Strain Profile for Specimens at 120 min in the X-Direction

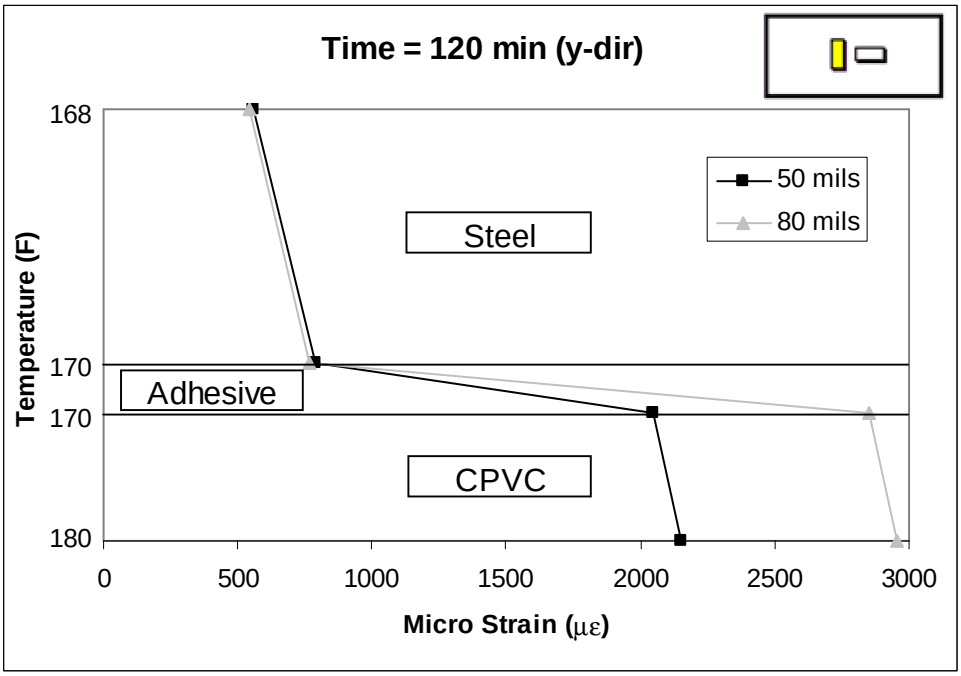

Figure 4.100 – Strain Profile for All Specimens at 120 min in the Y-Direction

applications steel strains are roughly 16 times greater than CPVC when subjected to any given temperature range (n.d.-a). Tests in this experimental study were essentially unrestrained, so such stress relationships cannot be applied. Temperature increase clearly has a negative influence on bond interaction strength between the steel and CPVC interfaces. This influence is much more pronounced in the short (y) direction, but still exists in the long (x) direction. Demands on bond strength are amplified at higher temperatures because of the difference in steel and CPVC coefficients of thermal expansion. The measured CTE of CPVC in the long direction is about six times larger than steel, while the short direction is about eight times larger. Plotted linearly, the strain difference between the steel and CPVC would only be amplified at higher temperatures.

To gain further understanding of the behavior of the induced shear strains within the adhesive layer, shear strains need to be quantified. Due to the significant strain

differences between the top of the CPVC and the bottom of the steel plates, denoted by $\Delta\varepsilon$, shear strains are developed. Adhesive layer shear strain, γ, is a function of the horizontal displacement within the adhesive layer and the thickness of the adhesive, t_a. It should be highlighted that the strains are not uniform across the width of the specimen due to the restraints provided along the perimeter of the specimen. The shear strains within the adhesive layer are directly proportional to $\Delta\varepsilon / t_a$ as expressed by Equation 4.4.

$$\gamma \propto \frac{\Delta\varepsilon}{t_a} \tag{4.4}$$

Since the strains were minimal in the long (x) direction, calculations are considered only to the short (y) direction. Table 4.14 shows the shear strain relationships for the specimens with 50 and 80 mils adhesive thickness. For the 80 minute time step, a 61 percent increase in the shear strain was observed by increasing the adhesive thickness from 50 to 80 mils. For the 100 minute time step, a 21 percent increase resulted. For the 120 minute time step, only a 3 percent increase resulted. Results show that the 50 mils thick adhesive specimen performs better at lower temperatures. However, at higher temperatures (around 170°F), the shear strain differences for the two adhesive layer thicknesses are negligible.

Table 4.14 – Shear Strain Relationships

Specimen Adhesive Thickness	$\Delta\varepsilon / t_a$ at various times		
	80 min	100 min	120 min
50 mils	5285	14666	25204
80 mils	8502	17746	26032

5.0 Summary and Conclusions

5.1 Summary

Severe environmental conditions and corrosive environments can significantly reduce the service life of steel tanks. To meet these challenges and to improve the service life of the tank, a fundamental understanding of the behavior of the materials used for lining these tanks must be studied. The main objective of this research program is to study the behavior of the various materials proposed for lining typical bleach tanks used in the pulp and paper industry. A cyclical heating environment, along with the corrosiveness of the chlorine dioxide bleach agent, presents considerable challenges to the proposed tank liner. The proposed tank lining material used in this study is chlorinated polyvinyl chloride (CPVC), which is a thermoplastic material that has excellent chemical resistance and has been shown to endure extreme thermal conditions. The selected structural adhesive, SS340, will be used bond the CPVC material to the wall of the steel tank. The adhesive is produced by a local company and is currently used by industry for bonding composites, metals, and other plastics. This thesis research program provided extensive analysis for some of the challenges facing the adhesive/CVPC tank liner and offered general guidelines to their behavior.

The primary goal of this research program is to determine the properties of the adhesive material, CPVC material, and the bond characteristics under the effect of severe environmental conditions typical to tank lining systems. The experimental program consisted of three phases. The first phase focused on the fundamental material properties of CPVC and SS340 when subjected to various environmental conditions. Test variables

included temperature and applied sustained loads, as well as time and soaking solution. For the second phase of testing, the investigation focused on the influence of environmental exposure on shear strength of the adhesive bond. Test variables included temperature and applied sustained loads. Test results for the first two phases provided limitations of the temperature and sustained load level which can be used safely under service loading conditions. The third phase of the experimental program investigated a cross-section of the proposed steel tank with an adhesively bonded CPVC lining. A small-scale model was constructed to determine the thermal gradient distribution and composite interaction resulting from temperature changes. In addition, finite element analysis was conducted to verify the measured results.

5.2 Conclusions

Test results of the experimental program to study the effect of the environmental conditions on the tensile strength of the CPVC material reveal that high temperature combined with high sustained loads has a significant effect on the behavior of the CVPC. The results indicate that temperature up to 180°F does alter the behavior of CPVC. Test results show that a combination of high sustained load with high temperature causes a significant reduction of the strength as well as brittle failure of the CPVC material. Based on the various levels of sustained loads and temperatures considered in this investigation, it is recommended to limit the sustained load to 30 percent of the ultimate strength if the temperature increased to 140°F. Results also suggest that if the temperature increased up to 180°F, the sustained loads must be limited to 10 percent or less. The effects of soaking time for both water and salt-water soaking does not have a significant impact on behavior of the CPVC material.

Based on the experimental program conducted to examine the effect of the environmental conditions on the tensile strength of the selected SS340 adhesive material, results indicate that the presence of sustained loads combined with high temperature dramatically reduce the tension strength and cause early failure of the adhesive. Results show that exposure to hot water without sustained loads could cause degradation and reduce the tensile strength of the material. In addition, water soaking does have an adverse effect on the deformability of the adhesive. Test results indicate that for the SS340 adhesive exposed to high temperature up to120^{o}F, the sustained stress should be limited to 10 percent of the ultimate strength. Soaking time has a minimal effect on the strength of the adhesive, however, the strength may slightly decrease as soak time increases. Salt water soaking does not have an adverse affect on the strength behavior or deformability.

Test results to study the effect of the environmental conditions on the shear strength of the SS340 adhesive for steel-to-CPVC lap slice specimens reveal that a substantial loss of adhesive shear strength and overall specimen displacement occurs when exposed to high temperatures in a water environment. Test results indicate that the shear strength of specimens tested at 140°F is reduced by a range of 25 to 35 percent compared to specimens tested at room temperatures. Similarly, the strength of specimens tested at 180°F was reduced by 50 percent compared to specimens tested at room temperatures. Test results show that the adhesive can carry sustained loads up to 15 percent at room temperature without any sign of degradation. Results also indicate that the adhesive bond did not survive under combined sustained stresses of 15 percent at a temperature range from 120°F and 140°F. Therefore, for in-service applications requiring 15 percent

sustained stresses the temperature should not exceed 120°F. To ensure a long service life of the adhesive, the sustained load should be reduced to 8 percent at a temperature of 120°F. Application of the adhesives should follow rigid bonding standards, such as surface preparation requirements and curing conditions to increase their service life. Bond overlap of 1/2" versus 1" does not produce a significant effect on the lap behavior. Failures occurring in the environmental exposure chamber resulted in an adhesive failure between the adhesive and steel substrate. Typical failure of specimens exposed to room temperatures of 73°F occurs in the adhesive layer, which is known to be cohesive failure. Some specimens exhibited a combination adhesive/cohesive failure. Results indicated no reduction in strength or deformation for specimens tested at room temperature soaked in salt-water compared to specimens soaked in water.

Coefficient of thermal expansion (CTE) measurements is critical to determining the overall structural behavior of the adhesively bonded steel and CPVC plates. For steel CTE measurements, test results showed that the behavior is influenced by the rate of temperature increase. Steady state temperature and strain recordings provided a smaller CTE value that more closely matches published CTE steel data. For CTE measurements of CPVC, test results showed the anisotropic nature of the material. CTE in one direction of the material is higher than the CTE in the other direction. Therefore, the measured strains in the short direction of the specimen (x-direction) were significantly higher than those measured in the long direction (y-direction) at all temperatures. This characteristic had a significant effect on the composite behavior of the bonded specimens. CTE measurements of the CPVC in the short direction produced a value 8 times that of steel in

the short direction and 6 times that of steel in the long direction. CTE measurements of the adhesive specimen showed a slightly smaller value than the CPVC material.

To study the influence of thermal gradient on the bond behavior of the proposed tank lining, three small scale models were constructed and investigated through a series of heated bath tests. Strain gages and thermocouples were attached to the top and bottom surfaces of the steel and CPVC materials. Strain gages were mounted in both the long (x) and short (y) directions on the top and bottom surfaces of both materials. Test results showed linear strain behavior to in both long and short directions for the steel. Conversely, a nonlinear behavior was observed in the strain-temperature relationship of the CVPC material. There are two main factors that contribute to the differences in the short and long directions. The first factor is the anisotropic nature of the CPVC. The second factor is the rectangularity of the specimens, which is influenced by the boundary conditions, as confirmed by finite element analysis. Results clearly indicate that as temperature increases the bond between the steel and CPVC deteriorates significantly. This behavior was evidenced by the highly nonlinear behavior of the CPVC material. Consequently, the CPVC is allowed to expand more freely at high temperatures, preventing the full composite action. Though the adhesive is much less effective at high temperatures, it still provides a restraining effect to the CPVC material. Results in the short direction may suggest a possible decay in bond strength over time, leading to an adhesive shear failure. Test results also showed that the adhesive thickness affects the performance of the specimen. The behavior of the steel plate was not considerably affected by thickness. However, the magnitude of strains induced in the CPVC for

specimen thicknesses of 30 and 50 mils were 20 to 30 percent less than those measured for the 80 mils specimen. Results suggest using a thinner adhesive layer for a more effective bond at lower temperatures.

Test results included in this study apply to only the specific materials used in the analysis. For the thermal gradient behavior of the proposed tank lining, the results are prescribed specifically for thicknesses of the steel (1/4") and CPVC (1/8"). Correlations to other materials would have to be made on a case by case basis.

5.2 Future Research

A continuation of this experimental program may be applied in several ways. An investigation of chlorine dioxide environments on the CPVC and adhesive materials may be necessary. The thermal changes within the tank may decrease the corrosive resistance of the CPVC material over time. Additionally, connection methods of the CPVC sheet linings must be designed. These connections must be able to absorb large strains produced at the ends of adjacent sheets. Ultimately, the connection method must be able to prevent chlorine dioxide penetration into the adhesive layer, since the adhesive will be extremely susceptible to the corrosive effects of the chemical solution. A design of a small-scale tank may also provide additional insight for the behavior of the composite liner. A circular steel tank will result in a confinement effect of the CPVC, which is not studied in this program. Finite element analysis of a circular steel tank should also provide similar insight for the behavior of the steel tank and CPVC lining. A nonlinear analysis would be ideal to include the decreases in the moduli of elasticity and the bond deterioration due temperature changes.

REFERENCES

ASTM D 638-03, *"Standard Test Method for Tensile Properties of Plastics.*" West Conshohocken, PA, American Society for Testing and Materials, 2003.

ASTM D 3528-96 (Reapproved 2002), *Standard Test Method for Strength Properties of Double Lap Shear Adhesive Joints by Tension Loading.*" West Conshohocken, PA, American Society for Testing and Materials, 1996.

Air Products and Chemicals (2001). "Epoxy Additives for Adhesive Applications." Retrieved August 28, 2006 from http://www.airproducts.com/epoxyadditives/content/pdf/AMR/125-0005.pdf.

Ambler, Roger E. "CVPC: The Material of Choice in Metal-Finishing Plants." *Metal Finishing.* 94.8 (1996): 24-28.

Ashcroft, I.A. "Fatigue." *Adhesive Bonding: Science, Technology & Applications.* R.D. Adams. Cambridge: Woodhead Publishing Limited, 2005. 209-239.

Bergquist, A. Nordstrom, J. "In Plant Corrosion Testing in Chlorine Dioxide Environments." *Tappi Journal.* 79.2 (1996): 187-196.

Bjorneklett, A. Kristiansen, H. Tuhus, T. "A Model for Thermal Fatigue of Large Area Adhesive Joints Between Materials with Dissimilar Thermal Expansion." *Proceedings - IEEE Semiconductor Thermal Measurement & Management Symposium*. Feb. 1994: 138-141.

Bogner, B. Sumbry, L. "Fiberglass-Reinforced Plastics Protect Aboveground Units Against Corrosion Inside and Out." *Chemical Engineering.* 100.1 (1993): 131, 32, 35.

Brewis, D. "Surfaces: How to Treat." *Adhesive Bonding: Science, Technology & Applications.* R.D. Adams. Cambridge: Woodhead Publishing Limited, 2005. 75-88.

Comyn, J. "What Are Adhesives & Sealants and How Do They Work." *Adhesive Bonding: Science, Technology & Applications.* R.D. Adams. Cambridge: Woodhead Publishing Limited, 2005a. 23-51.

Comyn, J. "Environmental (Durability) Effects." *Adhesive Bonding: Science, Technology & Applications.* R.D. Adams. Cambridge: Woodhead Publishing Limited, 2005b. 123-142.

Corzan Industrial Systems (n.d.-a). "Thermal Expansion and Thermal Stresses." Retrieved August 2005 from http://www.corzancpvc.com/DesignManual/Thermal_Expansion.pdf.

Corzan Industrial Systems (n.d.-b). "Corzan Industrial Sheet / Lining." Retrieved February 2005 from http://www.corzancpvc.com/designSpecInstallation/industrialSheet.asp

Corzan Industrial Systems (n.d.-c). "Thermal Conductivity of Corzan CPVC." Retrieved September 2006 from http://www.corzancpvc.com/DesignManual/Thermal_Conductivity.pdf.

Currier, R. Robinson, J. Sattelberger, A. "Inadvertent Production and Explosion of Liquid Chlorine Dioxide. *Chemical Engineering & News.* 80.49 (2002): 4-5.

Ewerszumrode, A. Hahn, O. "Influence of the Setting Conditions on the Property Profile of Adhesive-Bonded Joints between Adherents with Different Coefficients of Expansion." *Welding & Cutting.* 50.3 (1998): E47-E49.

Fay, P.A. "History of Adhesive Bonding." *Adhesive Bonding: Science, Technology & Applications.* R.D. Adams. Cambridge: Woodhead Publishing Limited, 2005. 3-22.

Ford, M. J. Gelfant, F.S. "Designing to Keep Monolithic Tank Linings Monolithic." *Pulp & Paper Canada.* 96.2 (1995): 28-31.

Habib, P. "Thermoplastic-Lined Fiber Reinforced Plastic Dual-Laminate Composites for Corrosive Applications. *Materials Performance.* 37.1 (1998): 25-29.

Hitzroth, A. Owen, D. "One Mill's Response to a Potential Significant Release of Chlorine Dioxide Solution from their Chlorine Dioxide Storage Tanks." *Pulp & Paper Canada.* 101.11 (2000): 31-34.

Kanderakis, G. N. Marioli-Riga, Z.P. Tsamasphyros, G.J. "Thermal Analysis by Numerical Methods of Debonding Effects near the Crack Tip under Composite Repairs." *Applied Composite Materials.* Oct. 2003: 149-158.

Kim, Y.G. Lee, D.G. Oh, J.H. "Strength of Adhesively-Bonded Tubular Single Lap Carbon/Epoxy Composite-Steel Joints." *Journal of Composite Materials.* 33.20 (1999): 1897-1917.

Lenntech. "FAQ's Chlorine Dioxide." 2001-2006. 28 August 2006 <http://www.lenntech.com/faqclo2.htm>.

Mitschke, H. "Effects of Chloride Contaminatino on the Performance of Tank and Vessel Linings." *Journal of Protective Coatings and Linings.* 18.3 (2001): 46-56.

Skabo, R.R. "A Survey of Tank Lining Materials." *Journal of Protective Coatings and Linings.* 4.2 (1987): 32-38.

Smith, G (2005). "Bond Characteristics and Qualifications of Adhesives for Marine Applications and Steel Pipe Repair." Retrieved June 2005 from http://www.ce.ncsu.edu/centers/rb2c/Publications/ConMat-BondCharacteristics.pdf

Stebbins Engineering (n.d.). "Pulp and Paper Industry." Retrieved August 2006 from http://www.engsw.com/drawroom/Stebbins/Pulp2.html

Sumbry, L. Klaiss, J. Trull, R. "The Sucessful Application of FRP Linings in Above-Ground Storage Tanks: A 20 Year History." *Journal of Protective Coatings and Linings.* 7.3 (1990): 40-44.

Vishay TN-513 (Tech Note). Measurement of Thermal Expansion Coefficient using Strain Gages Vishay Micro-Measurements. Document Number: 11063. Revision: 04-Jan-05.

Vishay B-137 (Instruction Bulletin). "Strain Gage Applications with M-Bond AE-10, AE-15, and GA-2 Adhesive Systems." Vishay Micro-Measurements. Document Number: 11137. Revision: 5-April-05.

Watts, J.F. "Surfaces: How to Assess." *Adhesive Bonding: Science, Technology & Applications.* R.D. Adams. Cambridge: Woodhead Publishing Limited, 2005. 52-74.

Zarnitz, C.E. "Chemical-Resistant Tanks and Linings." *Metal Finishing.* 100.1 (2002): 657-668.

APPENDICES

APPENDIX A

Table A.1 – Test I-A: CPVC Tabulated Results

Test Conditions		Tensile Strength (psi)	Stroke at Failure (in)
Temp (^{o}F)	Selected Percentage		
T_1 - 73 ^{o}F	0%	7962	2.99
		7864	2.89
	15%	7863	0.50
		7373	0.28
	30%	6214	0.12
		7837	1.15
T_2 - 140 ^{o}F	0%	8258	0.97
		8225	2.08
	15%	8312	0.29
		6936	0.14
	30%	7705	0.19
		8393	0.58
T_3 - 180 ^{o}F	0%	8595	0.56
		8423	1.10
	15%	5616	0.32
		6059	0.26
	30%	0	0.00
		4577	0.32

Table A.2 – Test I-B: CPVC Tabulated Results

Test Conditions			Soak Time (days)	Tensile Strength (psi)	Stroke at Failure (in)
Temp (^{o}F)	Solution	Selected Percentage			
T_1 - 73 ^{o}F	Water	0%	1	7781	1.78
			7	7178	2.21
			14	7779	1.31
			28	7823	0.60
		10%	1	7237	0.38
			7	7978	1.88
			14	7844	1.44
			28	7106	0.27
	5% NaCl	0%	1	7234	0.44
			7	7965	1.05
			14	7961	2.76
			28	7787	1.97
		10%	1	7098	0.37
			7	7773	0.72
			14	7913	0.72
			28	7890	0.93
T_2 - 140 ^{o}F	Water	0%	1	7835	2.63
			7	7332	1.46
			14	7994	1.24
			28	8172	1.16
		10%	1	7094	0.18
			7	8116	0.19
			14	7369	0.16
			28	8273	0.81
	5% NaCl	0%	1	8049	1.92
			7	8147	1.34
			14	8307	1.54
			28	8070	2.75
		10%	1	7511	0.21
			7	8507	0.31
			14	8488	0.22
			28	8314	0.26
T_3 - 180 ^{o}F	Water	0%	1	7912	3.78
			7	8182	1.80
			14	8302	0.90
			28	8444	0.65
		10%	1	7352	0.22
			7	8002	0.53
			14	7036	0.17
			28	7947	0.49
	5% NaCl	0%	1	8193	1.80
			7	7377	0.73
			14	7764	0.81
			28	7699	0.51
		10%	1	7955	0.50
			7	7406	0.22
			14	6340	0.28
			28	8387	0.19

Table A.3 – Test I-A: SS340 Tabulated Results

Test Conditions		Tensile Strength (psi)	Stroke at Failure (in)
Temp (^{o}F)	Selected Percentage		
T_1 - 73 ^{o}F	0%	2105	0.26
		2097	0.21
	15%	2458	0.31
		2275	0.32
	30%	2410	0.25
		2130	0.25
T_2 - 140 ^{o}F	0%	1923	0.24
		1803	0.18
	15%	NA	NA
		NA	NA
	30%	NA	NA
		NA	NA
T_3 - 180 ^{o}F	0%	1798	0.19
		1867	0.19
	15%	NA	NA
		NA	NA
	30%	NA	NA
		NA	NA

Table A.4 – Test I-B: SS340 Tabulated Results

Test Conditions			Soak Time (days)	Tensile Strength (psi)	Stroke at Failure (in)
Temp (^{o}F)	Solution	Selected Percentage			
T_1 - 73 ^{o}F	Water	0%	1	2152	0.48
			7	2138	0.38
			14	2100	0.39
			28	2128	0.46
		10%	1	2219	0.46
			7	2021	0.34
			14	2148	0.21
			28	2207	0.27
	5% NaCl	0%	1	1750	0.37
			7	1792	0.34
			14	1944	0.60
			28	1858	0.44
		10%	1	1753	0.42
			7	1789	0.36
			14	2088	0.45
			28	2123	0.44
T_2 - 140 ^{o}F	Water	0%	1	2023	0.23
			7	2122	0.21
			14	2020	0.26
			28	2001	0.29
		10%	1	2148	0.27
			7	2061	0.24
			14	1609	0.27
			28	1643	0.19
	5% NaCl	0%	1	1846	0.47
			7	1884	0.36
			14	1808	0.27
			28	1834	0.26
		10%	1	1850	0.30
			7	1947	0.47
			14	2124	0.83
			28	1813	0.30
T_3 - 180 ^{o}F	Water	0%	1	2242	0.32
			7	2251	0.22
			14	2071	0.29
			28	1966	0.26
		10%	1	NA	NA
			7	NA	NA
			14	NA	NA
			28	NA	NA
	5% NaCl	0%	1	2036	0.46
			7	2078	0.47
			14	2041	0.31
			28	2117	0.27
		10%	1	NA	NA
			7	NA	NA
			14	NA	NA
			28	NA	NA

APPENDIX B

Table B.1 – Test II-A: Lap Shear Tabulated Results

Test Conditions		Shear Strength (psi)	Stroke at Failure (in)	Days Survived
Temp (^{o}F)	Selected Percentage			
T_1 - 73 ^{o}F	0%	1007	0.078	30
		995	0.078	30
	15%	563	0.071	30
		1071	0.078	30
	30%	NA	NA	1
		NA	NA	1
T_2 - 140 ^{o}F	0%	742	0.050	30
		872	0.059	30
	15%	NA	NA	0.01
		NA	NA	2
	30%	NA	NA	0.007
		NA	NA	0.007
T_3 - 180 ^{o}F	0%	490	0.047	30
		539	0.049	30
	15%	NA	NA	0.014
		NA	NA	0.003
	30%	NA	NA	0.000
		NA	NA	0.004

Table B.2 – Test II-B: Lap Shear Tabulated Results

Test Conditions		Shear Strength (psi)	Stroke at Failure (in)	Days Survived
Temp (^{o}F)	Selected Percentage			
T_1 - 73 ^{o}F	0%	1231	0.117	30
		918	0.105	30
	8%	1457	0.256	30
		1133	0.114	30
	15%	1390	0.171	30
		1499	0.264	30
T_2 - 120 ^{o}F	0%	978	0.092	30
		748	0.075	30
	8%	1014	0.102	30
		NA	NA	29
		811	0.083	30
		975	0.087	30
	15%	NA	NA	5
		NA	NA	14
		NA	NA	6
		NA	NA	20
T_3 - 140 ^{o}F	0%	874	0.086	30
		710	0.069	30
	8%	797	0.090	30
		NA	NA	16
		NA	NA	6
		789	0.068	30
	15%	NA	NA	4
		NA	NA	9
		NA	NA	1
		NA	NA	1

APPENDIX C

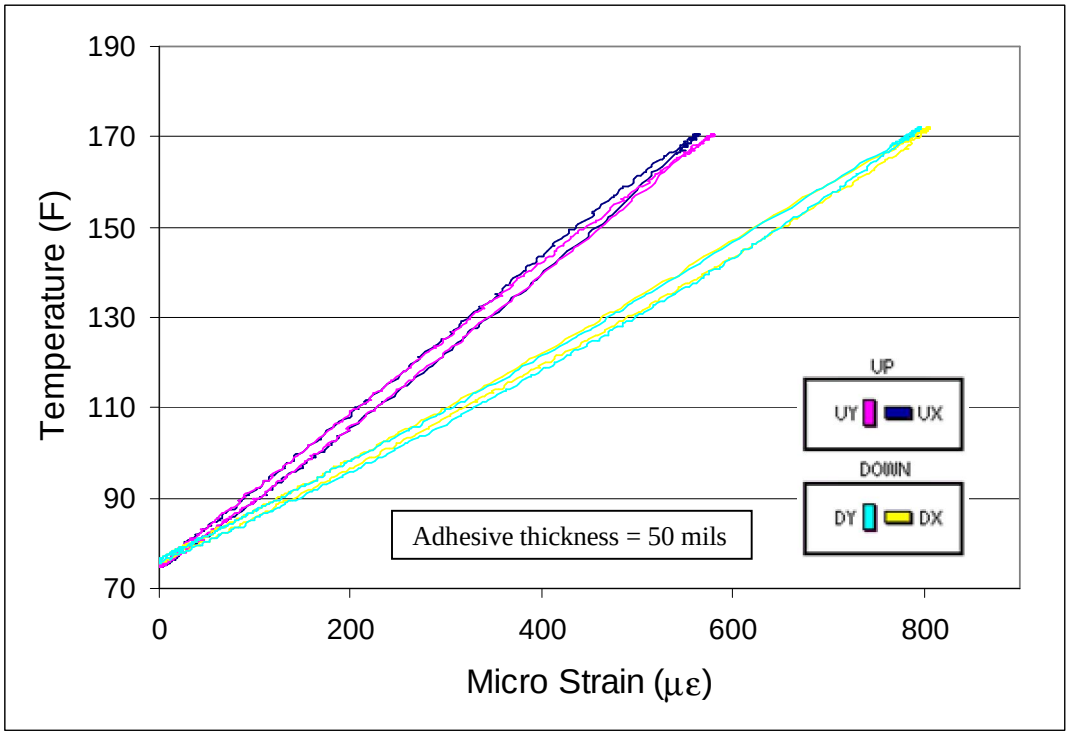

Figure C.1 – Measured Steel Strain of Specimen 2

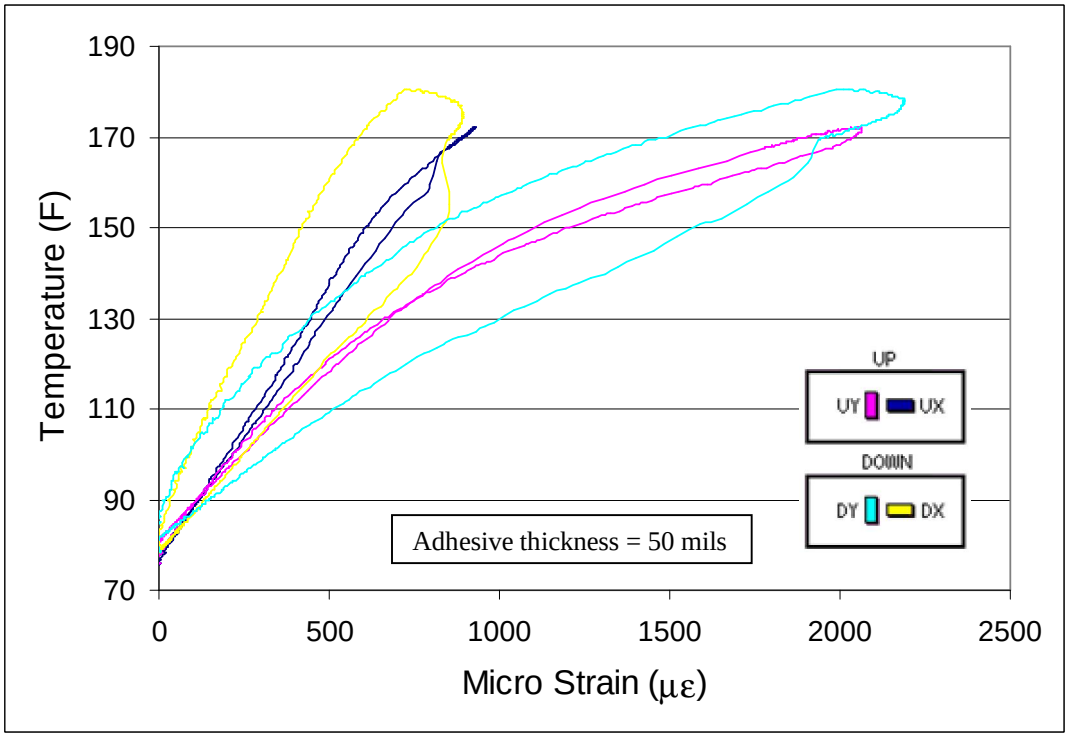

Figure C.2 – Measured CPVC Strain of Specimen 2

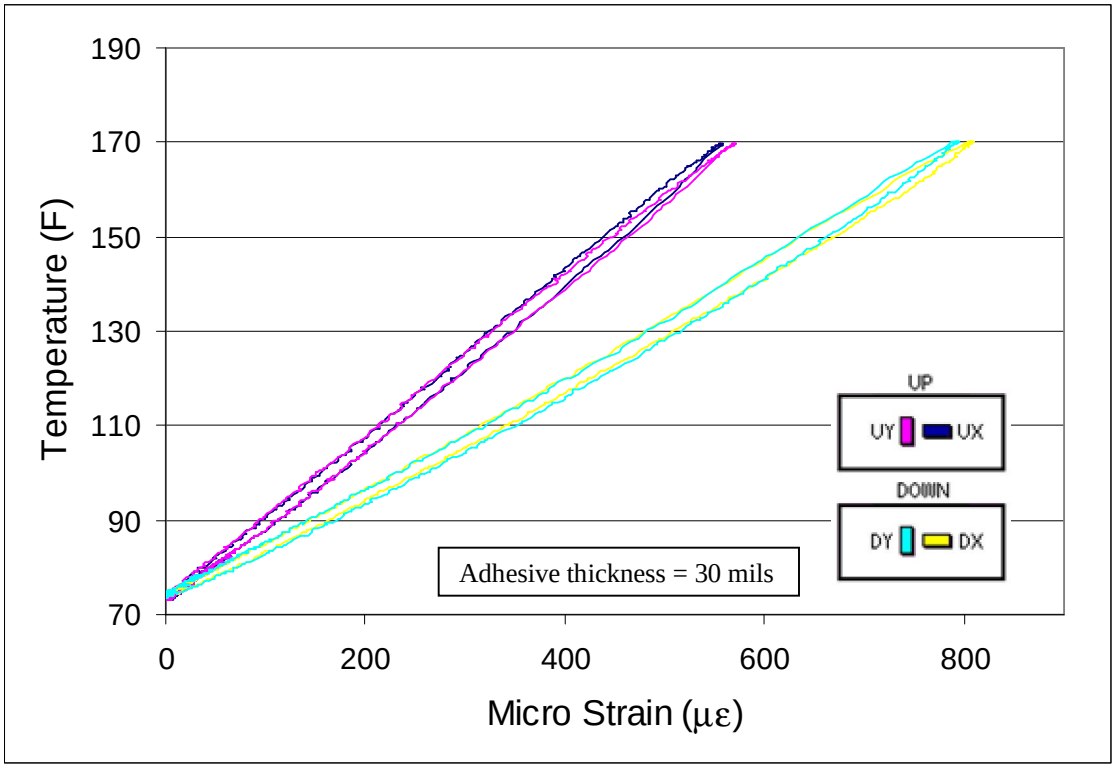

Figure C.3 – Measured Steel Strain of Specimen 3

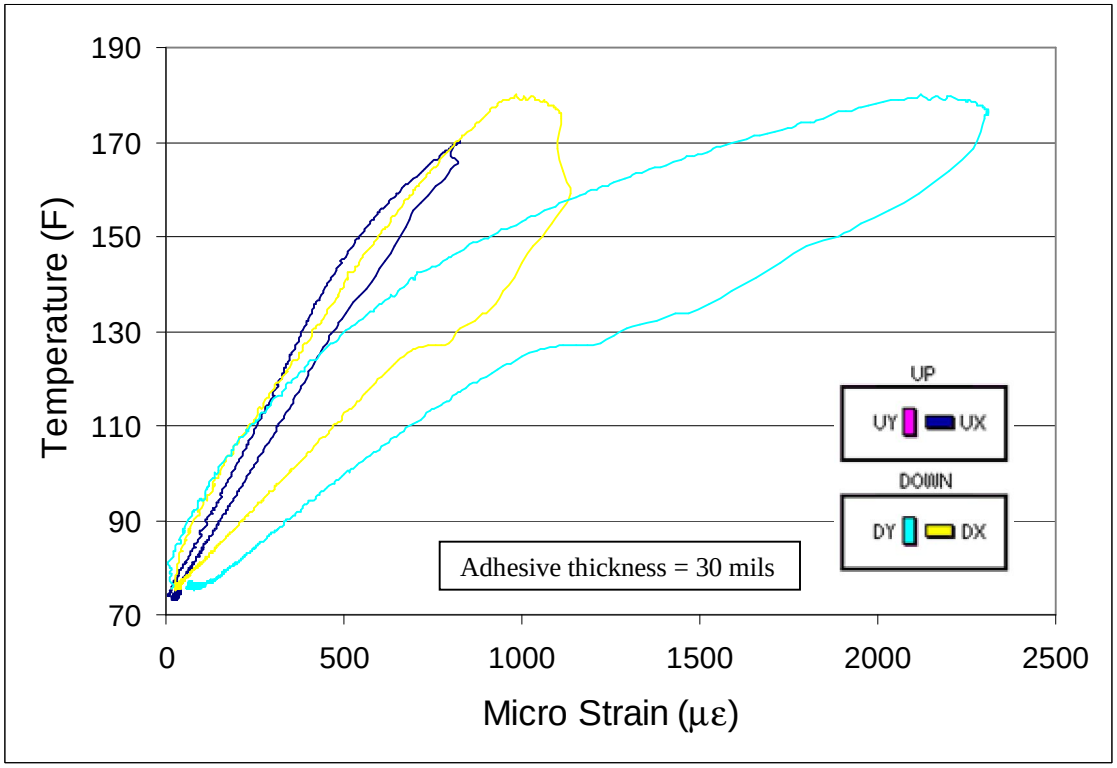

Figure C.4 – Measured CPVC Strain of Specimen 3

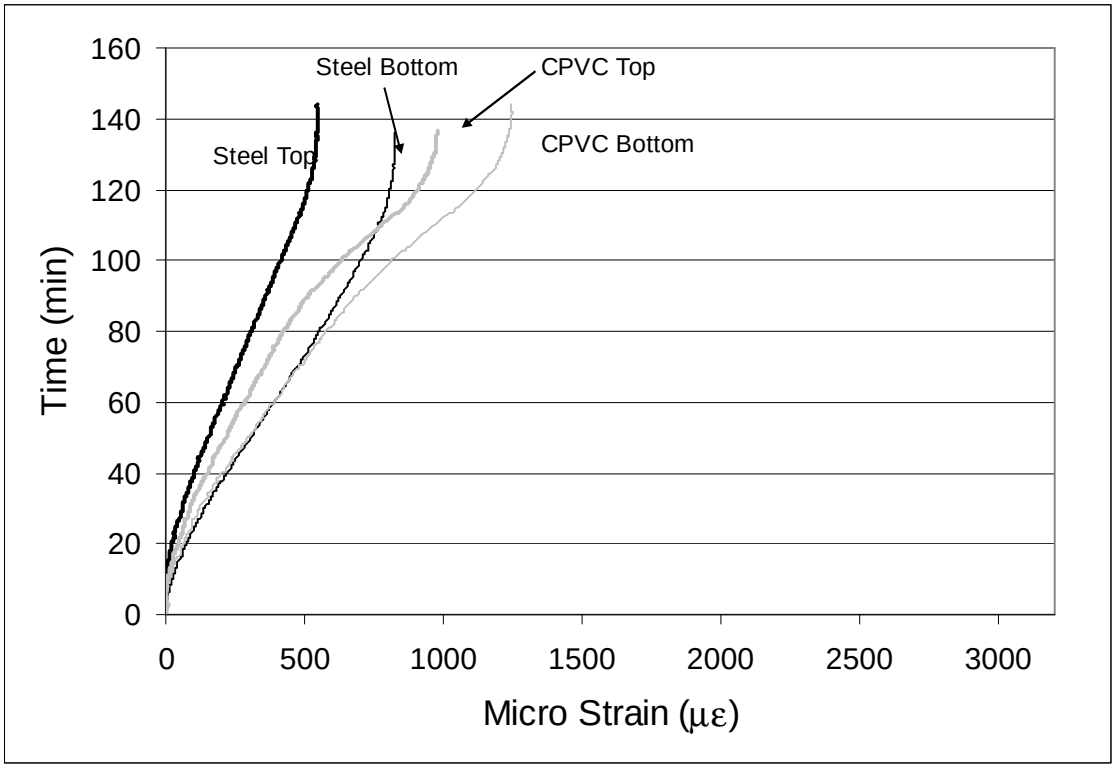

Figure C.5 – Time vs. Strain of Specimen 1 in Long Dir

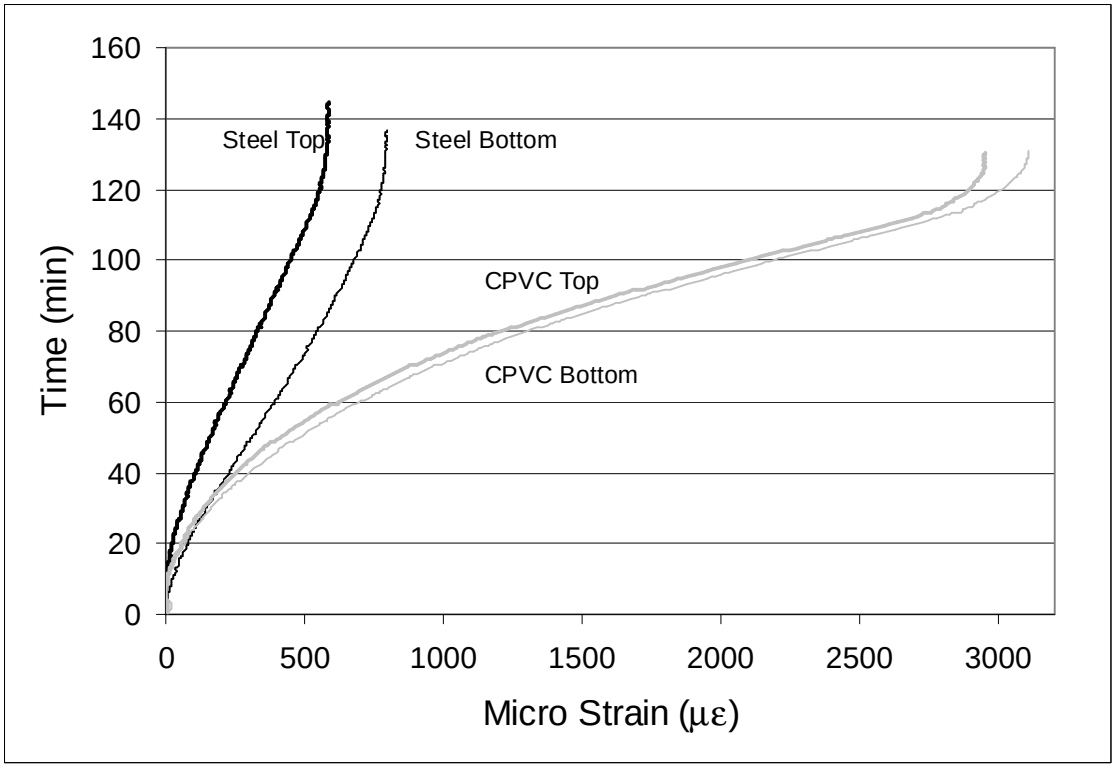

Figure C.6 – Time vs. Strain of Specimen 1 in Short Dir

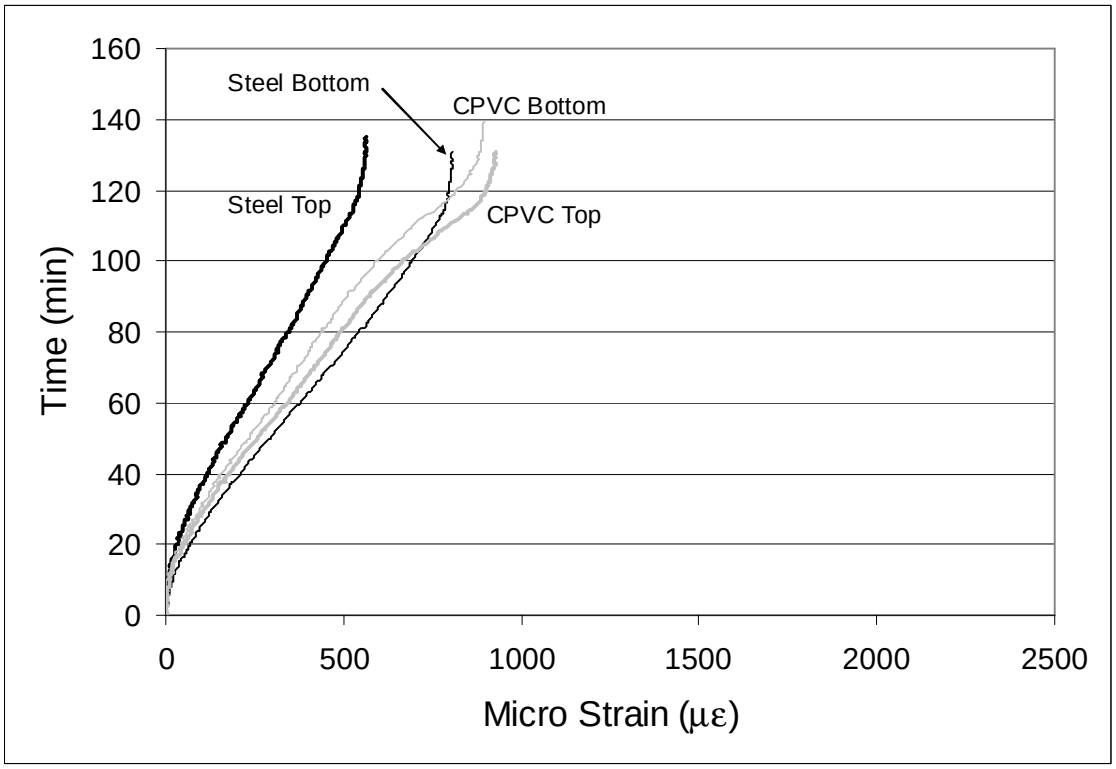

Figure C.7 – Time vs. Strain of Specimen 2 in Long Dir

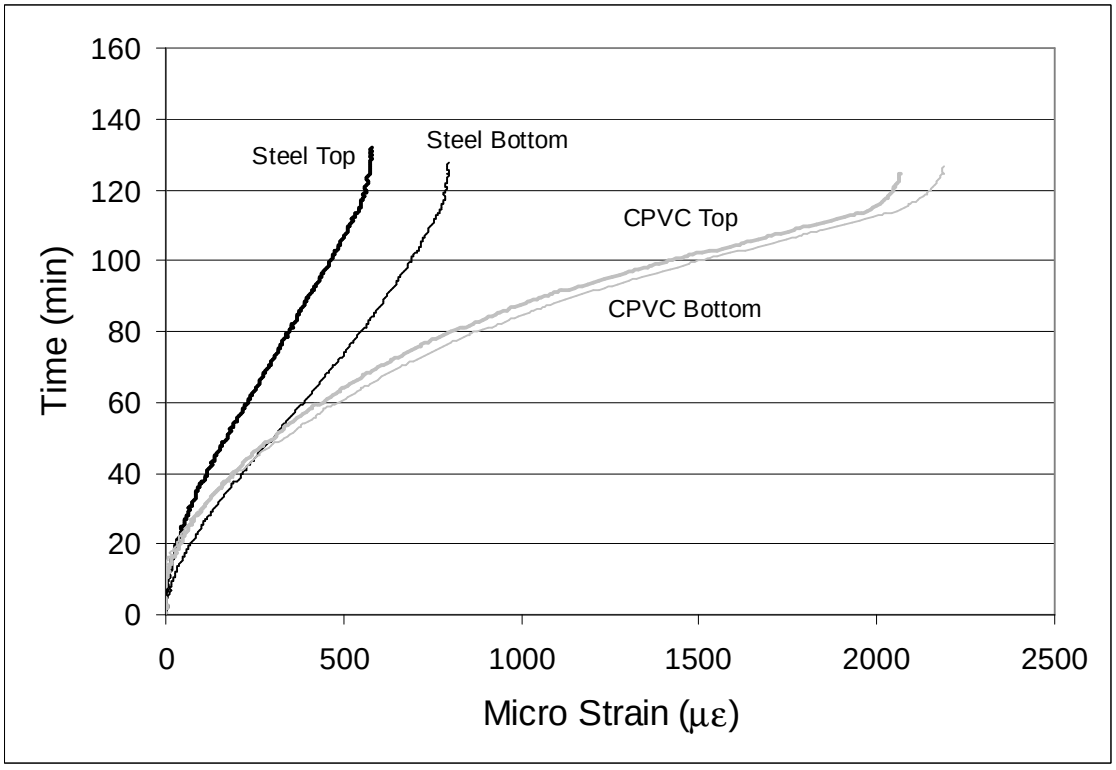

Figure C.8 – Time vs. Strain of Specimen 2 in Short Dir

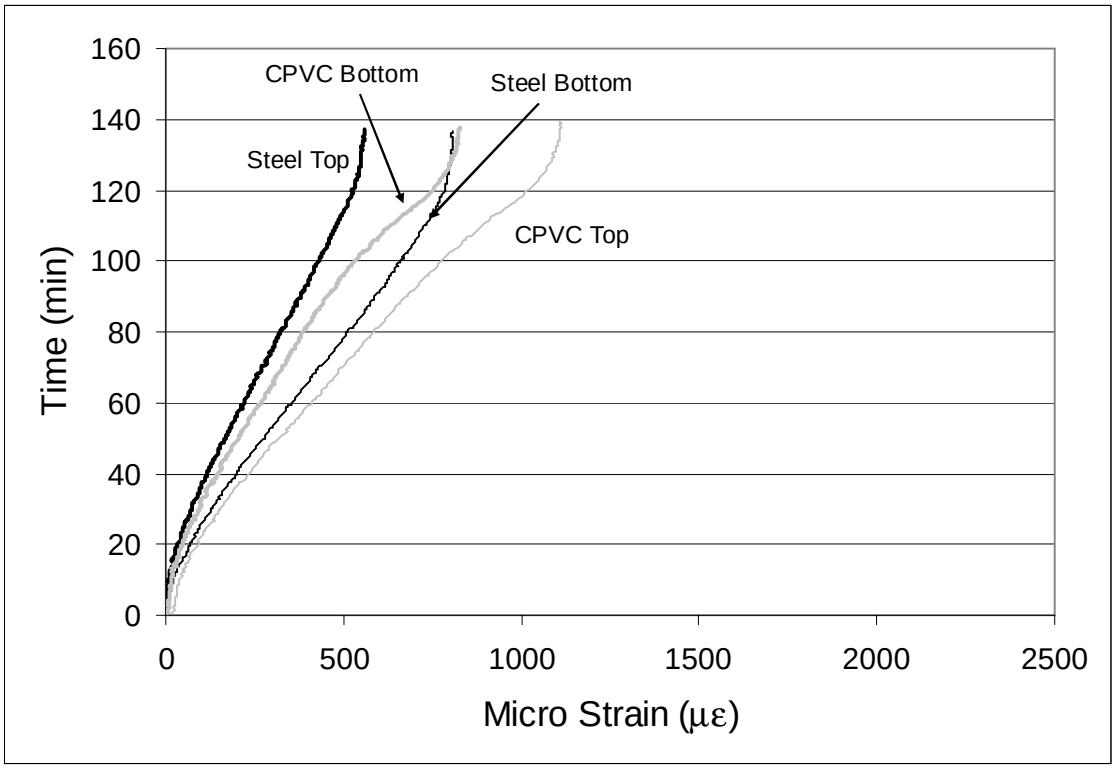

Figure C.9 – Time vs. Strain of Specimen 3 in Long Dir

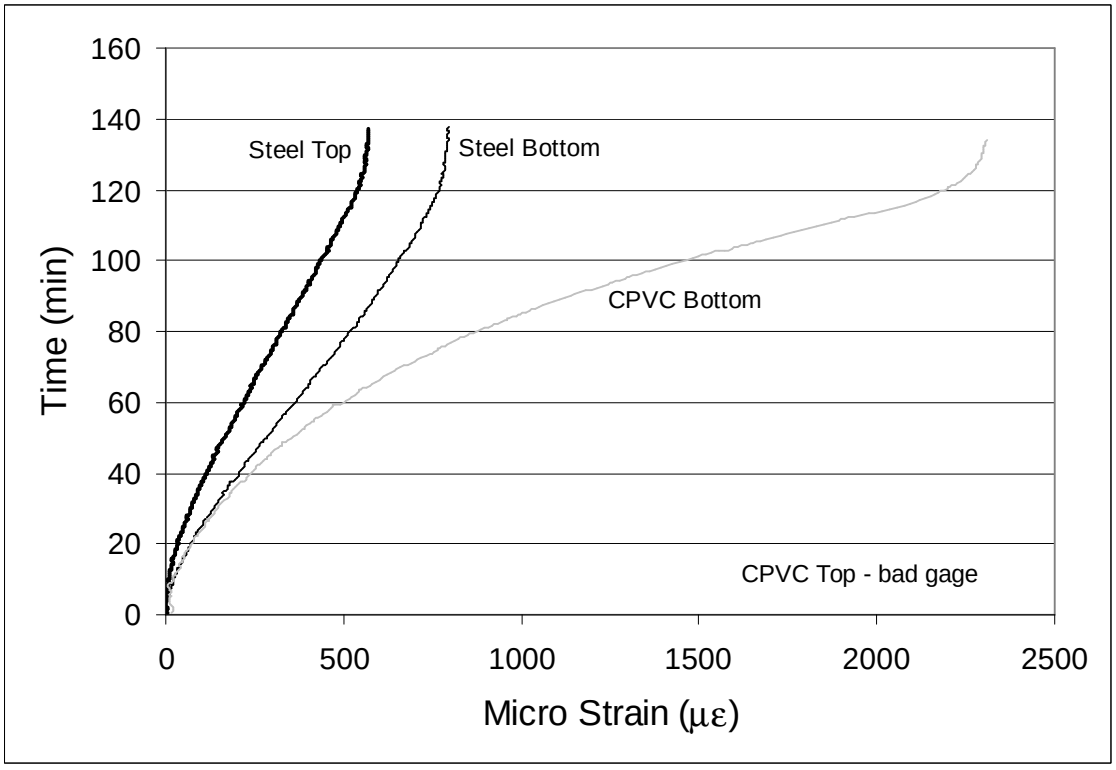

Figure C.10 – Time vs. Strain of Specimen 3 in Short Dir